Phosphorus transport in a Dutch lowland area: the role of high flow storm events and suspended matter

Master Thesis – 45 ECTS

Submitted in partial fulfilment of the requirements for the degree of Masters of Science in Sustainable Development

August 2014

Author	Arjen Kratz
Student number	3275426
Supervisors	Bas van der Grift (Deltares)
	Jasper Griffioen (Utrecht University)
	Paul Schot (Utrecht University)

Abstract

Phosphorus (P) is an essential macronutrient, which also has the potential to cause severe eutrophication issues in freshwater systems. Research done over the last decades has revealed the importance of the transport of particulate-P (PP) during high flow storm events to the annual total-P loading. The present study applied P speciation, by means of chemical sequential extraction, to analyse the temporal variability of P fractions during a high flow event and thereby allow a more detailed characterization of P mobility and the impact on eutrophication.

A sampling campaign was conducted in the Noordplas polder, a former lake in the Netherlands, featuring significant groundwater exfiltration. The polder exports large quantities of PP to downstream areas, often exceeding the regulatory limits on P concentration. A controlled high flow event was forced using the polder's water pumping station and a weir, thereby eliminating the interference of overland and subsurface drain flow that would have occurred during a natural high flow storm event in a free flowing system. Suspended matter samples collected by centrifugation and filtration were analysed to determine the P speciation, as well as the suspended matter (SM) concentration and particle size distribution.

The results showed that variation in the P concentration in the water column was significantly related to changes in the SM concentration. Changes in other parameters, including particle size distribution and the relative P content of SM, had no noticeable influence on the P concentration. Dissolved-P concentrations were at all times stable and only a minor component of the total P pool. Large increases in SM and P concentrations were associated with erosion during the highest flow velocities, the SM concentration remained largely unaffected if the flow velocity did not reach critical shear stress levels. The relative contribution of P fractions to PP (% PP) was a stable parameter, seemingly independent of other parameters like flow velocity or water quality. Iron-bound P (Fe-P) was the most dominant fraction (about 80% PP), at all locations and for all flow velocities. Organic P was the only other prominent fraction (about 15% PP on average). An important finding is that the P speciation of SM collected by centrifugation underestimated the exchangeable P and authigenic calcium-bound P fractions. This is explained by the inability of the centrifuge to capture the lightest particles. The mentioned %PP values were therefore based on filter samples only. The Fe-P contribution and relative P content of SM are high compared to values found in literature, most likely due to the influx of high concentrations of dissolved P and iron through groundwater, causing authigenic production of particulate Fe-P in the water column.

The findings of the present study implicate the necessity for water management to assess the effect that different pumping rates by pumping stations have on P transport. In this study, doubling the pumping rate led to twice higher PP concentrations in the channel near the pumping station. Spot samples might not be able to detected this spike during standard monitoring programs, therefore, estimations of P export that do not include a full range of pumping activity are prone to underestimate P export. Literature dictates that the dominant Fe-P fraction has to be considered biologically available; an eutrophication effect by the exported P is thus plausible.

Keywords Peak flow – Suspended matter – Phosphorus – Particulate phosphorus – Speciation – Fractioning – Sequential extraction

Contents

Acknowledgements

Writing this thesis as part of an internship at Deltares has proven to be an excellent choice. The freedom to find your own way, while knowing that help will be there the moment you ask for it, provided a stimulating and pleasant working environment. I am very grateful to all those people who have supported me in the process of writing this thesis, whether it was by answering a single question or joining me in the field during the sampling campaign.

My special thanks go out to my supervisors Jasper Griffioen and Bas van der Grift, for their trust and their guidance, and the entire BGK department, for all the small things. I'd also like to thank Paul Schot for agreeing to be my second reader and providing me with feedback on my proposal.

Best regards,

Arjen Kratz

1 Introduction

1.1 Phosphorus transport

Phosphorus (P) is an essential macronutrient for all living organisms and considered one of the major limiting nutrients for terrestrial ecosystems. The input of excessive amounts of biologically available P in surface water systems, often as the result of human action, can cause severe eutrophication. Negative effects include decreasing biodiversity and impairment of the use of water bodies for human purposes by harmful algal blooms (Correll 1998). Controlling P eutrophication in downstream areas requires detailed knowledge of transport pathways and retention of P in freshwater streams and rivers (Reddy et al. 1999).

The transport of P may vary significantly on a spatial and temporal scale. Research has shown that transport during high-flow storm events makes up a significant portion of the annual transport loads of P. It has also been observed that the increase in transport of particulate-P (PP) due to the occurrence of a storm event is significantly larger than the increase in dissolved-P (DP) transport (van der Salm et al. 2012; Vidon & Cuadra 2011; Evans & Johnes 2004).

PP is a term drawing together all kinds of particles that contain P in their molecular structure and/or have P absorbed to them. This can be organic and inorganic P. The various forms of PP have different physical and chemical properties, influencing their mobility (Poulenard et al. 2008). The transport characteristics of the overall term “PP” depend on the relative contribution of PP species to the total mixture of PP in the water column and the conditions that they are subjected to. P speciation (also referred to as fractionation) by means of chemical sequential extraction is a commonly used method to fractionate the overall inorganic P into groups of compounds with similar chemical release patterns (Ruttenberg 1992). P speciation allows a more detailed assessment of chemical and physical characteristics, while avoiding the logistical demands of particle by particle assessment. An overview of the various level of detail in P transport is presented by Figure 1.1. While a large amount of research has been done on the inorganic and organic scale of P transport, uncertainty persists regarding the distribution and relative mobility of the different particulate-P species, especially during storm events.

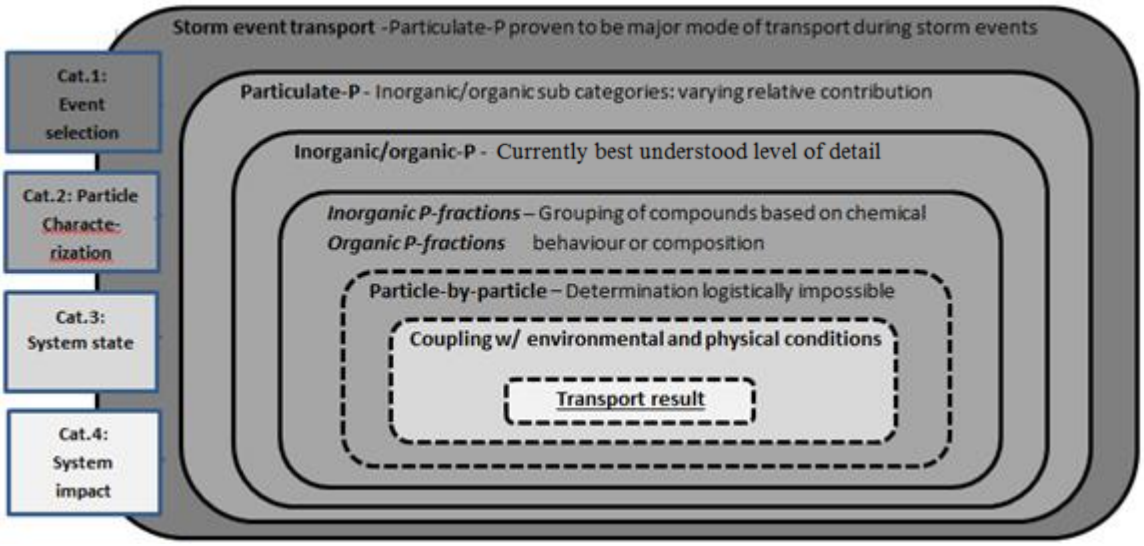

Figure 1.1: Assessing components of P transport in various levels of detail. Four categories, marked by colour, are distinguished. The dashed lines indicate a barrier (e.g. technological, logistical) for determining the respective component.

1.2 Phosphorus, suspended matter and storm events

The primary effect of storm events is that the increase in flow velocity induces shear stress on the sediments, which is the main factor in erosion and transport of sediment and suspended matter (SM) (Gailani et al. 1991). PP is a component of the overall sediment and SM groups, transport of PP is thus driven by the same principles. The variation in physical and chemical properties, especially particle size and density, influences the critical shear stress required for suspension of sediments as well as the sedimentation rate of SM upon the return to base flow conditions (Gailani et al. 1991; Pacini & Gächter 1999; Borah et al. 2004). Therefore, it can be expected that the flow conditions that favour transport and sedimentation will be different for each P fraction; however, no evidence could be found for attempts to map speciation of PP associated with SM transport loads during storm events in Dutch agricultural landscapes, at least not further than organic or inorganic.

The interest in the Dutch situation is based on the influence of iron-rich groundwater seepage, which is a common condition in the Netherlands and other lowland areas with a reactive subsurface. Production of ferrous authigenic sediment and authigenic suspended matter due to influx of dissolved iron (Fe) can be a significant component of total sediment and suspended matter input (Baken et al. 2013; Vanlierde et al. 2007; Hyacinthe & Van Cappellen 2004). Figure 1.2 shows a schematic overview of the various sources of particulate matter in water systems. The "stock" concept is borrowed from modelling and is defined as the historically present quantity of a substance, without making assumption about its origin.

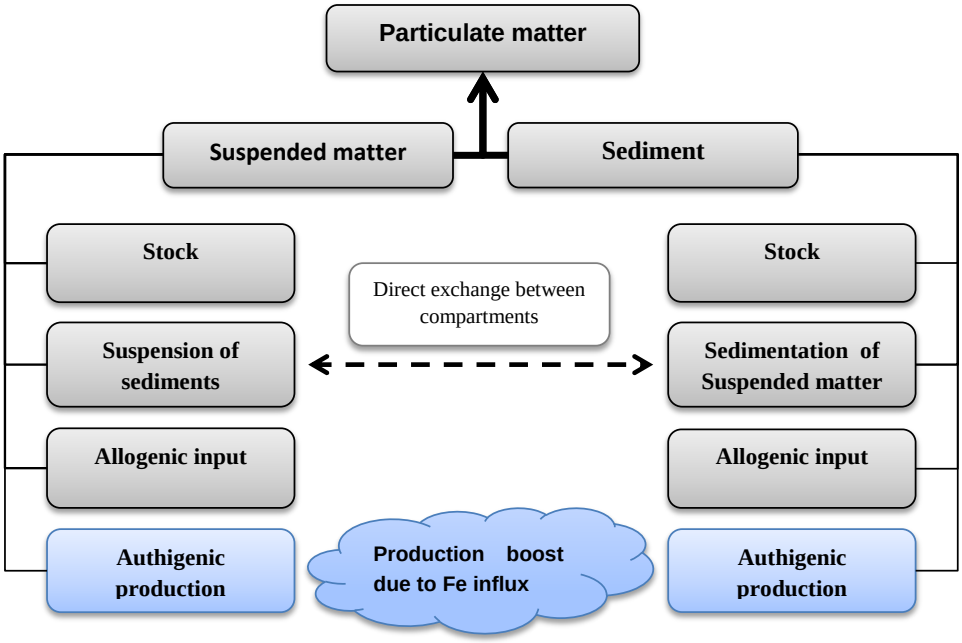

Figure 1.2: Basic overview of the sources of particulate matter in a water system.

Ferrous sediment and SM have great P binding potential, primarily through precipitation of dissolved P and dissolved Fe as ferric phosphates (FP) during the shift from anoxic to oxygenated conditions and through absorption of P species on the surface of hydrous ferric oxides (HFO) (Baken et al. 2013; Gunnars et al. 2002). Baken et al. (2013) investigated transport of authigenic sediment in a Belgian basin with iron-rich groundwater seepage and found the contribution of authigenic SM to total SM transport over a four-month period to range from 31% authigenic to "almost exclusively" authigenic. The authors also investigated the composition of freshly formed authigenic material (in the size range > 0.45 µm) and observed a large Fe component, on average 44% by weight. Contemporary results from the PhD research by Bas van der Grift indicate that the Fe-bound P fraction contributed 50-90% to the total SM-bound P in

grab samples gathered in two Dutch areas (Lissentocht polder & Hunze catchment), although no claims were made about the authigenic origin of the Fe-P fraction (pers. communication B. van der Grift). This study will expand on this knowledge by having a special focus on the transport of the Fe-P fraction, which is assumed to be highly authigenic, during storm events.

1.3 Research questions

This research will bring together the questions regarding the distribution of P fractions during storm events with special focus on the aspect of elevated authigenic (suspended) sediment production in Dutch water systems. The following *hypothesis* is stated based on the available data: *Surface water transport of P through freshwater systems with significant Fe-rich groundwater seepage consists mostly of particulate-P, contained in the overall suspended matter group. Most of the particulate-P consists of an inorganic Fe-P fraction. Different P fractions have their own specific mobility characteristics; their relative contribution to total-P thus varies with flow velocities. A significant part of the suspended sediment consist of very fine sediments and colloids, which have an long lasting effect on suspended matter concentrations that extends beyond the timespan of a storm event, as a result of slow sedimentation rates.*

The central research question that serves to investigate this hypothesis is as follows:

"How can the transport of phosphorus during storm events in freshwater systems with iron-rich groundwater exfiltrating be characterized, in particular its relation with suspended matter?".

The central research question is broken down into three sub-questions, aimed at different parts of the hypothesis:

i) How do the concentrations and loads of SM and the various fractions of P develop over the timespan of a storm event?

ii) Are there significant correlations between the observations of P, SM and other environmental parameters measured in the field?

iii) How does a storm event continue to influence P and SM transport in the period following the ending of the event?

The goal of the research is to improve understanding of the controls on P transport by generating field data relevant for the Netherlands that includes ferrous authigenic sediment as a factor. The results will strengthen the link between soil chemistry and transport and allow for more efficient water quality management. Furthermore, the development of surface water transport models can directly benefit from quantification of the mobility characteristics of dominant P-fractions that this study might find.

2 Theory

The theory section will expand upon some of the subjects mentioned earlier in the introduction and provide a background for the methodological foundation. The information provided is not meant to be entirely exhaustive, as a major part of the research effort will be focused at explaining the results in the discussion.

2.1 Fractioning techniques

Most of the classifications of P fractions in contemporary literature have been making a distinction based on state (dissolved/particulate/colloidal) and molecule type (organic/inorganic). The distinction up to these levels does not sufficiently explain mobility characteristics or environmental impact, due to the aforementioned diversity of P-species and their behaviour (Wang et al. 2013; Reddy et al. 1999; Poulenard et al. 2008) However, it is arguably impractical to determine all P species at a molecular level, not only for logistical reasons but also because the majority of the transport function might be explained by only a few specific fractions. A more functional approach to detailing transport dynamics is to use chemical sequential extraction to fractionate the major particulate inorganic-P (PIP) fractions by their associated metallic elements, e.g. iron (Fe), aluminium (Al), calcium (Ca), or required effort for extraction (e.g. loosely bonded P, detrital P). Different extraction schemes have been developed over the decades that utilize their own classifications of fractions and also each their own strengths and weaknesses (Wang et al. 2013). Some schemes are also able to distinguish between different forms of the same mineral. An important example is authigenic Ca-bound P and detrital P, which both contain apatite (Ruttenberg 1992). The term “authigenic” indicates that the calcium mineral was formed in the free environment, as opposed to detrital P, which generally refers to apatite of igneous and metamorphous origin.

2.2 Aquatic chemistry in marine polders

2.2.1.1 Effects of iron-rich groundwater exfiltration

Exfiltrating groundwater, containing dissolved Fe and P, has a positive effect on SM and sediment formation under most conditions. Exfiltration dissolved Fe reacts upon reaching the water-soil interface, forming hydrous ferric oxide and/or ferric phosphate authigenic compounds. Ferric phosphate has a preferred thermodynamic state at the water-soil interface and is thus the most common reaction product if Fe(II) oxidation occurs in the presence of dissolved P (Hyacinthe & Van Cappellen 2004; Gunnars et al. 2002). Given low pH values, the Fe(II) oxidation reactions are sufficiently slow for a portion of groundwater Fe to pass unhindered into the water column (pers. communication, Bas van der Grift), where most of the Fe oxides into HFO (Gunnars et al. 2002).

The produced HFO and FP colloids can move into a particulate phase through aggregation or to a truly dissolved phase by break-up processes. Colloids that resist change in either direction are considered to have a high colloidal stability. The colloidal stability of HFO colloids is heavily influenced by pH, salinity and organic matter (OM) parameters. High values of pH and salinity cause swift aggregation and subsequent precipitation, while higher OM values have a stabilizing effect (Gunnars et al. 2002). Declaring a single rule regarding the stability of colloids is not possible due to the dependency on local parameters. Gunnars et al. (2002) did, however, state that HFO colloids are generally stable under freshwater conditions.

2.2.1.2 Influence of particle size on suspension

Particle size has a large influence on the erosion and sedimentation characteristics of particles. The minimal flow velocity required to erode sediments (i.e. critical shear stress) and transport SM typically increases in an uniform direction with particle size and density, yet an exception exists regarding the erosion of the smallest size fractions; clays and silt . These particles are attracted to one another by cohesive forces, increasing their resistance to shear stress. This may result in

larger particles being eroded at lower flow velocities than is required for clay and silt. The sedimentation process of suspended particles is dominated by the gravity factor, making the finest particles require the lowest flow velocities for sedimentation. Based on the cohesive forces theory it is expected that storm events are important not only for the transport of the coarse sediments, but also for the finest sediments. Furthermore, these finest sediments are assumed to have a long-term impact on the system due to slow sedimentation processes. Determining size fractions of suspended matter is, therefore, crucial to estimating its long term fate.

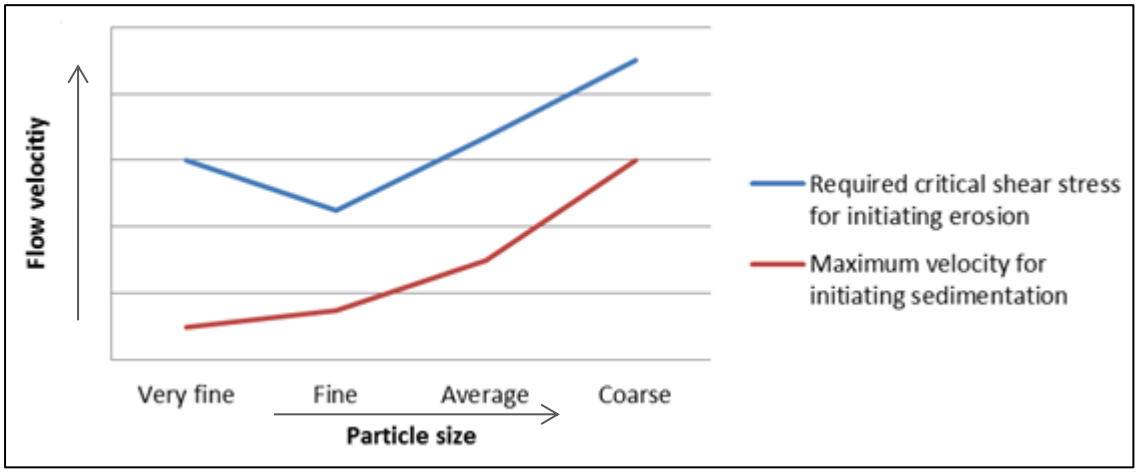

Figure 2.1: Schematic representation of the trends of the minimum and maximum flow velocities that are required for the erosion and sedimentation of particles, respectively.

2.2.1.3 *Influence of particle size on phosphorus concentration*

Aside from erosion and sedimentation, particle size is also related to the specific surface area (SSA) of particles. SSA refers to the amount of surface area per unit of mass or volume, this parameter largely determines the maximal absorption capacity of a particle. Smaller particles tend to have a significantly larger SSA than bigger particles, meaning they can store relatively large amounts of P (Evans et al. 2004). In contrast, studies showed that no significant relationship exists between SSA and P loading during storm events (Ballantine et al. 2008). The most probable cause of the conflict between the two theories is that mobilization of the large volume of coarse bed sediment provides the bulk of the P during a storm event.

3 Materials and methods

3.1 Sampling area

3.1.1 Description of the sampling area

The chosen fieldwork area is the Noordplas polder (NPP), a former lake in the province of Zuid-Holland, which is now used for agriculture and housing purposes. All necessary background information can be sourced from De Louw et al. (2004), who performed a very thorough assessment of the presence and origin of nutrients and salinity gradients in the NPP. The data in the remainder of this paragraph is based on this reference.

The NPP is situated 4 to 5 meters below sea level (by the Dutch NAP definition) and characterized by significant groundwater exfiltration, containing high levels of chloride, phosphorus and iron. Surface water levels are controlled through two pumping stations, Palenstein and Omringdijk. Inlet of external water is only a factor during dry periods in summer. The primary source of the groundwater in the polder is the Pleistocene sandy aquifer, situated below a confining peat layer and a Holocene cover layer of sandy marine clays. The peat layer is at some points intersected by sand lanes from former stream gullies. The groundwater exfiltration through the sand lanes is significantly stronger and often attracts groundwater from deeper in the aquifer. This phenomenon, visualized in Figure 3.1, is called upconing and has been estimated to results in five times higher exfiltration rates (1.4 mm/day) compared to the confined situation (0.35 mm/day). Chloride concentrations are also significantly higher in upconing areas, measuring 500-1000 mg/L compared to 100-200 mg/L elsewhere.

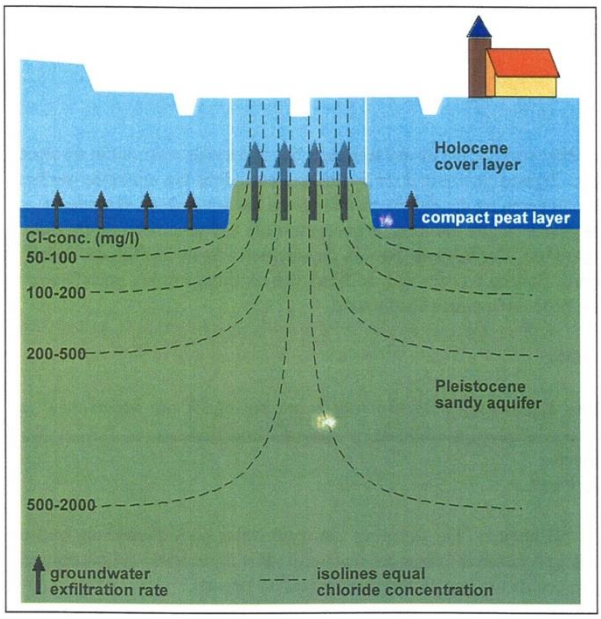

Figure 3.1 Representation of the upconing principle, caused by breaches of the impermeable peat layer. Both the quantity of the groundwater exfiltration and the salinity concentration are higher in upconing areas than on top of the confining layer. Picture taken from De Louw et al. (2004).

De Louw et al. (2004) found that most of the chlorine input comes from boils, that occur frequently in the sections of upconing areas where the Holocene layer is at its thinnest. Due to extremely high hydraulic conductivity boils often attract groundwater from the deepest and most saline parts of the Pleistocene aquifer. The location of the boils and their exfiltration rates are dynamic, but can be detected through their salinity profile.

The exfiltrating groundwater is low on sulphates. Most of the input of sulphate to surface waters results from nitrate-rich infiltration water, which oxidizes pyrite in the surface layer. The observation of high sulphate concentrations in the surface water has thus been linked to large contributions of precipitation water (De Louw et al. 2004).

Phosphorus in the surface water is estimated to originate for 75% from groundwater input. The remainder 25% is from input related to agricultural sources. De Louw et al. (2004) based their numbers on mass balances for entire parts of the polder, and for local situations these numbers might be different. The numbers do, however, indicate the importance of groundwater input for the presence of phosphorus in surface water.

3.1.2 Placement and description of sampling locations

Figure 3.2 shows a map of the NPP and the placement of the sampling locations. Three sampling locations (PLS, STW and SLT) were selected, each intended to provide an individual insight into the flow dynamics within the polder. Photo's 3.1-3.3 on the next page provide an impression of the conditions at the sampling locations.

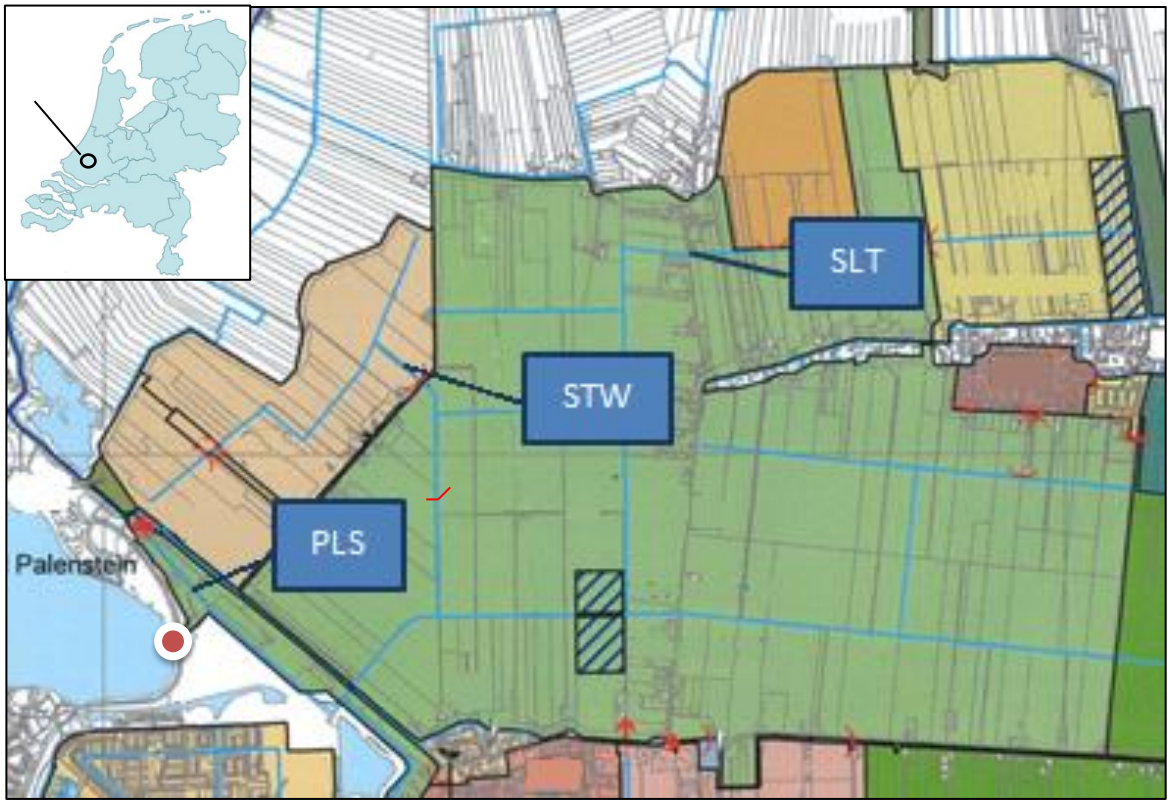

Figure 3.2 Map of the Noordplas polder. PLS, STW and SLT indicate the sampling locations close to the pumping station, a weir and in a backfield ditch, respectively. The different coloured areas indicate sections with separate water level management targets. The pumping station is marked the red-white circle. Weirs are marked by the red bracket symbols.

Sampling location PLS is set in the main waterway of the polder, 375 meters upstream from the pumping station Palenstein. The flow regime is governed almost exclusively by the activity of the pumping station. It is also the location where the water board performs its water quality measurements. PLS represent the most direct cause-effect relation between the working of the pumping station and flow velocity.

Sampling location SLT is set in a ditch with an open long flow connection, 5 kilometers long, to the Palenstein pumping station. Personnel of the local water board has observed some degree of water movement in response to pumping activity at SLT, but the effect is dampened due to the distribution of the flow from the single main waterway over multiple smaller channels and ditches. SLT is included to provide insight in the effects of a gradual pull of the water by the pumping station, in contrast to the expected sudden and powerful pull at PLS.

Sampling location STW is set 25 meters upstream of a weir, which controls a single section of the polder and separates the section from the influence of the pumping station. The outflow through the weir can be adjusted by inserting or removing a 20 centimetre high plank. The weir and the upstream water input are the only controls on the water flow at this measurement point. STW was picked with the purpose of creating a smooth and “natural” flow event (disregarding the initial peak flow when the weir is opened).


Photo 3.1 Downstream view of sampling location PLS, with the pumping station visible at the far end (left picture) and placement of the sampling equipment (right picture).


Photo 3.2 Upstream view of sampling location SLT (left picture) and placement of the sampling equipment (right picture).


Photo 3.3 Downstream view of sampling location STW (left picture) and placement of the sampling equipment (right picture).

3.2 Sampling moments

The timing of the sampling moments and their role within the study, duration of the investigated flow event and overall conditions during the sampling events are summarized in Table 3.1. The PLS and SLT samples collected on 25 February were collected during a flow event caused by a single continuous pumping session by the Palenstein pumping station, which was manipulated to fulfil the objectives of this study. Two teams of three people worked together on this field day.

Table 3.1 Description of all sampling moments, including role within the study (purpose), duration of the flow event (duration) and the conditions during the sampling event..

Location	***Sampling date***	***Duration flow event***	***Purpose***	***Flow conditions during sampling***
PLS	25 February '14	2.5 hours	Main data series	Relatively dry period, sampling targeted at system state before, during and after pumping by the Palenstein pumping station.
	6 March '14	Grab sample	Reference case	Relatively dry period, sample targeted at system state of rest (no pumping)
	21 March '14	1 hour	Reference case	Intense rainfall, sampling targeted at system state before, during and after pumping by the Palenstein pumping station.
SLT	25 February '14	2.5 hours	Main data series	Dry period, sampling targeted at system state before, during and after pumping by the Palenstein pumping station.
	6 March '14	Grab sample	Reference case	Dry period, sample targeted at system state of rest (no pumping)
STW	6 March '14	4 hours	Main data series	Dry period, sampling targeted at system state before and after opening the weir.

3.3 Field work procedure

3.3.1 Field set-up and collecting sample material

The core purpose of the field campaign was to log flow velocities and collect water samples. Flow velocity was measured at the same depth in the water column as the depth from where the water samples were pumped up. The velocity meter and pump tubing were installed at a water depth of approximately 20 centimetres at the start of the field campaign. The surface water level in the field work area decreased as the flow event progressed, causing temporal variations in the exact sampling depth. Visual inspection of the sampling containers indicated that no leaves and other undesirable floating material was sucked into the tubes at any point of the experiment.

The water sample collection is done with Eijkelkamp peristaltic pumps. The pumping rate was kept as stable as possible throughout the experiment. The inlet tubes were placed just downstream of the velocity meter to avoid any interference between the equipment.

Unfiltered water samples were analysed for total-P and particle size distribution, obscuration and particle concentration. Filtered water samples were analysed for pH, EC, alkalinity and concentrations of dissolved-P, cations, anions, DOC and suspended matter. Suspended matter for further SEDEX analysis was extracted from the water samples by filtration and centrifugation. See Table 3.2 for an overview of the sample containers, treatment and the parameters that the containers were used for. All container bottles, except the 15-25 L tanks, were topped off carefully during sampling, to minimize the presence of oxygen and limit any disaggregation due to shaking during transport.

Table 3.2 Overview of sampling containers, sample treatment and the parameters that were derived from the sample. Obscuration and particle concentration are

Sample container	Volume	Sample treatment	Target parameter / purpose
HDPE bottle	60 mL	Acidification	total-P
	60 mL	Filtration and acidification	dissolved-P, dissolved cations and dissolved anions
PE bottle	100 mL	Filtration	EC, pH and alkalinity
	500 mL	None	Particle size distribution of suspended matter, obscuration, particle concentration, total-P
Dark glass bottle	60 mL	Filtration	DOC (measured as NPOC)
Glass bottle	2 L	None	Suspended matter concentration and suspended matter extraction (by filtration)
Plastic water tanks	15-25 L	None	Suspended matter extraction (by centrifugation)

Filtration and preservation by acidification were performed in the laboratory for the PLS and SLT samples, on the same day as the sample collection. For STW the filtration was performed in the field and the acidification in the lab on the same day. Filtration was done using 0.45 micrometre cellulose-nitrate membrane filters. 600 µl of 67%-pure HNO_3 was used for the acidification. The 2 L glass bottles were cleaned with 0,1 M HCl and rinsed three times with ultrapure water prior to use in the field. The 15-25 L water tanks were rinsed three times with tap water before use.

Sampling intervals were based on the relatively importance of the parameters, with P concentrations being the core of the data, and the necessity to gather sufficient SM for chemical analysis. Test runs of the sampling protocol, combined with the available pumping equipment, indicated that approximately 20-30 minutes were needed to collect the necessary water samples, as described in Table 3.2. It was decided that a 30 minute sampling cycle was the best option. Separate total-P measurements were added to the protocol at a 15 minute interval since it could not be excluded that shifts in parameters would occur on time-scales shorter than 30 minutes. In such an event, regular intervals of total-P measurements can help explain the data derived from the P measurements in suspended matter.

3.3.1.1 Location-specific planning and adaptions – 25 February

In preparation for the field work it was agreed with the water board to deactivate the water pumping station in order to build up sufficient water for an estimated two hours of continuous pumping. The station has two pumps that can be activated separately. Each pump provides a constant capacity of 110 m^3/minute. It takes approximately five minutes from standstill for the pump to build up to this pumping rate according to the manager of the umping station. When stopping the pumps it also takes five minutes to gradually reduce the pumping rate to zero again.

Sampling material was collected during various stages of the pumping cycle, e.g. stand still – one active pump – two active pumps – stand still. The pumps were kept active till water level reached

a minimum level, which provided sufficient time to complete four sampling cycles for the main series of both the PLS and the SLT location.

3.3.1.2 Location-specific time planning and adaptions – 6 March

The weir at the STW location was closed six days prior to starting the field work, in order to build up water behind the weir for the flow event.

At the time of the experiment, it was unknown if and when any peaks in SM and P transport would occur after opening the weir. Also no control can be exerted on the water flow once the weir was opened. Therefore, it was even more important to gather data in small time steps, improving the isolation of peaks from more average moments. Furthermore, the initial results from the first field day indicated the need for less water for the centrifuge and thus also less needed pumping time. In light of these considerations, the frequency of primary sampling cycle described in paragraph 3.3.1 was increased to one measurement round per 20 minutes. In the end eight full sampling cycles were completed.

3.4 Measurement techniques

3.4.1 Flow velocity

Flow velocities in the water column were measured using a programmable electromagnetic liquid velocity meter (hereafter referred to as P-EMS) and a Sensa RC2 electromagnetic flow meter (hereafter referred to as EMP). The P-EMS is an automated continuous measurement system, which was set to logging at a 5 second interval. Figure 3.3 shows how it measures the flow in the horizontal and vertical plane, perpendicular to each other. Not knowing the sideways displacement in the water column is acceptable as the dominant influence of the pumping station or weir on the flow velocity is expected to pull the water in a single direction. Sideways displacement is also dampened by the smooth profile of the streambeds and stream banks in the study area.

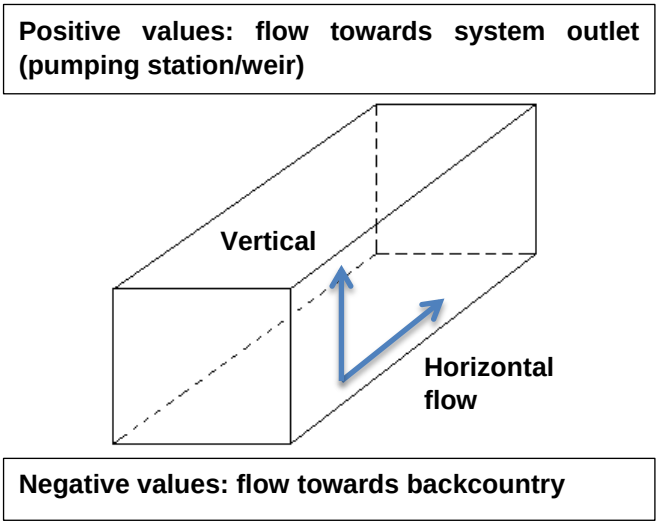

Figure 3.3 Schematic representation of flow directions for the P-EMS

The EMP was used without an automated continuous logging system, thus requiring manual notation, and measures the flow velocity as vector instead of a quadrant. This makes the EMP inferior to the P-EMS, particularly in cases where the flow velocity undergoes rapid change.

Only one P-EMS was available for the first sampling day, while there were two locations to be sampled. The choice was made to use the EMP at the SLT location, where the change in flow velocity was expected to be gradual as a result of the large distance from the pumping station.

This freed the P-EMS for the PLS location, where the close distance to the pumping station was sure going to create a very strong flow velocity gradient, something which was known from visual observation of a previous start-up of the pumping station.

3.4.2 Suspended matter

3.4.2.1 Centrifugation procedure

A single-speed continuous flow centrifuge was used to extract SM from the water phase. The water sample is inserted from the top through a funnel, directed at the centre of the column. Centrifugal forces then push the water out from the centre and up against the walls of the column. The walls of the column are covered with extractable teflon collection sheets which capture particles that they come into contact with. The more water is inside the column, the thicker the water layer against the wall and the quicker the water is able to overflow out of the column. Samples from the overflowing water were captured and stored to determine the weight of the remaining suspended particles, this data is available on request but not included in the report.

The SM scavenging efficiency of the centrifuge is dependent on the throughput rate of the water sample (influencing the residence time of water inside the centrifuge) and the particle size of the SM (influencing the ease by which particles can be entrained by the swirling water) (Ministerie van Verkeer en Waterstaat 1990). The influence of particle size is best described by the Law of Stokes. The variation in scavenging efficiency makes it important to select a throughput rate that forms a good balance between maximum extraction of the SM from the water phase and the required time. Although no official standards could be found, the assumption is that higher throughput rates will result in a lower total SM extraction yield per volume of water sample. This is confirmed by test runs. Test runs also found that the SM yield per unit of time is larger at higher throughput rates. Furthermore there is significant variability in the results for both yield per time and yield per volume, making it difficult to set a general rule for the extraction of the centrifuge. Therefore, it was chosen to maintain the centrifuge at maximum throughput, as defined by the maximum amount of water that the funnel would allow through. This gives the best chance for creating similar conditions between the centrifugation rounds and has shown to extract near-maximum SM from the water samples during test runs.

The contents of all sample tanks were continually mixed by stirring and shaking during the separated centrifugation rounds. Peristaltic pumps were used to transfer the water from the bottom of the tank into the funnel of the centrifuge. All the equipment, including the tubing and centrifugation column of the centrifuge, was cleaned with tap water and demi water between sessions.

Following centrifugation, the material on the teflon collection sheet was scraped off with a rubber wiper, removing roughly 90% of the material, and stored in plastic containers. Approximately 50 mL water would remain in the centrifuge column at all times after finishing a run, this fraction was collected separately for weight determination of the suspended matter. The SM samples obtained from the teflon sheets was freeze-fried at the earliest opportunity. Sample weights and water volumes were tracked throughout the entire procedure.

3.4.2.2 Filtration procedure

Filtration of the water samples from the 2 L glass bottles was performed in the laboratory, using 0.7 micron glass fibre filters (type: Whatman GF/F) and vacuum pumps. The untreated filters were laid down on top of a piece of aluminium foil in a labelled petri dish and covered with a (labelled) lid. The petri dish was then pre-weighted. After pre-weighing the filter was ready to be used for the filtration procedure. The amount of used filtrate per filter was tracked by using a measuring cup to fill the filtration devices and weighing the cup before and after adding filtrate. Once filled, filtration devices were always fully drained. Multiple (3-5) filtration samples were

obtained from each storage bottle, using 75-100% of the available water sample volume. In a few select cases, time restrictions and extremely long filtration times (requiring more than 45 minutes to process as little as 500 mL of water) made it impossible to use the entire sample bottle. A set of blanks (some untreated from the box, some flushed with ultrapure water) was included in every daily batch of filter samples in order to assess the weight loss effect of the filter substrate.

The used filter samples were oven-dried at 45 ºC for 48 hours on the day of filtering. After the drying the samples were set down to settle at room temperature, as tests showed that the weight of the filters changes significantly in the first 30-60 minutes after drying. This is most likely due to absorption of air moisture. The weight of the filters is considered to be sufficiently stable after one hour, the weight of randomly picked filters was measured a second time after about two for verification purposes. Filters were stored in an excitator once the second measuring round had confirmed that the observed weights indeed represented a stable state.

3.4.2.3 Determining suspended matter concentrations

In order to determine the suspended matter concentrations at the sampling site, the dry weight of the SM caught on the used filters samples is divided by the weight of the filtrate. The weight of filtrate is assumed to be translatable to volume, with a constant ratio of 1000 gram to 1 L.

The dry weight of the SM is calculated by taking the dry weight of the entire filter and subtracting the weight of the filter in its unused state. This value is corrected for the weight loss of the filter blanks, based on the average of all blanks in the experiment. The weight of the filtrate is determined by weighing and needs to calculation. The steps are combined in the equation below:

$$SM\ conc. = \frac{[dry\ weight\ used\ filter\ ] - [weight\ unused\ filter\ ] + [weight\ correction\ blanks]}{[filtrate\ weight]}$$

However, multiple filters are used per sample bottle. Therefore the volume-weighted average of all filters is calculated by dividing the *sum of the (corrected) weight of all SM material on all filters* by the *sum of the filtrate of all filters.* See also the equation below:

$$SM\ conc. = \frac{[SM\ conc.filter\ x_1] * [weight\ filtrate\ x_1] + [SM\ conc.filter\ x_2] * [weight\ filtrate\ ] + \ \ldots}{[weight\ filtrate\ x_1] + [weight\ filtrate\ x_2] + \ \ldots}$$

According to NEN-6600-2, filtration is the primary method for measuring SM concentrations in the Netherlands (Nederlands Normalisatie Instituut, 2009) and is therefore accepted as the official result for this study.

There is additional data available from the Malvern Mastersizer that is used to determine the particle size distribution and also provides particle concentration and obscuration measurements as side-products. The manual of the Mastersizer (Malvern Instruments Ltd, 2007) defines obscuration as "*a measure of how much sample is in the beam at any one time*" (p.108), expressed as a percentage of lost light intensity. Particle concentration is expressed in parts per million (ppm), independent from particle's weight and density (Malvern Instruments Ltd, 2007). Particle concentration and obscuration are used as indirect measures of SM concentration. Their main limitation is that the Mastersizer can only analyse a sample in suspension and as such it does not measure the SM fraction in terms of weight, like a scale would do. Providing a value with the unit in the shape of [weight]*[volume]$^{-1}$ is therefore not possible. Instead, the Mastersizer software uses calculations, based on assumptions of the dominant particle type (arbitrarily set by the user) and the measured laser diffraction. The fact that particle concentration and obscuration depend on calculations of the size and quantity of particles makes them useful indirect measures for validating the upward and downwards trends of SM concentration derived from the official

filtration method. The methodology for determining obscuration and particle concentration is the same as the methodology for the particle size distribution, described in the next paragraph.

3.4.2.4 Particle size distribution

The particle size distribution (PSD) of the suspended matter was measured using the Malvern Mastersizer 2000 particle size analyser, which is based on laser diffraction technology. 10-20 runs were performed for each sample, continuing till stability was reached. Some runs were arbitrarily excluded from the results if there were suspicions that air bubbles or macro size material distorted the signal. The PSD was calculated by taking the average of the accepted runs.

PSD samples were stored in the refrigerator at 4 ºC after collecting and analysed for the first time within 24 hours. The goal was to most accurately retain the field conditions of the samples, the samples were therefore left untreated. The expert judgement of the laboratory personnel was that there would not be significant change in the state of untreated samples as long as the 48 hour time window was not exceeded. The PSD of two samples was analysed a second time, after having been stored in a refrigerator for 10 days. This was done to check for the influence of time and storage on the stability of the distribution.

The classification of particle types (clay, silt, sand) in this study follows the standards set by NEN 5104, with one alteration: the increase of the size range of clays from <2 µm to <8 µm, based on Konert & Vandenberghe (1997) who proved experimentally that the clay particle size category of <2 µm is commonly misrepresented by the laser diffraction technique.

3.4.3 Water quality parameters

The pH and EC of filtered samples were determined in the field for PLS and STW. The pH and EC of SLT samples were measured in the lab due to a lack of field equipment. Alkalinity of filtered samples was measured in the lab using the titration method. Anion concentrations (Cl, NO_3, SO_4) of filtered samples were measured by ion chromatography (IC). Cation concentrations of filtered samples (Al, Ca, Fe, K, Mg, Mn, Na, Si) were determined by inductively coupled plasma atomic emission spectroscopy (ICP-AES). Dissolved organic carbon (DOC) was measured as non-purgeable organic carbon (NPOC) on a TOC analyser.

The P concentration of the filtered and unfiltered water samples was determined colorimetrically on an Auto-Analyzer for dissolved-P and total-P, respectively. The P content of the SM used in the SEDEX was determined through manual analysis of the extractants with the molybdenum-blue method, using ammonium heptamolybdate as reagent.

3.4.4 SEDEX procedure

The used SEDEX procedure is based on Ruttenberg (1992) and altered by Slomp et al. (1996). The complete protocol for the SEDEX can be found in appendix A. The SEDEX features the sequential extraction of the following five fractions, in the order they are mentioned:

1) Exchangable P (Exch-P). Extracted by $MgCl_2$.
2) Fe-bound P (Fe-P). Extracted by Citrate-Dithionite-Bicarbonate (CDB) and a $MgCl_2$ rinse afterwards.
3) Authigenic Ca-bound P (Authi & Ca-P). Extracted by acetate and a $MgCl_2$ rinse aftwards.
4) Detrital P (Detri-P). Extracted by HCl.
5) Organic P (Orga-P). Extracted by combustion (three hours at 550 ^{0}C in a muffle oven) and HCl.

The P concentrations of the five fractions were added up to yield a sum of extracted P. Although the assumption is that all P has been removed from the sample after the last step, it is not correct to refer to the sum of all fractions as particulate-P (PP). Standard PP data is collected by taking a whole water sample, analysing it as a single fraction, with and without filtration, and then applying the formula PP=TP-DP. The SEDEX procedure has many more analytical steps than standard PP measurements and with every step comes uncertainty. Because of this compounding uncertainty it was chosen not to define the sum of all extracted fractions as PP.

3.4.4.1 Selection SEDEX samples

Due to logistic limitations the capacity for the SEDEX procedure is less than 60 samples. However, the total amount of available unique samples exceeds the hundred, divided over different locations (PLS/SLT/STW), SM gathering techniques (filters/centrifuge) and points of time. Therefore it was necessary to select samples and duplicates based on the goal of the SEDEX and the preliminary results that became available before starting the SEDEX (i.e. SM content, flow velocities and PSD). This paragraph will from here on be restricted to presenting the general selection criteria. An overview of the individual selection is found in the appendix.

Note that duplicates are defined differently for filters and centrifuge samples due to the nature of the material. For filters “duplicates” means that the used filtrate originated from the same sampling bottle. Despite efforts to make sure that the water poured into the filter device is homogeneous over all sessions, the relationship between size, shape and movement rate makes it inevitable that different sizes of particulate matter respond differently to the transfer process. Therefore, the term “double” should be read with a certain reservation when it concerns the filters. For the centrifuge samples, the term “double” is more accurate. Centrifuge sessions yielded anywhere between 200 and 750 milligrams of dry weight SM. Since the original SEDEX only requires 100 milligram, doubles can be made by simply taking another 100 milligram from the same sample.

The most important goal of the study is to gain a complete overview of P speciation, with a high temporal resolution. Therefore a minimum of one SEDEX sample was used per available measurement point. To investigate the comparability of SEDEX results for the same sample, duplicates were used for some PLS and STW samples, but not for SLT. This decision was based on contemporary results that indicated that there was no significant trend in SM concentration and flow velocity at the SLT location. The PLS and STW samples selected for duplicates were those that resembled the beginning-end scenarios, rather than intermediate scenarios. This translated into samples from time periods with one pump active and two pumps active (for PLS) and the period directly after the opening of the weir and directly before closing the weir (for STW). Blanks were also included in the SEDEX, consisting of clean filters and empty reagent tubes, to test the influence of the filter material and the purity of the extraction reagents.

3.4.4.2 Execution of the SEDEX and accounting for uncertainties

The procedure of separating sample from extraction fluid by means of centrifugation and pouring inherently leaves behind some extraction fluid at every stage. This was corrected for by weighing the sample tubes before and after every addition and extraction step and using the weight differences to calculate the remaining extraction fluid. This also allows for correction of the obtained phosphate concentrations of the extraction fluid, where it is assumed that remainders of extraction fluids always mix perfectly with new additions. This assumption of perfect mixture is also applied to any and all cases of loss of material.

For the sake of calculation it is assumed that no particulate sample material (i.e. SM and/or filter substrate) is lost during the process of separation and transportation. To be entirely sure about any material losses would require the drying and weighing of the used filters and syringes before and after every single extraction step. However, this is an overly arduous task and logistically

unfeasible. It is very much questionable if it is even at all possible to completely dry the used 0.45 micron cartridge filters.

3.5 Data analysis

Primary data analysis was done by means of visual interpretation of graphs, for identifying trends. Scatter plots and basic linear regression statistics were employed to investigate relationships between parameters. More complicated statistical tests are deemed unreliable due to the low number of data points for most parameter (4-5 for PLS and SLT, 8 for STW).

Phosphorus speciation is the core element of this research. In order to gain a complete overview P speciation was assessed on three different levels, including an increasing number of measuring parameters:

%PP	P-fractions scaled to the total extracted P, representing the relative contribution of fractions (expressed in %). The %PP parameter is derived directly from the SEDEX.
P/SM ratio	P-fractions per unit of SM, representing the relative P content of the SM in the water column (expressed as mg/g). The P/SM ratio is derived directly from the SEDEX.
$PP_{WATER.SEDEX}$	P-fractions per volume of water, representing an approach of the in-situ field situation for PP concentration (expressed in mg/L). The $PP_{WATER.SEDEX}$ concentration is calculated by multiplying the P/SM content with the SM concentration derived from the filtration procedure.

4 Results

4.1 Sampling location 1: PLS

4.1.1 Field observations

The weather on the sampling day featured strong winds and minor precipitation. The influence of rain on the SM measurements is deemed negligible, given that the rain was not of sufficient quantity to cause overland flow and also that major rainfall events in the preceding week can be assumed to have flushed the drain pipes clean. Major input of particulate matter to the surface water is therefore unlikely.

4.1.2 Flow velocity

Figure 4.1 shows the recorded flow velocity as a vector. The four stages of the experiment, i.e. no pumping - one pump active - two pumps active - no pumping, are recognizable in points A,B,C and D, respectively. The vertical flow velocity component ranged between 0 and 0.05 m/s at all times and horizontal flow velocity ranged between -0.1 and 0.35 m/s.

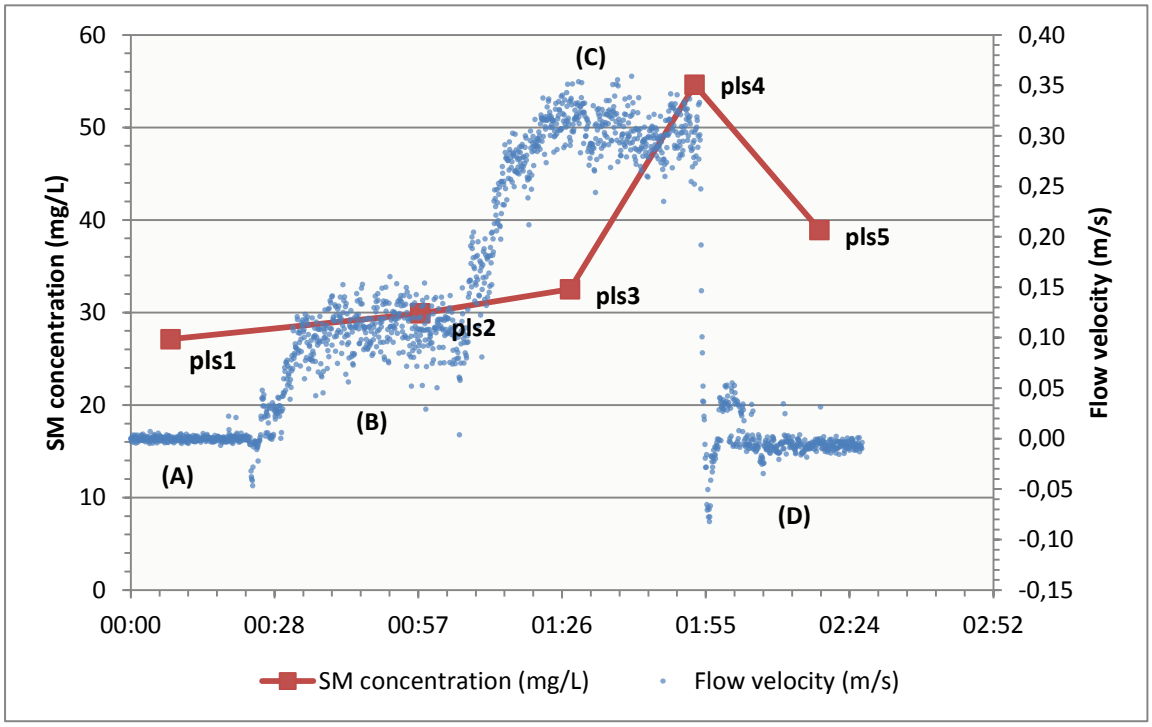

Figure 4.1 SM concentration and flow velocity at the PLS location (close to the pumping station) as a function of time.

The relatively small variation in vertical direction compared to the horizontal direction indicates that the water flowed towards the pumping station with little vertical mixing. The two negative spikes in the horizontal plane are most likely caused by waves rebounding from the pumping station as the suction of the pumps ceases and the flowing water is forced to a sudden stop. The phenomenon of rebounding waves has been observed in the field by water board personnel (pers. communication H. van Wolfswinkel, 2014). The cause of the first drop in suction is unknown, while the second drop is caused by deactivation of the pumps at the end of the experiment. The effect of a gradual decrease in pumping power upon deactivation, predicted by the water board personal, is unexpectedly absent from the results.

4.1.3 Suspended matter

4.1.3.1 Suspended matter - concentration

The results depicted in Figure 4.1 indicate that the SM concentration at PLS follows the absolute upwards and downwards trends of flow velocity. A clear peak is observed at pls4, coinciding with a period of maximum flow velocity. In pls3, however, the rise in flow velocity has not yet led to considerable increases in SM concentration. Overall the rate of change of the SM concentration varies significantly and is not always in proportion to the change in flow velocity.

Table 4.1 shows the change in SM concentration and flow velocity between measurement points. The most notable observation is that the stongest change in SM concentration *per second* occurs between two measurement points (pls3-4) with equal flow velocity, indicating a delay in the response of the SM concentration to increased flow velocities. When flow velocity declines to zero between pls4 and pl5, pls5 does not immidiately fall back to the level at the start of the experiment, indicating delayed or stretched out response to a decline in flow velocity as well. The low frequency of the sampling process and the lack of a gradual decrease of flow velocity makes it difficult to state if the fraction that was added to the SM pool between pls3-4 is equally resistant to decreasing flow velocities as it is to increasing flow velocities. For now it can only be concluded that SM as a whole responds strongly to decrease in flow velocities.

Table 4.1 Change per second in SM concentrations and flow velocity for various stages of the pumping cycle.

Section	Transition pumping stage	ΔSM conc. per second ($x10^{-2}$)	Δflow velocity per second ($x10^{-4}$)
pls1-pls2	Standstill => one pump active	0.10	0.8
pls2-pls3	One pump => two pumps active	0.14	1.7
pls3-pls4	Two pumps active (continued)	1.47	0
pls4-pls5	Two pumps active => standstill	1.04	-5.6

Validity of the measurements

Taking into account that the flow velocity has already reached maximum at the time of pls3 and remains stable between pls3-pls4, it was expected that pls3 and pls4 would had have similar SM concentrations. To assess the validity of pls3, the particle concentration and obscuration measurements of the particle size distribution analysis are plotted in Figure 4.2. The results of these indirect measures of SM concentration indicate a higher increase between pls2 and pls3 than the determination of SM concentration by filtration suggests.

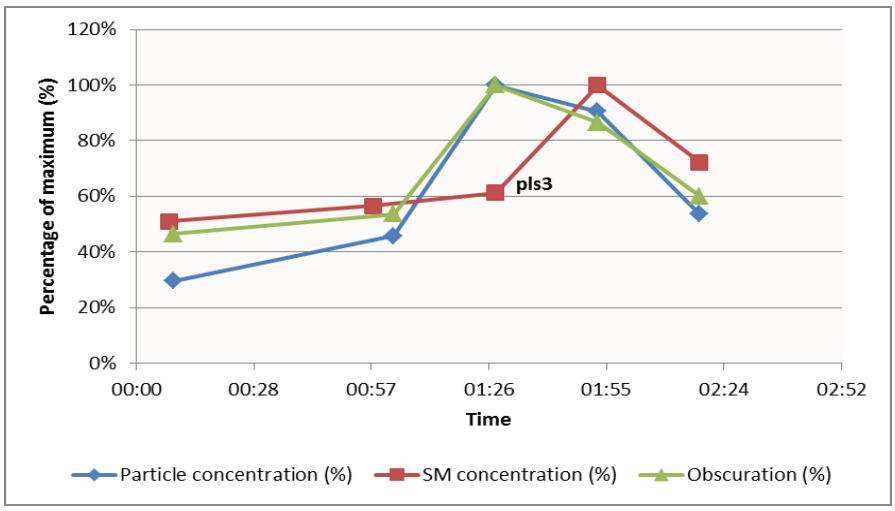

Figure 4.2 Comparison of the SM concentration, particle concentration and obscuration for samples from the PLS location (close to the pumping station), calculated as percentage of the parameter's maximum.

Even though obscuration and particle concentration are in conflict with the pls3 SM concentration measurement, outright dismissal is not an option. Table 4.2 shows that the standard deviation in the concentrations derived from the various filters that were used for pls3 is lower than for any other PLS measurement point. Furthermore, no irregularities were noted during sampling or analysis that point towards a polluted sample or erroneous measurement for pls3.

Table 4.2 SM concentrations for the Palenstein location (PLS), with (a) number of filters used to calculate the volume-weighted average,(b) volume-weighted average, (c) standard deviation of the volume-weighted average, (d) minimum concentration of used filters, (e) maximum concentration of used filters.

	Number of used filters	Average SM concentration	Std. deviation	Minimum	Maximum
	#	mg/L	mg/L	mg/L	mg/L
pls1	4	29.2	3.7	24.0	32.1
pls2	4	32.4	2.6	31.0	36.3
pls3	5	35.1	1.5	32.8	36.6
pls4	5	57.3	9.6	48.5	71.4
pls5	4	41.4	2.1	38.5	43.1

4.1.3.2 *Suspended matter - particle size distribution*

The particle size distribution (PSD) depicted by Figure 4.3 shows a clear change over time. Key features are a general shift towards larger particle sizes for pls1-4, made visible by the continuously increasing d(0.1), d(0.5) and d(0.9) values (see Table 4.3), and the development and subsequent decline of a secondary peak A (see Figure 4.3) in the sand size range between 170 and 850 micrometre. What is particularly notable about peak A is that it occurs even before the major rise in overall SM concentrations occurs and has almost entirely disappeared by the end of the flow event. Furthermore, there are the characteristics of pls5 to consider, which features stagnant water along with the second-highest SM concentration levels, but even less large particles in the 120-850 micrometre peak area than the starting situation, pls1. Together these findings indicate that the larger size-fractions of SM are more vulnerable to changes in flow velocity than the overall concentration and that major changes in the PSD can occur simultaneously with limited changes in SM concentration.

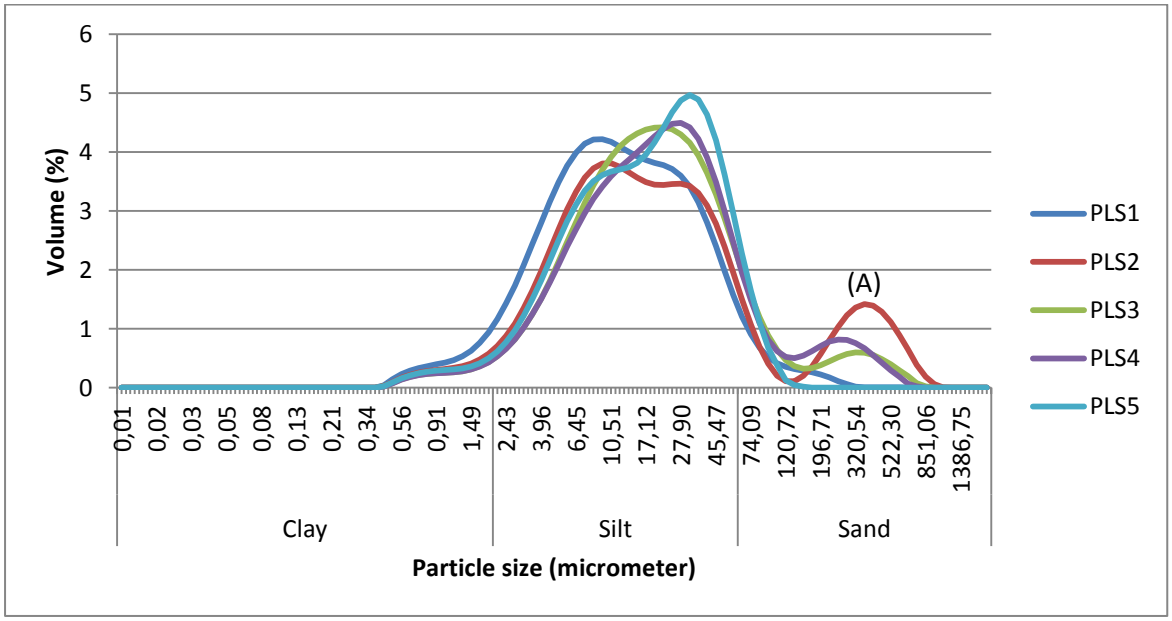

Figure 4.3 Particle size distribution for the PLS location. Point (A) marks the secondary peak

The PSD results also indicate that stock depletion and/or particle disaggregation could be a factor at PLS. This is deemed the most viable explanation for the observation that the largest particles under peak A (see Figure 4.3) of pls2 are gone by the time of pls3, even though flow velocity has increased between these points. Sedimentation of the particles between pls2 and pl3 is unlikely during times of increasing flow velocities.

Table 4.3 Characteristics (d(0.1), d(0.5) and d(0.9) of the particle size distribution for the PLS location. The d-percentiles are volume-based. The measuring points match those of Figure 4.3.

	Time sample taken (hh:mm)	**d(0.1) (µm)**	**d(0.5) (µm)**	**d(0.9) (µm)**
pls1	00:09	2.8	11.1	43.6
pls2	01:03	3.6	15.8	248.2
pls3	01:28	4.3	17.5	70.9
pls4	01:53	4.5	19.6	76.5
pls5	02:18	3.9	17.0	50.0

4.1.4 Chemical properties of the water column

Table 4.4 on the next page shows the results of the water quality analysis. The general water quality parameters pH, ECE and alkalinity were relatively stable throughout the experiment, remaining between 90% and 100% of their maximum value. This is also the variation range for the DOC and anions, with the exception of Cl (which has an 80%-100% range). Cations are also stable within a 90%-100% range, with the exception of Fe and Na (80%-100%). The similarity in the pattern of Na and Cl indicates that the concentration changes for these compounds are a result of varying freshwater contribution, containing less dissolved NaCl salts than the saline groundwater. Table 4.4 also shows that DP has extremely low values (0.01-0.03 mg/L) compared to TP (0.24-0.48 mg/L) indicating the dominance of PP in the system.

Overall, the measurements of the water quality parameters are sufficiently stable to assume that the composition of dissolved compounds will be similar throughout the flow event.

Table 4.4 Water quality parameters (pH, alkalinity, EC, anions, cations, DOC, DP and TP) for the Palenstein (PLS) location. TP data was provided as background to DP data, more TP measurement points are available.

		PLS1	PLS2	PLS3	PLS4	PLS5
Sampling time	hh:mm	00:09	01:03	01:28	01:53	02:18
pH	[-]	7.23	7.26	7.28	7.26	7.45
Alkalinity	mg/L	481	485	480	501	488
EC	mS/m	2.09	2.07	2.13	2.12	2.06
Cl	mg/L	341	347	377	306	315
NH_4	mg/L	2.9	2.8	3.0	3.0	3.1
NO_3	mg/L	6.4	6.7	6.8	6.3	6.5
SO_4	mg/L	193	199	193	205	208
DOC	mg/L	14.7	13.8	13.5	14.1	14.3
DP	mg/L	0.02	0.02	0.01	0.02	0.01
TP	mg/L	0.24	0.27	0.48	0.45	0.31
Al	mg/L	< 0.07*	< 0.07*	< 0.07*	< 0.07*	< 0.08*
Ca	mg/L	219	219	223	222	225
Fe	mg/L	0.19	0.22	0.20	0.20	0.20
K	mg/L	12.8	12.8	13.3	12.8	13.1
Mg	mg/L	35.5	35.7	37.9	34.8	35.9
Mn	mg/L	0.70	0.71	0.73	0.76	0.77
Na	mg/L	173	172	191	161	168
Si	mg/L	10.0	10.0	10.0	10.2	10.4

* Value was lower than the calibration limit for the analysis equipment.

4.1.5 Phosphorus analysis

4.1.5.1 Relative contribution of P fractions

The results of the SEDEX regarding the relative contribution of P fractions are displayed in Figure 4.4 and Table 8.1 (of appendix E). As there are no shifts larger than 5% in any fraction of either filter or centrifuge samples, the relative P contribution is considered stable throughout the entire flow event. Fe-P is the dominant fraction at all times, ranging from 79% to 83% for filter samples and from 87% to 89% for centrifuge samples. Orga-P is the most significant of the remaining fractions, contributing 12-13% and 9% for filter and centrifuge samples, respectively.

The Authi & Ca-P fraction shows the most notable differences between centrifuge and filter. The contribution of this fraction is significantly larger for the filter samples (5-6%) than for the centrifuge samples (<0.5%).

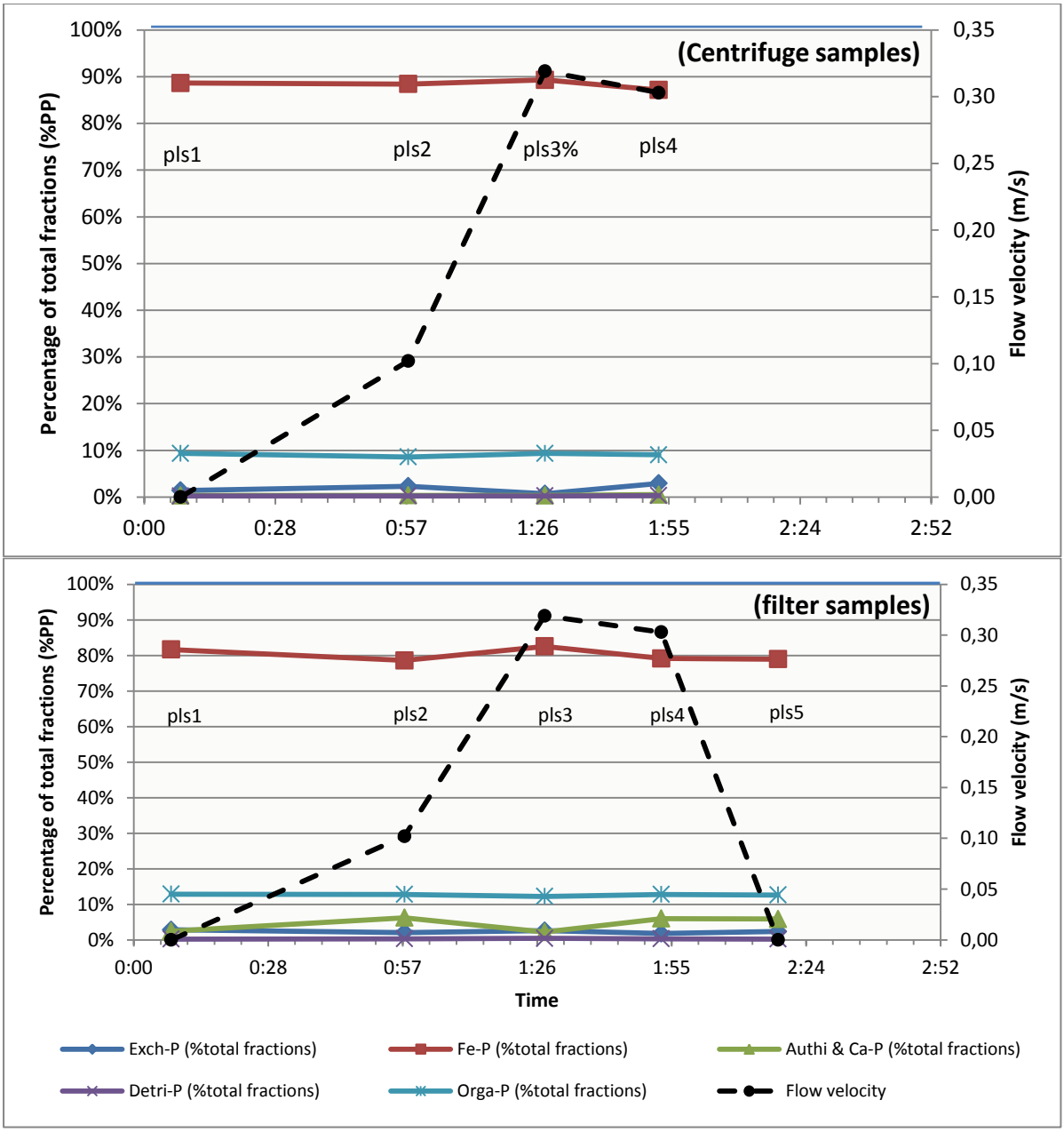

Figure 4.4 Relative P contribution of the different fractions (%PP) for the location close to the pumping station (PLS).

4.1.5.2 *P content of suspended matter*

The results for the P/SM ratio, depicted in Figure 4.5 and Table 8.2 (of appendix E), indicate that there is a notable variations over time and between sample types. The total of all fractions varies between 8.4-9.3 mg/g and 8.3-6.8 mg/g for filter and centrifuge samples, respectively. The increase/decrease pattern of both sample types is similar, even though the centrifuge samples have a relatively lower P/SM ratio and feature stronger fluctuations.

The change in P/SM ratio does not correlate linearly to the change in flow velocity; the development between 0:00 and 1:26 in Figure 4.5 shows that the trend of P/SM can switch independently between positive and negative direction, also if the trend of flow velocity maintains the same direction.

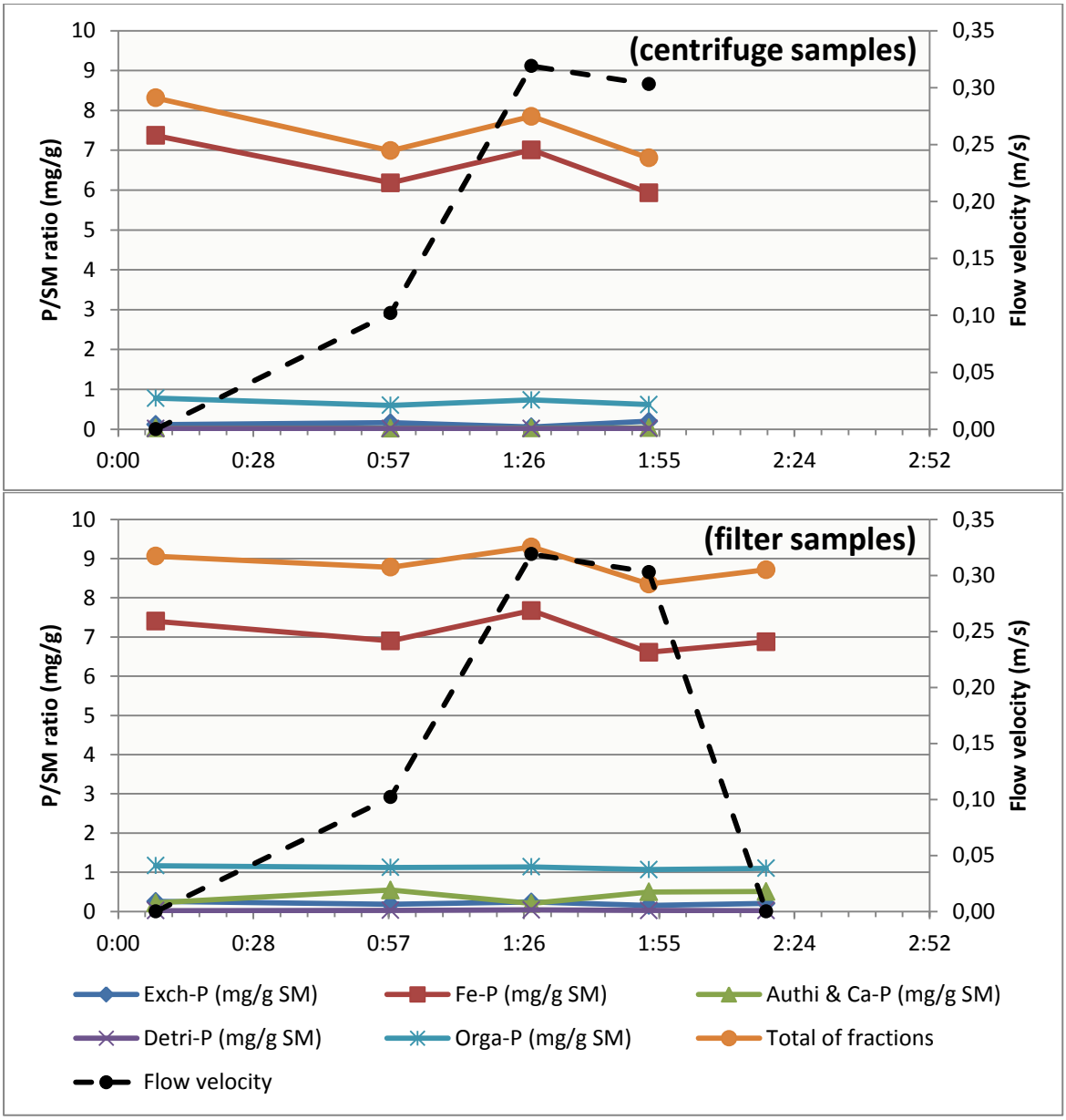

Figure 4.5 P/SM ratio (in mg/g) for the location close to the weir (PLS)

4.1.5.3 P content of the water column

The results for the concentration of P fractions in the water column ($PP_{WATER.SEDEX}$) are depicted by Figure 4.6 and Table 8.3 (in appendix E). The trend of the total $PP_{WATER.SEDEX}$ is similar for both centrifuge and filter samples. Filter samples follow the trend of SM concentration slightly closer than centrifuge samples. The closer match is due to the relatively low P/SM ratio of the centrifuge samples pls2 and pls4. Point pls2 also features the only occurrence where the trend of the total $PP_{WATER.SEDEX}$ was decided by the P/SM ratio, in all other cases the SM concentration was the deciding factor in the equation. The total of all fractions continues to rise from pls1 till pls4, maxing out at 0.39 mg/L for centrifuge samples and 0.48 mg/L for the filter samples. The pls5 (filter) indicates that the P content of the water column goes down after pls4, which coincides with a drop in SM concentration and flow velocity.

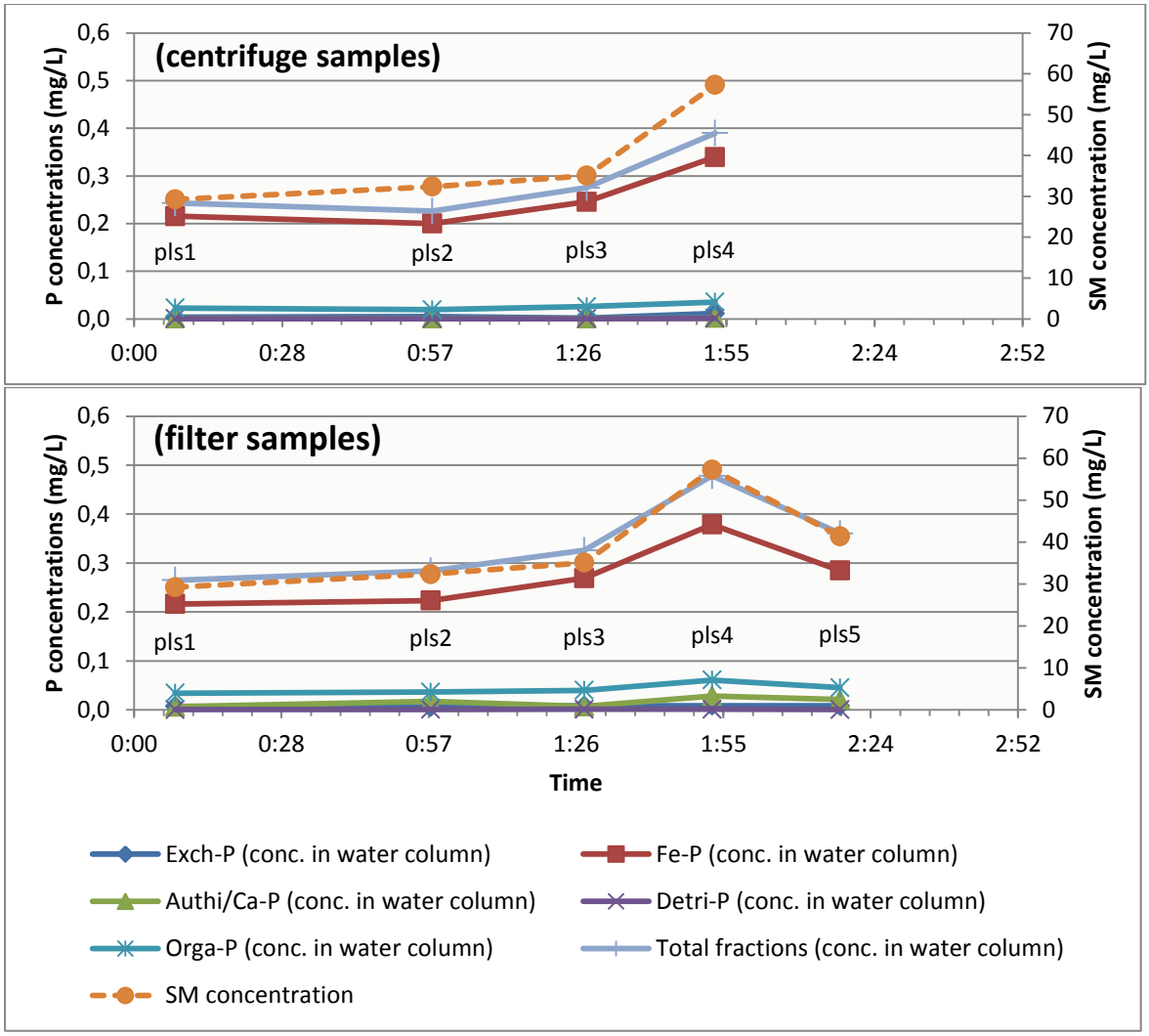

Figure 4.6 $PP_{WATER.SEDEX}$ (mg/L) and SM concentration for the PLS location.

In addition to the $PP_{WATER.SEDEX}$ calculations (i.e. multiplying the P/SM ratio with SM concentration), PP concentrations in the water column were also determined by direct TP and DP measurement (calculated into PP) of separately collected samples. The result for each method is depicted in Figure 4.7, which shows that the differences between PP concentration and the $PP_{WATER.SEDEX}$ are relatively small, except for the peak in PP at point A. The PP concentrations generally fall between the total of all SEDEX fractions for centrifuge and filters samples; the centrifuge samples seem to be underestimating the P concentrations compared to PP, while the filters overestimate compared to PP. The similar range of PP and SEDEX indicates that the SEDEX protocol has been successful. The deviation in peak A is most likely a result of an erroneous SM concentration measurement for pls3.

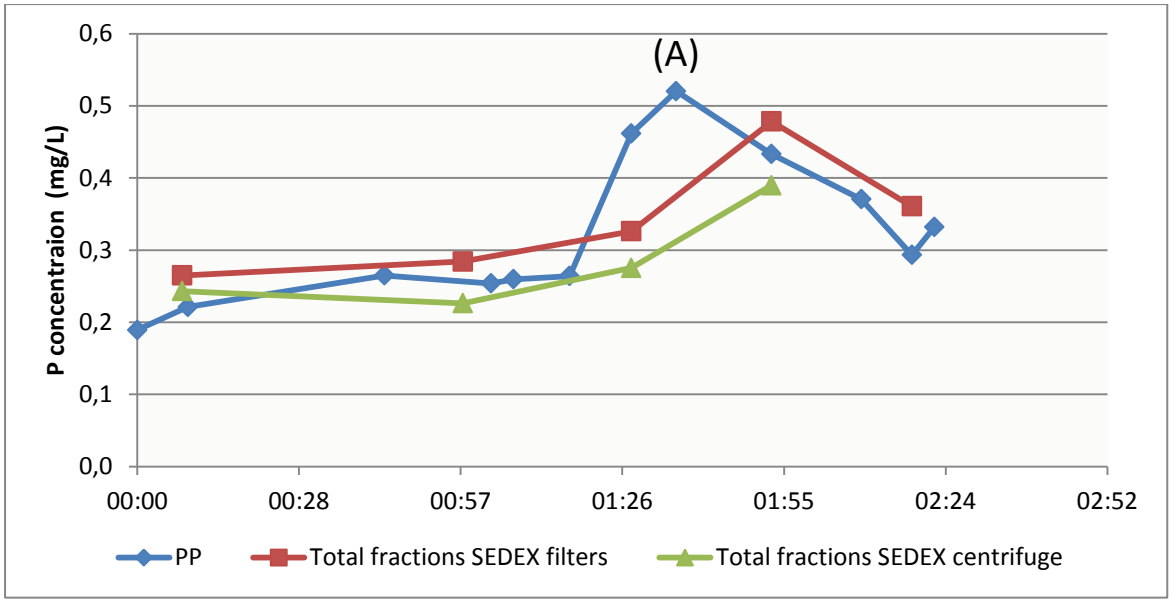

Figure 4.7 Comparison of different methods for assessing P concentration in the water column of the PLS location.

4.1.6 Comparison between multiple sampling days

The overview of the SEDEX results for different sampling days is shown by Figure 4.8 and Figure 4.9 (next page). The P/SM ratio is considered stable between sampling days, as all results for the plsx and plsy series fall within the range of the main series (pls1-5).

The concentrations of the different P fractions in the water column are similar between plsy and the main series. The result for plsx1 deviates, falling about 20% below the main series' minimum value.

The overall result indicates that the SEDEX results for the different sample days were within range of each other, but that there is still noticeable temporal variation.

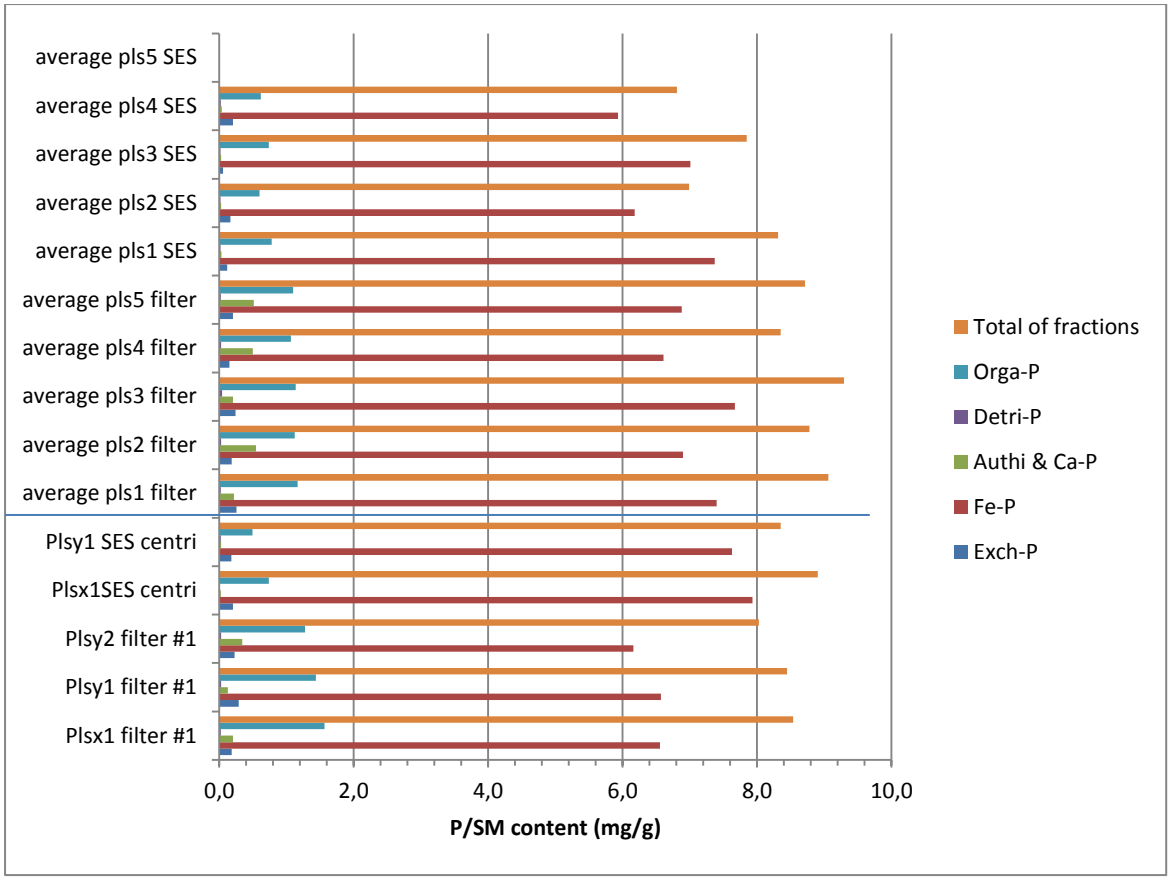

Figure 4.8 P/SM ratio on different sample days (pls versus plsy and plsx).

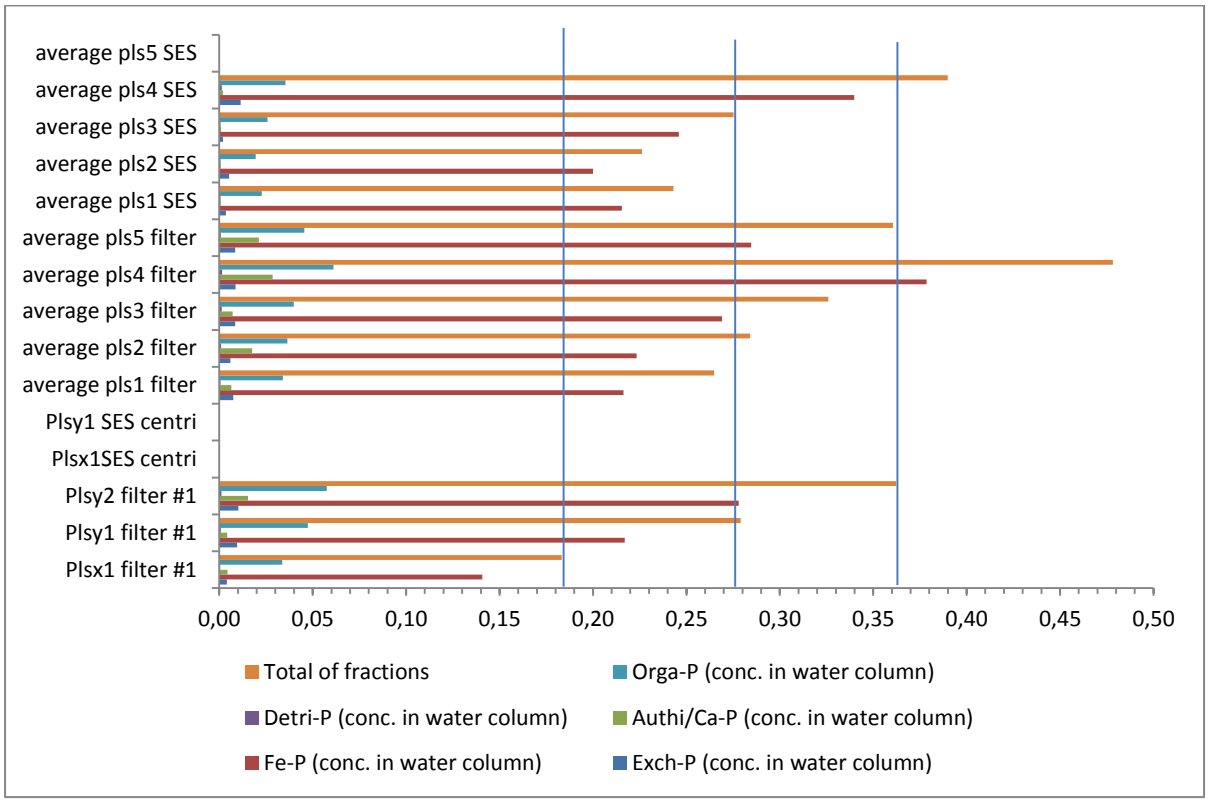

Figure 4.9 Overview of the concentration of P fractions in the water column on different sample days (pls series versus plsy and plsx). The vertical blue lines indicate the isotherms for the total of all fractions.

4.1.7 Summary of results

The experimental set-up of creating a flow event with a strong influence on SM succeeded: the results have clearly shown that flow velocity is the primary driver of change in SM concentration. The pumping regime was very visible in the pattern of flow velocities. The water quality parameters behaved relatively stable throughout the experiment, indicating that the water type remained the same.

The particle size distribution of the SM changed significantly; from a composition of mainly small size particles, to larger particles and finally back to mainly small particles. The results indicate that particle size distributions respond more rapidly to changing (flow) conditions than the SM concentration. However, the evidence for the expected (negative) correlation of a higher size range with P/SM ratio was not found to be sufficiently strong to make definitive claims regarding the influence of particle size distribution.

Subtracting DP from TP data showed that approximately 91-98% of the TP was made up from PP. PP concentrations ranged from 0.19 to 0.52 mg/L. Minor deviations were noted between the PP data obtained by the TP-DP method and the total $PP_{WATER.SEDEX}$ obtained from multiplying P/SM ratio and SM concentration. The only significant deviation occurred in measurement point pls3, which featured a much higher PP than is warranted by the PP/SM concentration ratio of the other measurement points. Application of obscuration and particle concentration as indirect SM concentration estimation methods indicates that the SM concentration is indeed higher than the official filtration method suggests.

The contribution of the different P fractions is stable throughout the experiment and largely unaffected by flow velocity and/or the particle size distribution of SM. Fe-P (78-89%) and Orga-P (9-13%) dominate the relative contribution of the fractions. Although the relative contribution was stable, the P/SM ratio did vary through time (6.8-8.3 mg/g). Its influence on the eventual P concentrations in the water column is limited however, as the change of SM concentration had a far stronger relationship with the change of the P-fraction concentrations in the water column.

4.2 Sampling location 2: SLT

4.2.1 Field observations

The field work at the SLT location was performed under the same conditions as PLS, i.e. rainy and windy weather. However, the wind in particular seemed to have much more effect at SLT. During the sampling it was observed that the flow at the water surface was directed away from the pumping station, while the velocity meter (approximately 20 centimetres below the water surface) was still indicating a flow towards the pumping station. It is unknown to what extent the oppositional surface flow affected the sub-surface flow. Also, miscommunication between the two teams performing the measurements on the first field day led to a one-hour gap in the measurements, during which no samples were taken.

4.2.2 Flow velocity

Figure 4.10 shows the development of the flow velocity. The four stages of the experiment (no pumping- one pump active – 2 pumps active - no pumping) are less apparent than they were at PLS. Regular observation of the manual velocity meter did however indicate two stable levels in the ranges 0.07-0.08 m/s and 0.10-0.12 m/s. The assumption is that these levels represent pumping with respectively one and two pumps. At the end of the field experiment there still was no sign of a drop in flow velocity. The total variation in flow velocity is also relatively mild compared to PLS. These findings indicate that the response of the flow in the ditch to pumping by the pumping station is not only dampened, but also elongated. This concept is supported by water level measurements from the water board, depicted by Figure 4.11, which indicates that the downward trend at the SLT location continues for a significantly longer time than at PLS.

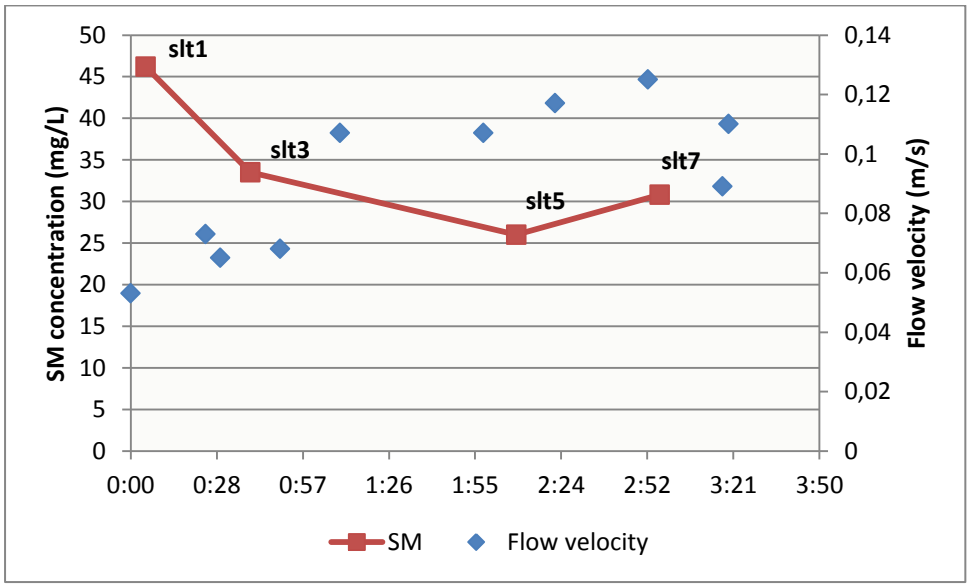

Figure 4.10 Flow velocity and SM concentration for the ditch location (SLT).

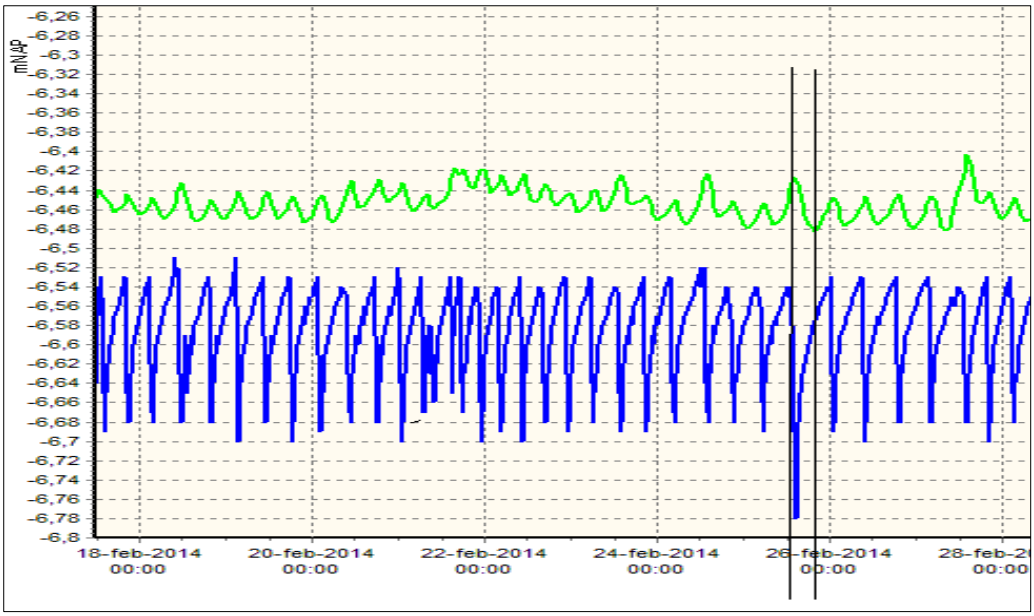

Figure 4.11 Water levels at the Palenstein pumping station (blue) and Bentweg (green), which are comparable to respectively PLS and SLT. Picture sourced from Hoogheemraadschap Rijnland.

4.2.3 Suspended matter

4.2.3.1 Suspended matter - concentration

Figure 4.11 shows that the concentration of SM is at its maximum at the start of the experiment, after which it declines towards a relatively stable level. There seems to be no significant link between flow velocity and SM for the SLT location.

The spread in the separate filter samples used to calculate the average SM concentration is shown by Table 4.5. The minimum and maximum values follow the same trend as the average and the standard deviation is within 15% of the volume-weighted average. These differences are all within acceptable ranges.

Table 4.5 SM concentrations for SLT, with (a) number of filters used to calculate the volume-weighted average, (b) volume-weighted average, (c), minimum value (d) maximum value, (e) standard deviation of the volume-weighted average.

MP	# used filters	Average	Minimum	Maximum	Std. deviation
	[-]	mg/L	mg/L	mg/L	mg/L
slt1	5	49,2	48,6	50,0	0,5
slt3	5	36,4	28,4	41,1	5,1
slt5	3	28,6	24,4	34.0	4,0
slt7	3	33,4	29,3	36,5	3,0

For added certainty, the obscuration and particle concentration patterns are compared to the SM concentration. As shown by Figure 4.12, there is a chance that the first measurement point is somewhat overestimated or that the other three are underestimated.

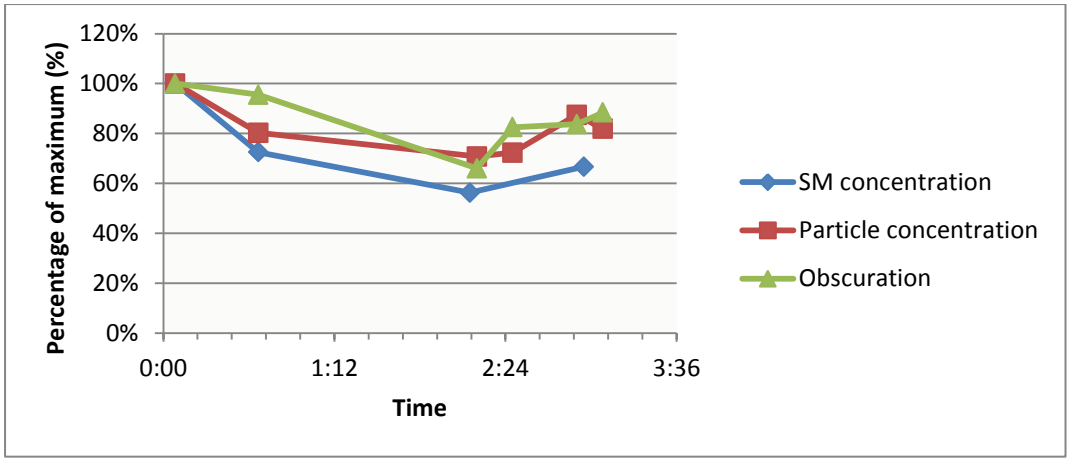

Figure 4.12 Comparison of the SM concentration, particle concentration and obscuration for samples from the ditch location (SLT), calculated as percentage of the parameter's maximum.

4.2.3.2 *Suspended matter - particle size distribution*

Figure 4.13 shows the progression of the particle size distribution from a distribution with a single peak in the clay and silt categories (peak A) to an almost bimodal distribution. The secondary peak B is in the sand size category, which is quite unexpected given the relatively low flow velocities at SLT.

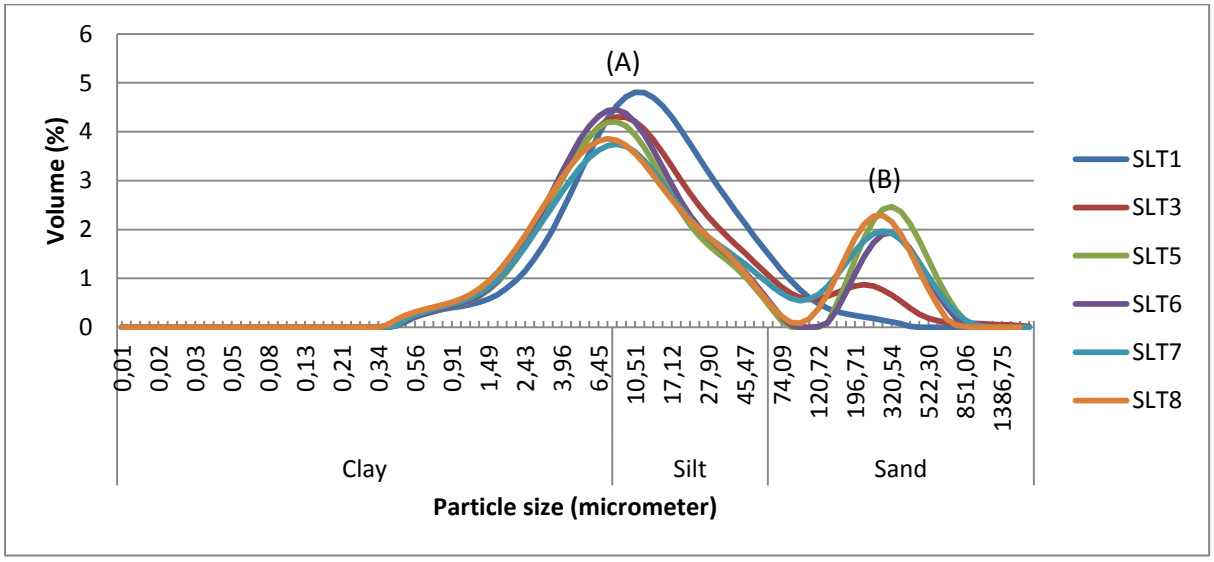

Figure 4.13 Particle size distribution for the ditch location (SLT). The main peaks are marked (A) and (B)

One of the more notable features of Table 4.6 is that when flow velocity goes up, there is a simultaneous decrease in the d(0.1) and increase in d(0.9) values. This indicates that relatively more of the tiniest and the heaviest of particles were picked up at higher flow velocities.

Table 4.6 Characteristics for the ditch location (SLT). The d-percentiles are volume-based

	Sampling time (hh:mm)	d(0.1) (µm)	d(0.5) (µm)	d(0.9) (µm)
slt1	00:05	3.1	11.5	47.8
slt3	00:40	2.4	9.7	88.3
slt5	02:12	2.6	10.4	315.6
slt6	02:27	2.5	9.6	261.4
slt7	02:54	2.8	13.5	391.9
slt8	03:05	2.6	11.9	292.4

4.2.4 Chemical properties of the water column

Table 4.7 shows that that there is very little variation in the general water quality parameters pH, alkalinity, both parameters staying within the same 90-100% of maximum as PLS. The Cl and NO_3 concentrations are somewhat variable within an 80-100% boundary of their maximum value. Cations concentrations also fall within a 90-100% boundary of their maximum value. The DP concentration (0.04-0.06 mg/L) is somewhat higher than measured at PLS (0.01-0.03 mg/L). It is unknown why DP is relatively more abundant; however, PP is still the dominant component of TP.

Overall, the measurements of the water quality parameters are sufficiently stable to assume that the aquatic reaction chemistry of the water is similar throughout the flow event.

Table 4.7 Water quality parameters (pH, alkalinity, EC, cations and anions) for the ditch location (SLT). TP data was provided as background to DP data; more TP measurement points are available than shown.

		slt1	slt3	slt5	slt7	slt8
Time	hh:mm	00:05	00:40	02:12	02:27	02:54
pH	[-]	7,55	7,6	7,52	7,41	7,23
Alkalinity	mg/l	576	571	583	586	592
Cl	mg/l	252	244	238	267	280
DOC	mg/l	20,2	19,6	20	19,7	20,1
NH_4	mg/l	3,42	3,42	3,42	3,42	3,42
NO_3	mg/l	7,4	7,7	6,5	6,8	7
DP	mg/l	0,04	0,05	0,06	0,06	0,06
TP	mg/l	0,42	0.39	0,36	-**	0,37
SO_4	mg/l	202	203	196	198	195
Al	mg/L	< 0.07*	< 0.07*	< 0.06*	< 0.06*	< 0.07*
Ca	mg/L	213	215	206	211	217
Fe	mg/L	0,2	0,2	0,2	0,2	0,2
K	mg/L	14,26	14,13	14,41	14,57	14,83
Mg	mg/L	34,4	34,6	34,2	35,5	36,5
Mn	mg/L	0,99	1,03	0,98	0,98	0,99
Na	mg/L	159	159	158	168	175
Si	mg/L	11,5	11,7	11,6	11,5	11,5

* Value was below the calibration range of the equipment.

** Missing data point.

4.2.5 Phosphorus analysis

4.2.5.1 Relative contribution of P fractions

The results for the relative contribution of P fractions are displayed in Figure 4.14 and Table 8.4 (in appendix E). No P fraction for centrifuge or filter samples shifts by more than 5% throughout the entire flow event, therefore, the contribution from the different fractions to the total extracted P is considered to be stable. There are some minor changes below the 5% threshold, primarily the decrease of Authi & Ca-P (from 5% to 2%), and simultaneous increase of Fe-P (from 80% to 84%) in the filter samples. For the centrifuge samples the changes in relative contribution are even smaller, with an increase of Exch-P (from 1% to 2%), primarily at the cost of Fe-P (decrease from 93% to 91%). Compared to the filters, the centrifuge samples contain relatively

less of every fraction but Fe-P. This results in an extreme Fe-P dominance for the centrifuge samples (over 90% of the total). For filters, the Fe-P fraction is also dominant, but slightly less so (over 80% of the total).

Although both centrifuge and filter samples share the same stability and Fe-P dominance, there are also notable differences. Most importantly, the Authi & Ca-P fraction is almost completely absent in centrifuge samples (<1%), just as it was for the PLS location. The contribution of Exch-P is also higher for filter samples than for centrifuge samples, although the difference is less than for Authi & Ca-P.

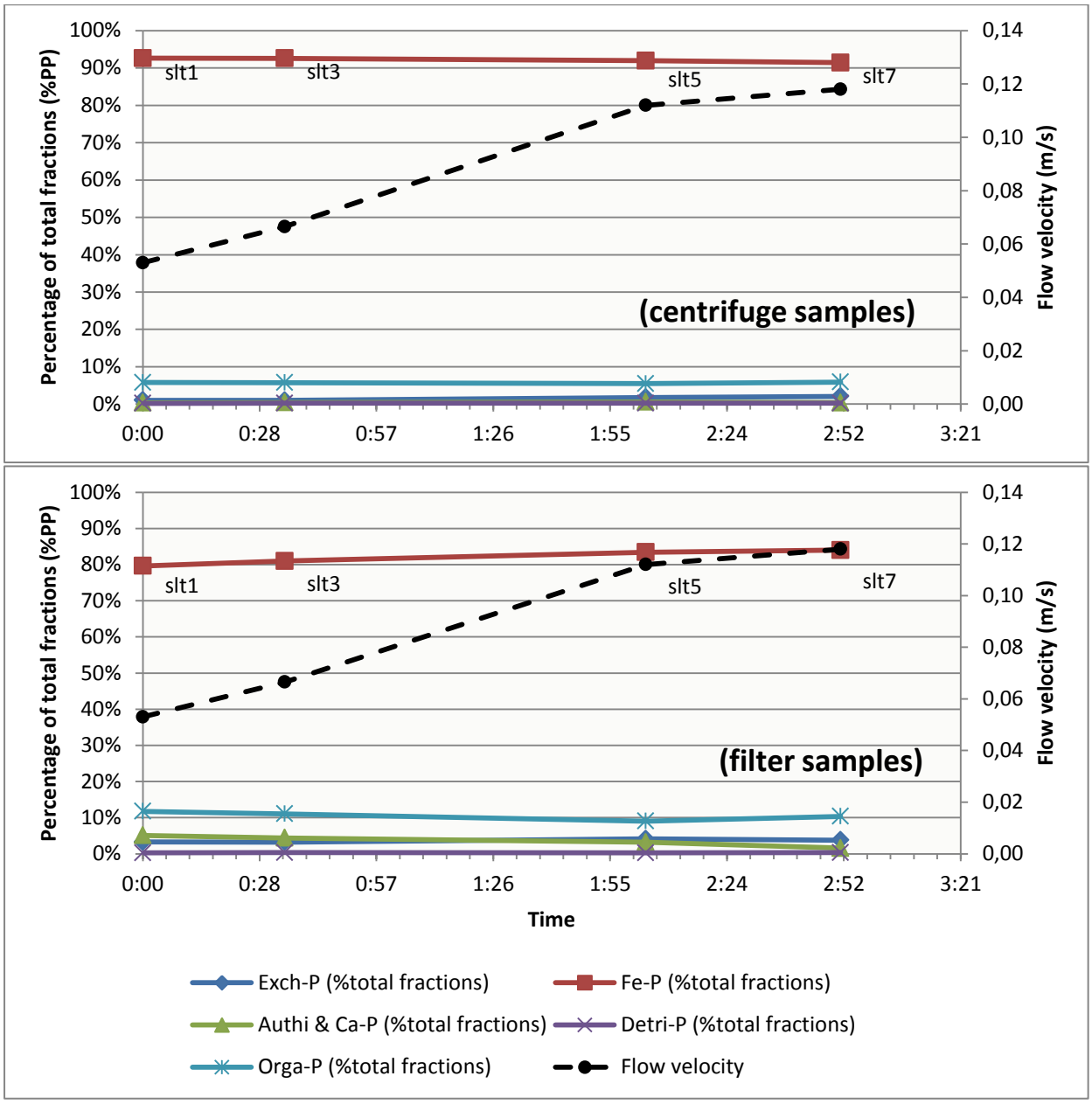

Figure 4.14 Relative P contribution of the different fractions for the ditch location (SLT).

4.2.5.2 *P content of suspended matter*

Figure 4.15 and Table 8.5 (in appendix E) show the P/SM content for SLT. The overall pattern is deemed quite stable, with a maximum variation of 10% for both filter and centrifuge samples. The total P/SM is generally slightly higher for the filter samples, up to a 0.9 mg/g (10%) difference at the end. Unlike at PLS, however, changes in the total of all fractions are not only caused by Fe-

P. For slt3, slt5 and slt7 the sum of the changes in the Exch-P, Authi-P & Ca-P and Orga-P fractions is greater than the change in Fe-P. The relatively low amounts of Exch-P and Authi-P & Ca-P in centrifuge samples reflect the results for PLS.

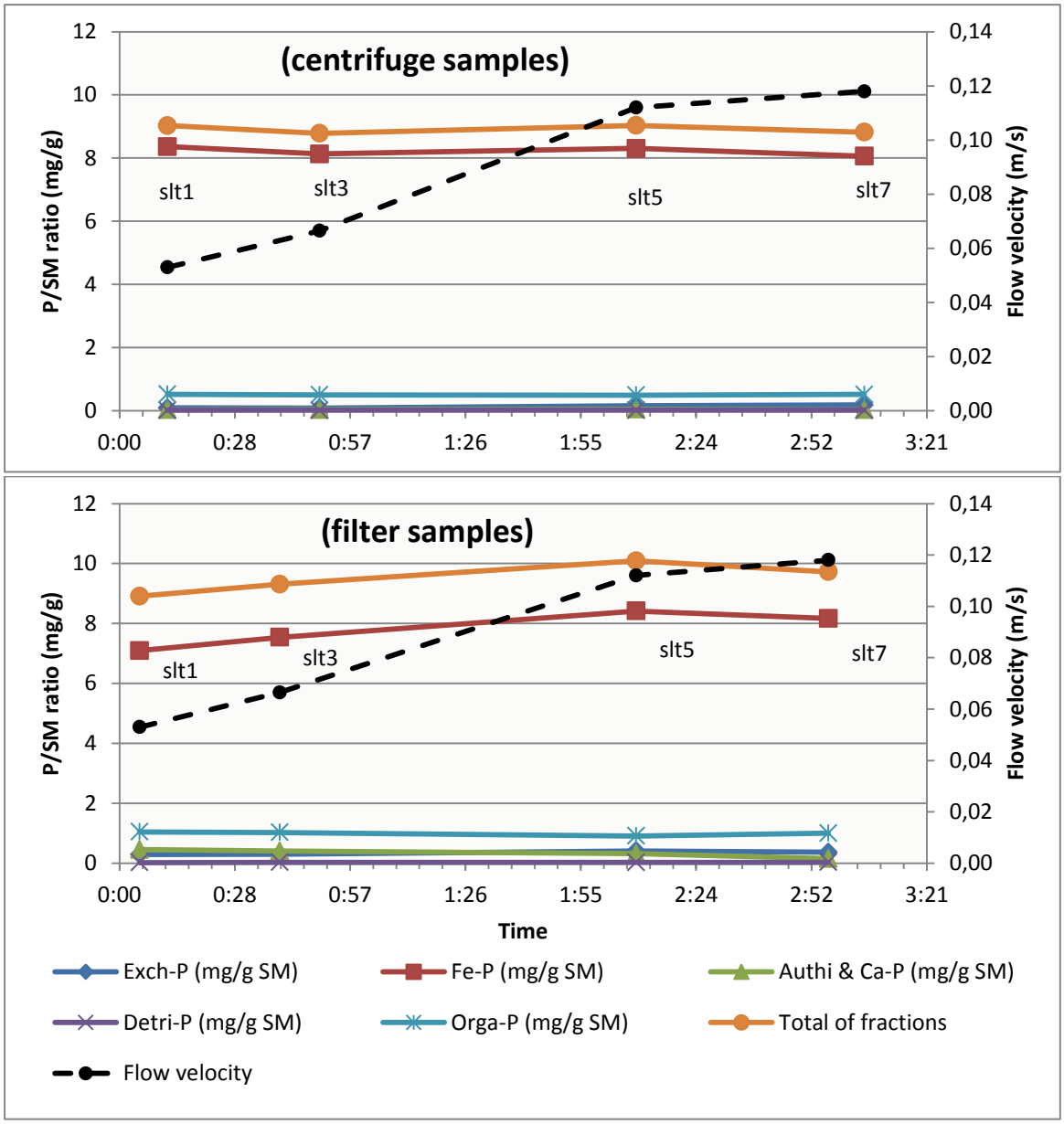

Figure 4.15 P/SM ratio (in mg/g) for the ditch location (SLT).

4.2.5.3 *P content of the water column*

The results for the $PP_{WATER.SEDEX}$ are shown in Figure 4.16 and Table 8.6 (in appendix E). The P concentration decreases for the first three measurement points, picking up slightly at the end of the experiment. There is little difference between the sum of all fractions for the centrifuge and filter samples (maximum deviation: 0.03 mg/L on a total of 0.26-0.44 mg/L). This is to be expected, given the stability of the P/SM content.

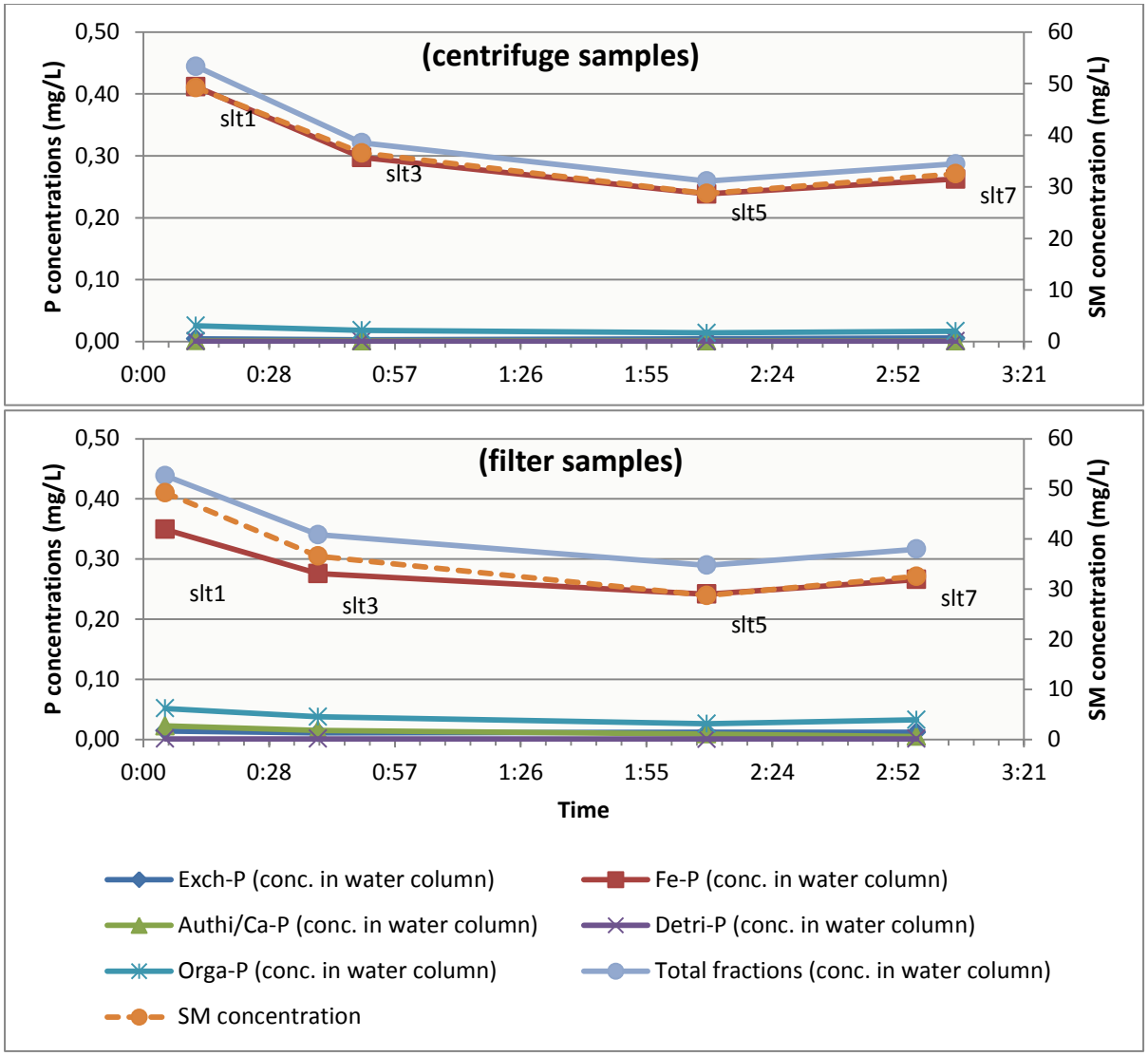

Figure 4.16 $PP_{WATER.SEDEX}$ for the ditch location (SLT).

Comparing the results of the SEDEX to the direct PP measurements (see Figure 4.17) shows that both methods yielded similar values. PP values ranged from 0.24 to 0.38 mg/L, SEDEX filter results are equal or slightly above that range, while centrifuge samples remained below for three of four measurement points. Only for the first measurement points at the very start of the experiment (see point A) did the SEDEX of both sample types seemingly overestimate the P concentrations by 0.7 mg/L, but the difference is already decreased for the next PP measurement point. Earlier in the report it was shown that the SM concentration that was used to calculate point A is most likely overestimated. The overall SEDEX result is thus accepted as trustworthy.

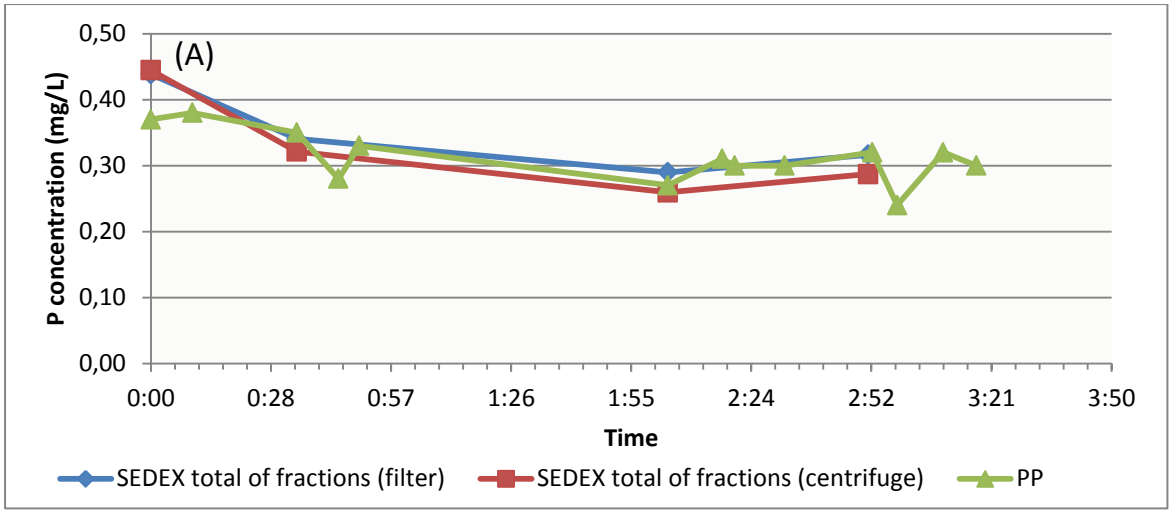

Figure 4.17 Comparison of different methods for measuring P concentrations in the water column for SLT. (A) marks the most deviant set of SEDEX measurement points.

4.2.6 Summary of results

The SLT location was sampled simultaneously with the PLS location. The pull effect of the pumping station was observed at both locations, although flow velocities at SLT were of significantly smaller magnitude. The maximum velocity was 0.12 m/s, which is more than 50% lower than at PLS. Flow velocity did not seem to have any influence on either SM or P concentration at this location. The particle size distribution was the only affected parameter, showing the presence of an increasing volume of larger particles as the flow velocity increased. In contrary to expectations this did not coincide with elevated SM concentrations. SM concentrations initially seemed to decrease through time, but the obscuration, particle concentration and PP parameters all indicated that the first measurement point is overestimating SM concentrations and that the decrease is in fact more neutral.

The results of the SEDEX indicate that the relative contribution of P fractions and the P/SM ratio are all stable parameters. Fe-P was the largest P fraction, especially for the centrifuge samples (91-93%), but also for filters (79-84%). The PP concentration in the water column varied with the SM concentration and was not found to be related to any other parameters. Furthermore, the PP measurements formed a good match to $PP_{WATER.SEDEX}$, confirming the validity of the SEDEX results.

4.3 Sampling location 3: STW

4.3.1 Field observations

The sampling at the STW location was done on a day of good weather. There was no rain and hardly any wind, the preceding days were also clear of precipitation. The site was inspected upon arrival. The first thing that stood out was the layer of organic material on the water surface in front of the weir. The reddish-brown colour and oily sheen indicated the presence of iron oxidizing and/or sulphur bacteria. Water was already flowing over the weir from the moment of arrival, but the floating organic material stuck together and was trapped behind the weir.

Photo 4.1 Pictures of the set-up of the STW location and the floating organic matter.

4.3.2 Flow velocity

The sudden increase and consequent smooth decline of the flow velocities for STW are evident in Figure 4.18. Technical problems with the automated logging system led to partly missing data for the first 45 minutes of the field work, only five manual notations were available for that time period. This data loss was compensated for by closing the weir at the end of the experiment, visible by the sudden drop in flow speed at point (A), and letting the water build up before opening it again. The results indicate that the manual notations of the flow velocity in the first hour give the correct picture of a sudden response of the flow velocity to opening the weir.

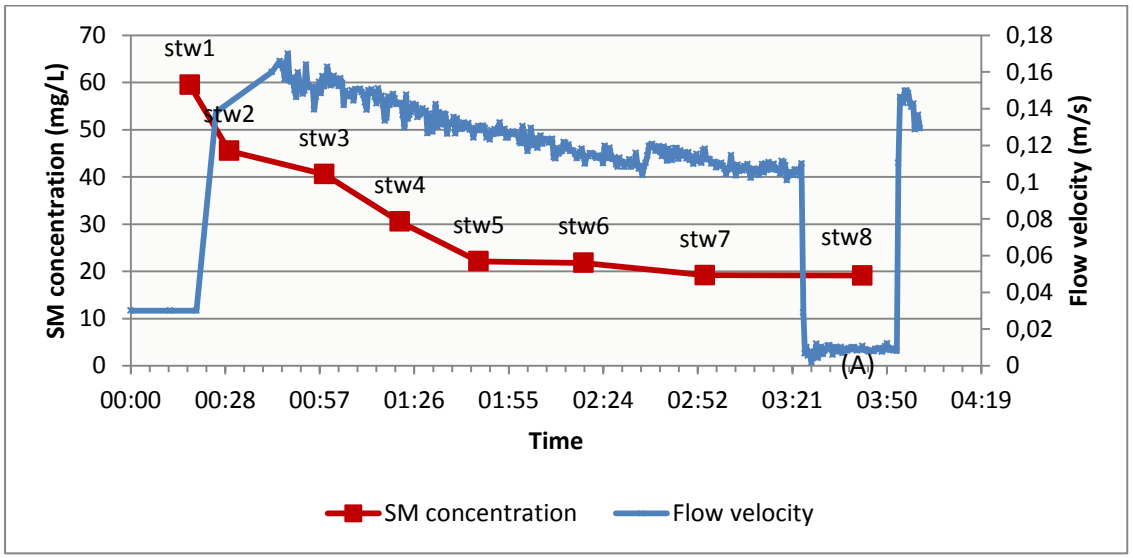

Figure 4.18 Development of flow velocity and SM concentration for the weir location (STW). Point A depicts the time period where the weir was temporarily closed.

4.3.3 Suspended matter

4.3.3.1 Suspended matter - concentration

Figure 4.18 shows that the SM concentrations at the STW location started at their maximum and proceeded to go down with time. Flow velocity did not seem to affect the pattern, not even when dropping to almost zero. Point A in Figure 4.18 shows how the SM concentration remains stable while flow velocity drops). It was expected that the water flow would erode particles and thus increase SM concentrations at higher flow velocities. Two explanations are provided for why this effect is not observed in Figure 4.18:

i) The water flow did not erode a significant amount of SM. A possible reason is that the flow velocity does not reach the critical shear stress level of the streambed sediments.

ii) The water does entrain a new fraction of eroded SM at higher flow velocities, but the effect on the total concentration is obscured by a simultaneous process with a contrasting impact. The most likely candidate for such a process would be the depletion of build-up stocks of organic matter.

The spread in the SM concentration of separate filter samples used to calculate the average is shown by Figure 4.19. With the exception of stw5, the minimum and maximum values follow the same directional up/down trend as the average. The minimum of stw5 is much too low for this trend. Throwing out the stw5 filter with the minimum value would raise the average to 26.4 mg/L, which would not change the absolute direction of the up/down trend. Since the trend remains the same and there were no observed irregularities during the filtration, it has been chosen to keep all filters of stw5 included in the average number.

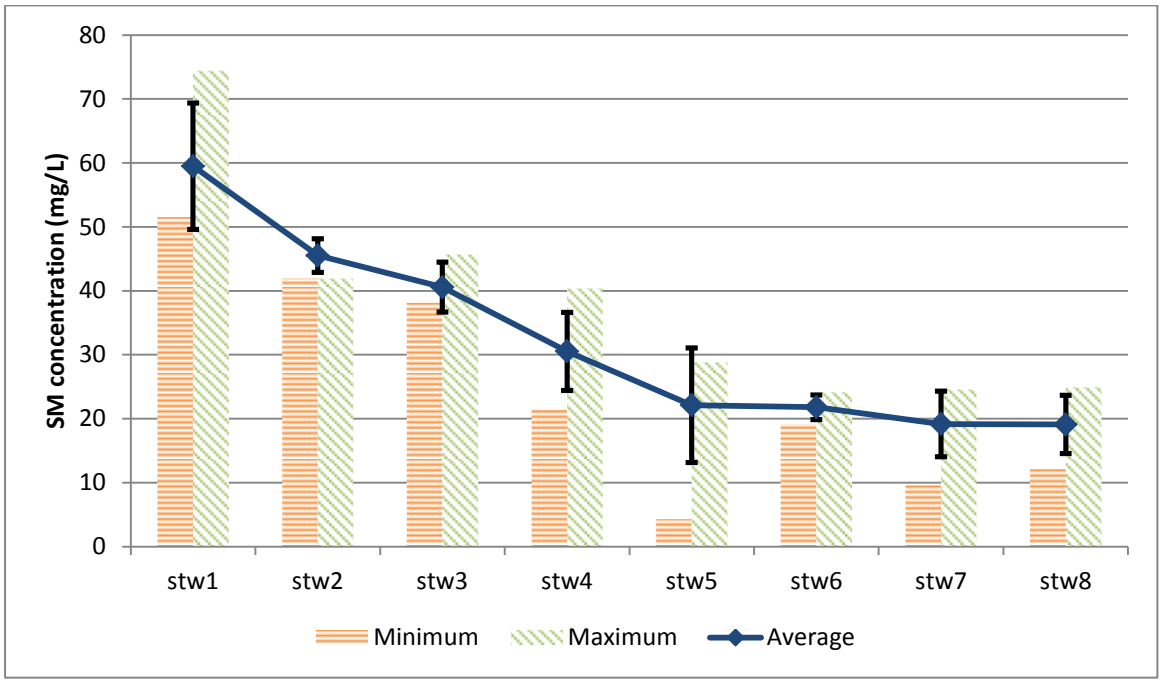

Figure 4.19 Characteristics of SM concentrations for STW, showing the volume-weighted average, standard deviation of the average (in error bars), and the minimum -and maximum concentrations .

Plotting the SM concentration against the particle concentration and obscuration shows that trend for SM concentration deviates from the latter two during the beginning of the experiment (see Figure 4.20). Determining exactly if a measurement is accurate for its point in time is hardly possible given the large differences at short timescales; however, it is plausible to assume some level of overestimation of the SM concentration at stw1.

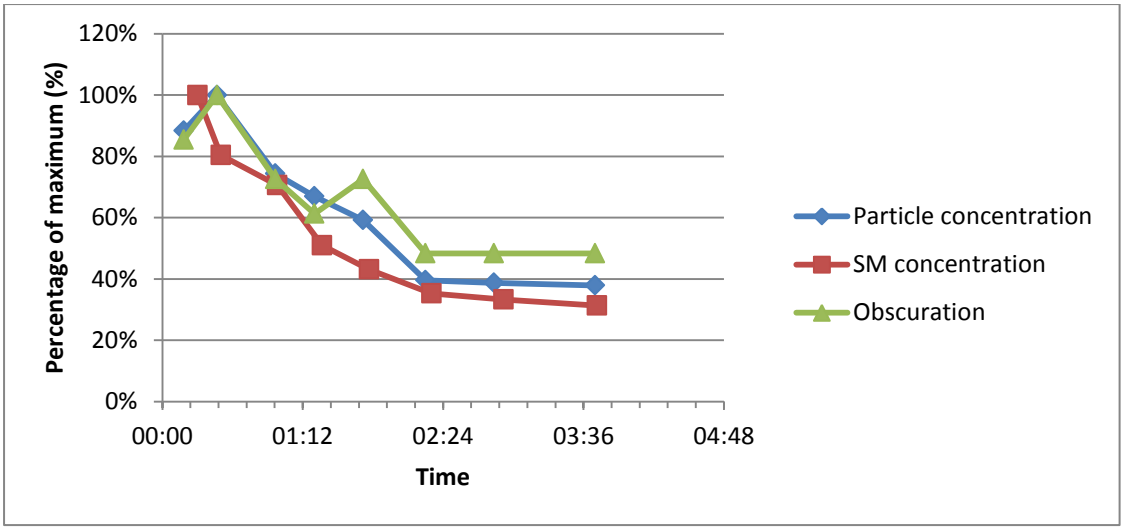

Figure 4.20 Comparison of the SM concentration, particle concentration and obscuration for samples from the weir location (STW), calculated as percentage of the parameter's maximum.

4.3.3.2 *Suspended matter - particle size distribution*

The particle size distribution for STW, depicted by Figure 4.21, is uncharacteristic for a freshwater system (pers. communication M. Verheul). Most notably it displays a system with three peaks, even four if one also counts point D. The main peak remains in the 0.0063 - 0.002 micrometre range for medium silt during stw1-7. At the time of stw8, the main peak has shifted to the left, but is still within this range. The fact that the system still includes a significant amount of large particles (sand) even though flow velocity is close to zero is another indicator that the PSD analysis did not perform as it should, sand particles cannot remain suspended if the flow is that low. The most likely explanation is that aggregates or large organic particles are disturbing the signal.

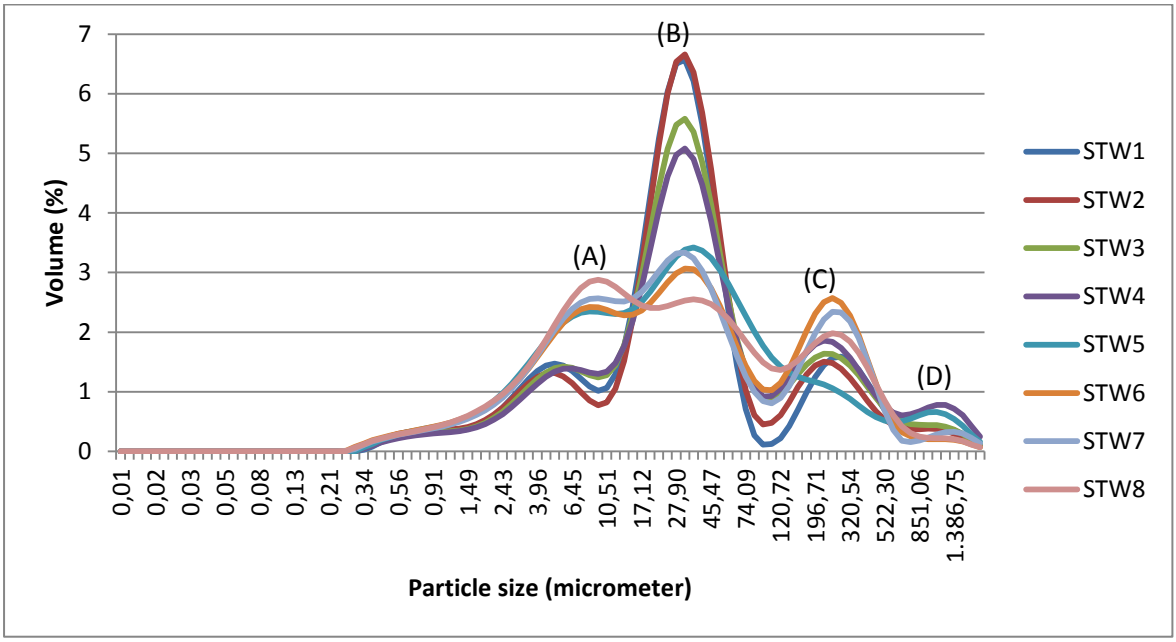

Figure 4.21 Particle size distribution for the weir location (STW). A, B,C and D mark the peaks in observed particle sizes.

4.3.4 Chemical properties of the water column

The results for the chemical properties of the water column are displayed in Table 4.8. Two of the three general water quality parameters (alkalinity and EC) vary by more than 10% of their maximum level, only pH remains within that 10%. In general, Figure 8.1 points towards the existence of two stable states, one at the beginning (stw1-2) and one at the end (stw5-8), with a transient phase in between (stw3-4). The assumption is that the changes are primarily due to a shift from long-time stagnant saline water at the weir to fresh and less saline water inflow from the backcountry. Judging by the development of Cl it is assumed that shifts due to biological or chemical processes at the site are not a likely explanation, as Cl is a fairly inert substance in aquatic chemistry and still varies the most of all water quality parameters. Additionally, salinity measurements performed by De Louw et al. (2004) indicated that the STW sampling location is situated in a part of the stream with boils, while Cl measurements in the ditch 350-400 meters further upstream indicated a relatively fresh environment. Given the elapsed time and flow velocity between the start of the flow event and stw3 (roughly 36 minutes and 0.15 m/s), water from this distance could very well have reached the sampling location by the time of stw3. However, the location of boils is dynamic and the situation might have changed since the sampling by De Louw et al. (2004).

Table 4.8 Water quality parameters (pH, alkalinity, EC, anions, cations$_4$, DOC, DP and TP) for the weir location (STW). TP data was provided as background to DP data, more TP measurement points are available.

	[unit]	stw1	stw2	stw3	stw4	stw5	stw6	stw7	stw8
Time	hh:mm	00:13	00:30	00:56	01:18	01:42	02:15	02:50	03:42
pH	[-]	7,11	7,1	7,17	7,19	7,14	7,21	7,28	7,3
Alkalinity	mg/l	543	555	491	492	453	459	464	468
EC	[mS/m]	2610	2800	2250	2160	1883	1852	1850	1867
Cl	mg/l	462	508	334	288	188	178	179	192
DOC	mg/l	22,5	23,8	23,5	24,8	29,9	28,3	27,2	26,7
NH_4	mg/l	3,4	3,2	2,4	1,9	1,7	1,5	1,6	1,6
NO_3	mg/l	5,7	5,6	5,7	6,4	6,2	n.a.	6,8	7,1
SO_4	mg/l	289	286	300	339	385	382	358	366
DP	mg/l	0,02	0,02	0,02	0,03	0,02	0,03	0,02	0,02
TP	mg/l	0,41	0,73	0,44	0,45	0,32	0,34	0,32	0,30
Al	mg/L	< 0.08*	< 0.08*	< 0.07*	< 0.09*	< 0.06*	< 0.07*	< 0.07*	< 0.06*
Ca	mg/L	> 257*	> 260*	> 248*	> 263*	> 265*	> 259*	> 257*	> 258*
Fe	mg/L	0,86	0,65	0,68	0,55	0,59	0,40	0,38	0,29
K	mg/L	17,1	17,3	15,9	15,1	13,9	13,9	14,2	14,2
Mg	mg/L	51	51	44,9	42,5	37,1	36,8	37,6	37,9
Mn	mg/L	1,02	1,07	0,97	1,02	1,14	1,08	1,05	1,03
Na	mg/L	> 240*	> 240*	179	157	107	103	107	112
Si	mg/L	10,6	10,7	10,3	10,3	10,5	10,1	10,3	10,3

* Value is below (<) or above (>) the calibration range of the equipment

The cation measurements in Table 4.8 exhibit the same pattern as anions: initial values are high and stabilization occurs after stw5. Dissolved Fe is the only parameter which does not stabilize at any point, also not the estimated total Fe calculated from Fe in the extract of the SEDEX (see also Figure 8.2 in appendix E). The change in Fe is assumed to have little consequence for

phosphate binding, as the DP measurements are constant throughout the entire experiment (0.02-0.03 mg/L) and very low compared to TP (0.30-0.73 mg/L). The relatively large drop in Na and Mg compared to the other cations is most likely related to the decreased salinity of the water, which is also held responsible for the drop in Cl concentration.

4.3.5 Phosphorus analysis

4.3.5.1 Relative contribution of the P fractions

The relative contribution of the P fractions is depicted by Figure 4.22 and Table 8.7 (in appendix E). Fe-P and Orga-P compromise the bulk of the fractions for STW. The Fe-P fraction varies between 65-81% for the filters and 81-90% for the centrifuge samples. Orga-P contributes 12-28% for the filter samples and 9-17% for the centrifuge samples. Measurements of Exch-P are stable for the centrifuge samples (1-3%), but vary significantly for the filter samples (3-10%).

The relative contribution of P fractions during the first two hours of the experiment (stw1-5) is more unstable for the filter samples than for the centrifuge samples. The trends of the sum of all fractions for both sample types are also reversed during this time, mostly due to large variations in Orga-P and Fe-P in the filter samples. The conflicting trends of centrifuge and filter samples indicate a considerable variability in the relative contribution of P fractions, on a timescale as short as one centrifuge sample period.

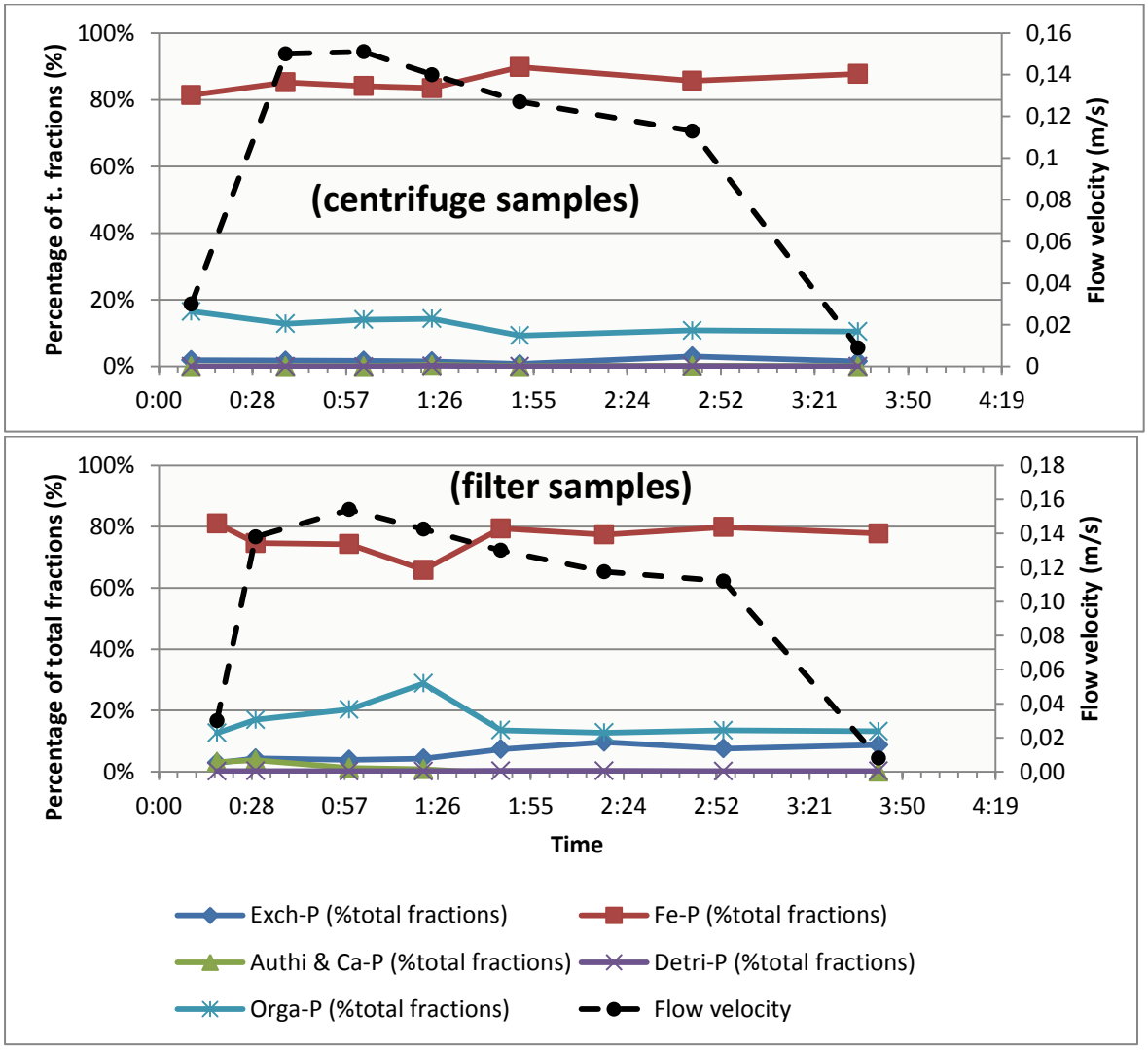

Figure 4.22 Relative contribution of the different P fractions for the weir location (STW).

4.3.5.2 *P content of suspended matter*

The P/SM ratio is shown by Figure 4.23 and Table 8.8 (in appendix E). Due to an issue in the experiment there is no data available for measurement point stw6 centrifuge. This coincides with the questionable measurement point stw7 centrifuge, which features a decrease of almost 50% in the total P per SM from the previous measurement point (stw5). The assumption is that stw7 is erroneous. This is primarily based on the relatively stable flow velocity and other conditions at the time of sampling that argue against an extreme change (see also the stabilizing trend in the general water quality parameters) and also on the absence of a similar dip in the corresponding filter sample.

The development pattern of the P/SM content is relatively stable for both sample types, excluding for stw4 (filter) and stw7 (centrifuge). The total of all fractions varies between 10.2-14.0 mg/ g for the filter samples and 6.1-13.0 mg/g for the centrifuge samples. Excluding stw7 from the centrifuge samples changes the range for centrifuge samples to 10.7-13.0 mg/g. The total P/SM content of the filter samples shows a rising trend towards the end that the centrifuge samples do not portray.

The missing and faulty measurement points of the centrifuge induce some uncertainty, but based on changes in fraction composition and the sum of all fractions it seems like there is *some variation in the type of particles being transported* during the first two hours of the experiment (stw1-5). After this time the change in relative contribution and P/SM ratio stabilizes.

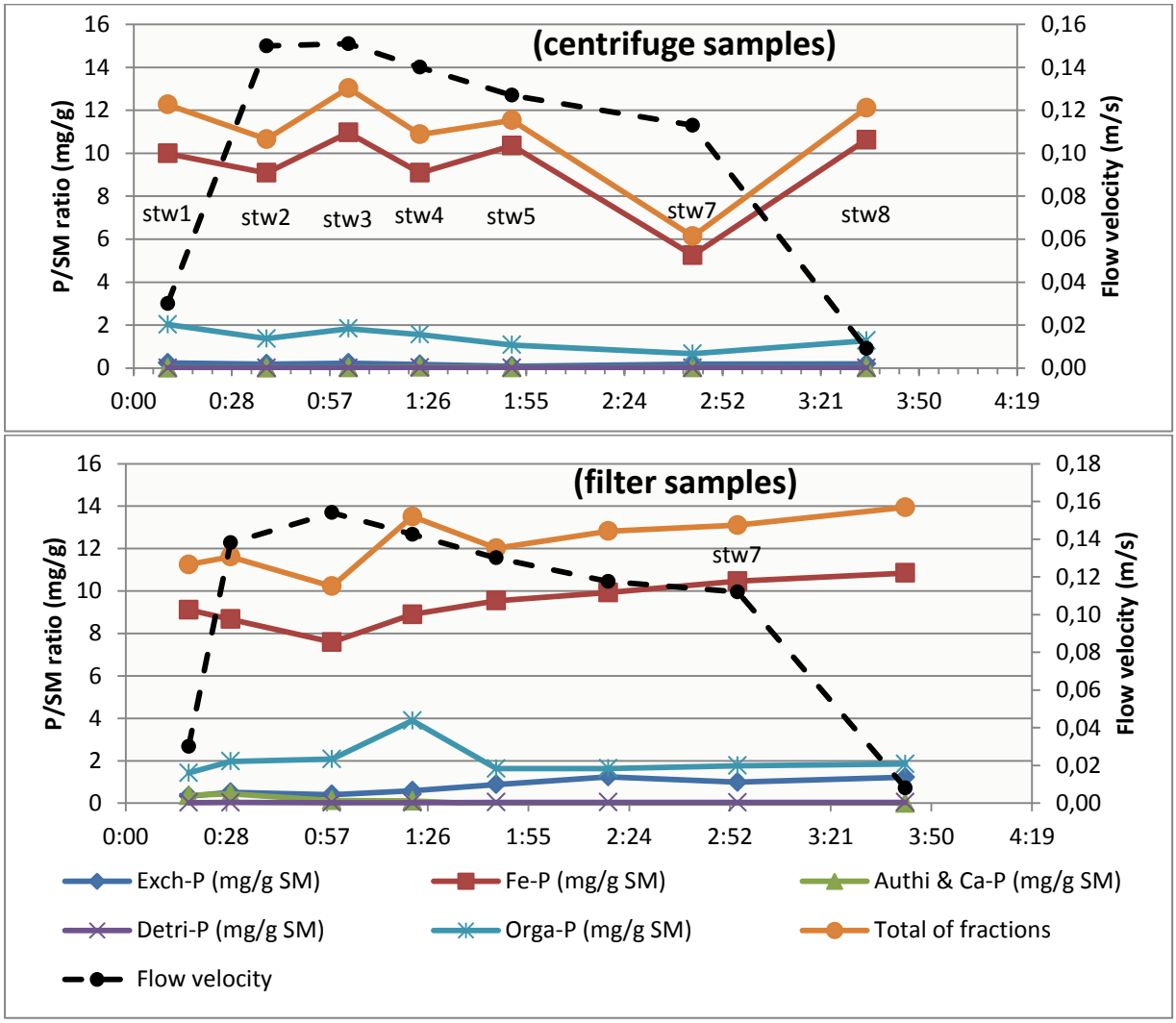

Figure 4.23 P/SM ratio and the average flow velocity for the weir sample location STW

4.3.5.3 *P content of the water column*

The trend of the final P concentration in the water column, shown by Figure 4.24, is strongly related to the SM concentration. Figure 4.25 shows that the match of the $PP_{WATERSEDEX}$ with the PP measurements is better for filter samples than for centrifuge samples. The latter tend to underestimate the concentrations towards the end of the experiment. This is particularly noticeable in stw7, which supports the theory that this is an erroneous measurement point. The P concentration of stw1 deviates strongly from PP for both the filter and centrifuge samples, most likely due to the aforementioned overestimation of the SM concentration.

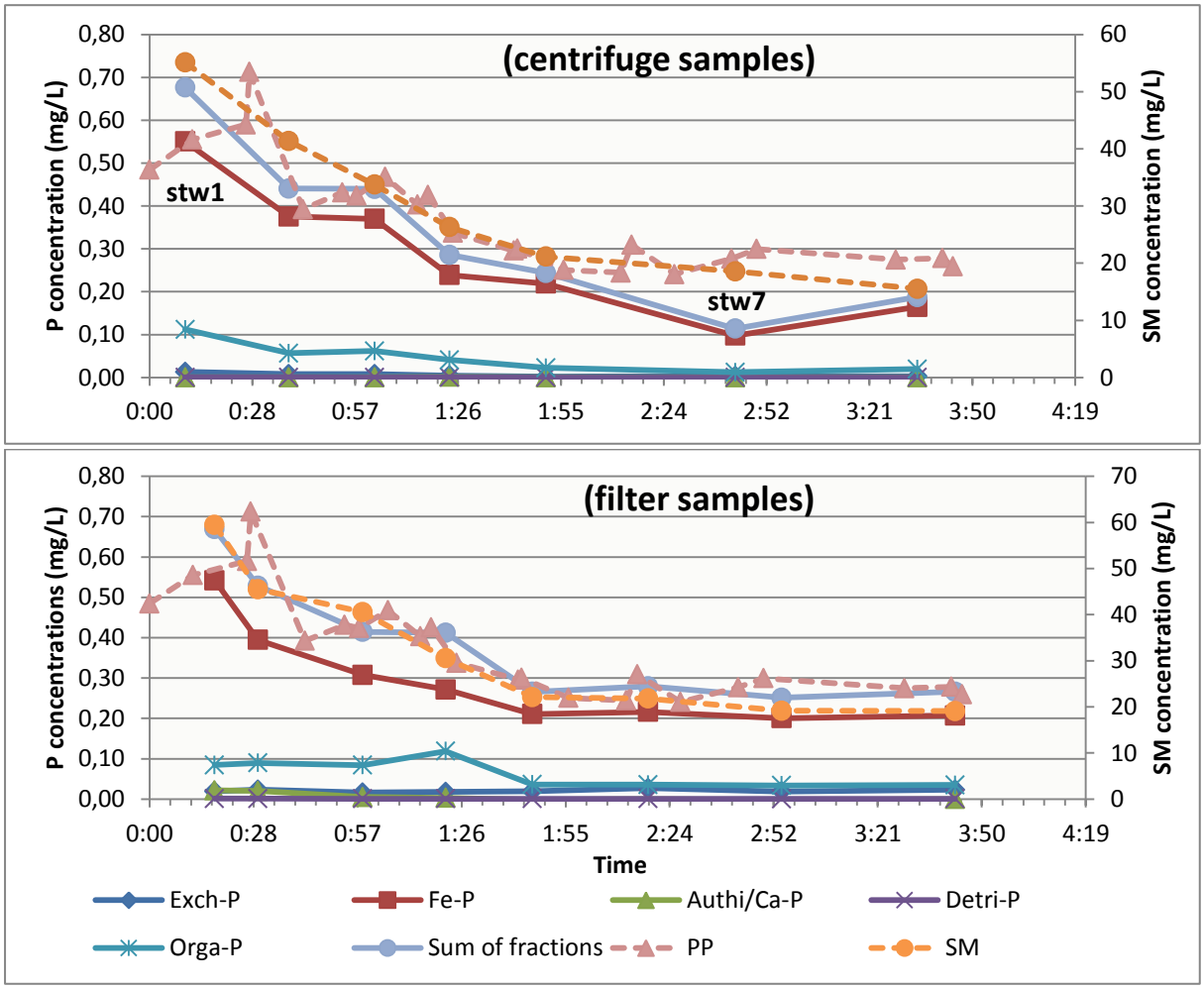

Figure 4.24 P concentration in the water column for the weir location (STW). Both $PP_{WATER.SEDEX}$ and PP are plotted.

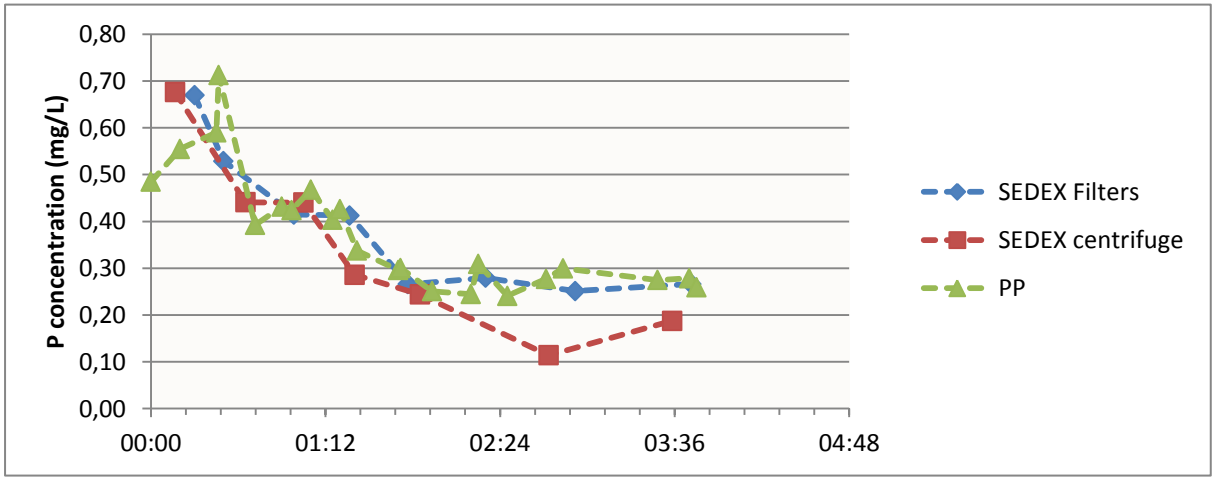

Figure 4.25 Comparison of methods for measuring P concentrations in the water column for the STW location.

4.3.6 Summary of results

The opening of the weir at STW caused a sudden increase in flow velocity within the first 45 minutes, which proceeded to go down gradually over the next three hours. The SM concentrations were at their highest before the opening of the weir and only decreased from there on. STW is the only location where the chemical properties of the water column changed between two distinctive states. The particle size distribution also varies between two distinct states. It is hypothesized that the initial situation is the result of a build-up of SM behind the weir, boosted by high local groundwater influx. The decrease in OM is also very visible in the decline of the main peak in the particle size distribution.

Besides the drop in Orga-P, the relative contribution of the P fractions remained stable. Fe-P (66-90%) was again the most dominant fraction and also took over the share of Orga-P (9-29%) at later measurement points. The P/SM ratio varied significantly throughout the experiment, particularly during the time period where the flow velocity and water quality indicators had not yet stabilized. An interesting result were the opposite trends derived from respectively filter samples and centrifuge samples; filters are the closest thing this research has to spot sampling and the differences between filters and the long-period data from the centrifuge indicate that the changes in P/SM ratio are highly volatile at small timescales. The difference between SEDEX results for filters and centrifuge samples largely disappeared when analysing the total concentration of P in the water column. It was concluded that that this is due to the dominant influence of SM concentrations on the calculation of $PP_{WATER.SEDEX}$. Separate PP measurements confirmed the trend of the SEDEX results.

5 Discussion

The overall results of the study indicate that the methodological approach was successful in providing reliable data for explaining the controls on P transport. The findings for the three separate locations are joined together with a thorough assessment of the available literature. First, the differences in the SEDEX results for filter and centrifuge samples will be discussed. After that the controls on P concentration, P speciation and the temporal variability will be debated. The chapter will end with discussing practical implications of the study and provide a short recommendation for future research.

5.1 Differences in SEDEX results for filter and centrifuge samples

Based on the SEDEX extraction, centrifuge samples have been shown to differ from filter samples by having lower average P/SM ratios for each location (-15%, -6% and -11% for PLS, SLT and STW, respectively), especially in regards to the Exch-P and Authi & Ca-P fractions. The reliability of the SEDEX sample types can be evaluated by comparing the $PP_{WATER.SEDEX}$ concentration from the SEDEX results to the direct PP concentration calculation, obtained from subtracting DP from TP measurements. The results indicate that the $PP_{WATER.SEDEX}$ of filter samples tends to overestimate the PP concentration, while the $PP_{WATER.SEDEX}$ of centrifuge samples tend to underestimate PP. Filters seem to provide a better match to PP than the centrifuge samples (for SLT and STW, undecided for PLS), but $PP_{WATER.SEDEX}$ for both sample types generally falls within 10-20% of the PP value. The differences in accuracy are therefore considered to be marginal; both sample types provide acceptable simulations of PP despite differences in P/SM ratio. This is explained by the dominant influence of the shared SM concentration parameter on the P concentration calculation.

The frequent underestimation of PP by the centrifuge samples, coupled with the slightly lower P/SM ratio, gives reason to assume that the centrifuge did not collect the entire Exch-P and Authi & Ca-P fraction from the water. According to Poulenard et al. (2008) and Pacini & Gächter (1999) the Exch-P fraction is most abundant in the finest of particles, which arguably have insufficient mass to be affected by the centrifugal force that is supposed to separate particles from the water phase during centrifugation (Ministerie van Verkeer en Waterstaat, 1990). The same principle of insufficient mass most likely also applies to the lower measurements of Authi & Ca-P, although no literature could be found that supports this assumption.

As consequence, the choice was made to base the numerical expression of the P/SM ratio and relative contribution of fractions solely on the SEDEX obtained for filter samples. The results from the centrifuge samples for the total P concentration in the water column do retain their value as a representation of periodic sampling versus spot sampling.

5.2 Phosphorus concentrations and speciation

5.2.1 Explaining P concentrations in the water column

Three factors were assumed to influence the P concentration in the water column: P/SM ratio, SM concentration and flow velocity. DP concentration was assumed to be an insignificant factor and thus excluded from the plot, given that the DP concentration (<0.06 mg/L) and its maximum spread (<0.03 mg/L) for the time period of any location were very low compared to TP concentration measurements.

The relevant factors were plotted against the sum of the SEDEX fractions in the water column, in order to determine the coefficient of determination (see Figure 5.1). The results of all SEDEX measurement points were included in the plots. Ultimately, the only correlation with an R^2 score greater than 0.25 was between *SM concentration* and the *total of all SEDEX fractions in the water column* (R^2=0.70). This remains the only correlation with R^2>0.25 if the data points are separated into filter and centrifuge samples, the correlation strengths are then R^2=0.67 (centrifuge) and R^2=0.78 (filter). Separating the results by location yielded additional correlations with R^2>0.25, for flow velocity with the total of fractions for PLS and STW, although this does not get carried over into the total combined correlation plot due to the weak correlation for SLT. The influence of flow velocity on SM and P concentration will be discussed more elaborately later on in the discussion.

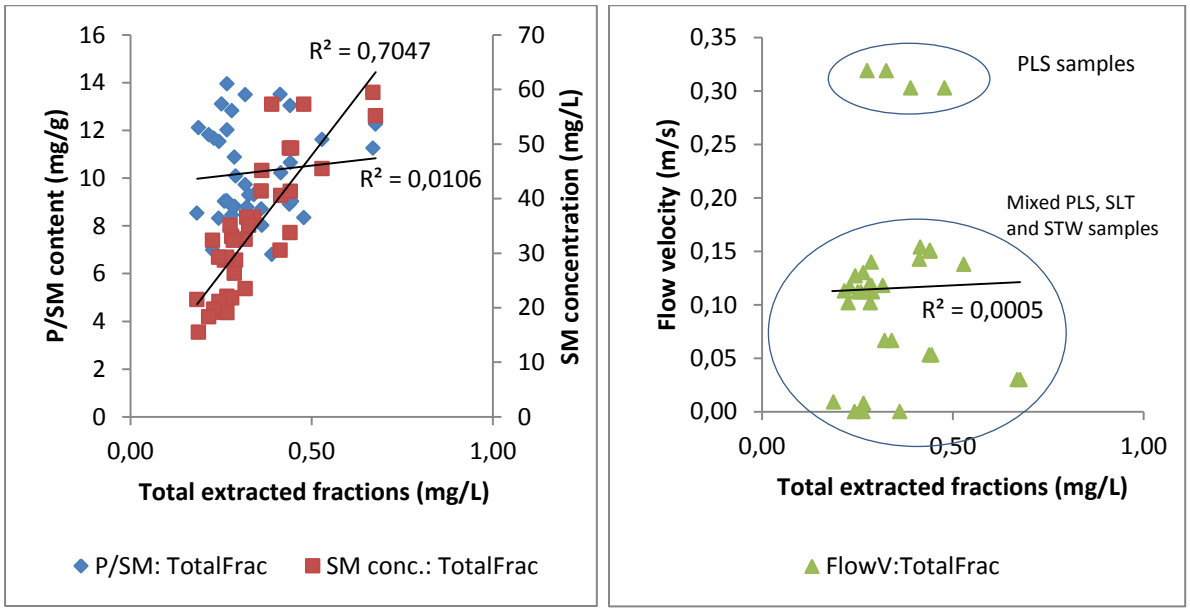

Figure 5.1 Scatter plots of the P/SM ratio, SM concentration (SM conc.) and flow velocity (FlowV) set against the total P concentration in the water column (TotalFrac).

Literature has also stated the importance of SM concentrations for PP concentrations (van der Salm et al. 2012; Vidon & Cuadra 2011; Evans & Johnes 2004), but that the variation of the P/SM ratio would have so little influence on PP concentrations in the present study came as an unexpected result. A possible explanation would be that the P/SM ratio was relatively stable compared to variation in literature; other studies have found the P/SM ratio to range between 1.0 and 2.5 mg/g (Pacini & Gächter 1999; Evans & Johnes 2004). These studies took place in free-flowing rivers and are therefore not directly comparable to the results of the present study, but it does indicate that the change in P/SM ratio can be much stronger.

5.2.2 Controls on SM concentration

Given that P concentrations are best explained by SM concentration, it is then imperative to understand how the presence of the latter can be explained. Most important for the set-up of this study is the relationship with flow velocity. The results already made clear that flow velocity and SM concentration do not have a similar relationship for all three locations; at PLS the link was positive, at SLT negative and for STW it could not be determined with certainty if flow velocity actually had an influence on SM concentration. The lack of a *linear* relationship between flow velocity and SM concentration was confirmed by R^2 scores of 0.33, -0.75 and 0 for PLS, SLT and STW, respectively.

A possible explanation for the correlation differences between the three locations is the influence of bed sediment and whether or not there is sufficient critical shear stress to suspend this potentially significant source of SM. The maximum flow velocity for PLS (around 0.3 m/s) was double that of SLT and STW (0.10-0.12 m/s), which speaks in favour of this explanation. However, SLT and PLS both showed a secondary peak in the sand particle size category, (maximum size of 1000 µm), which is indicative of streambed erosion, while featuring only a relatively mild increase in SM concentrations. It is possible that the peak in particle size is caused by aggregates rather than actual sand size particles. Judging by the commonly applied Hjülstrom diagram; transport, but not erosion, of particles with a maximum size of <1000 µm is possible at the measured SLT flow velocities (see Figure 5.2). Additionally, Gailani et al. (1991) argued for the existence of an “easily resuspendable layer” on the surface of the streambed which defies the regular calculations for critical shear stress. Combining these findings indicates that the peak observed in the particle size distribution of SLT and PLS could be the suspension of aggregates from the easily resuspendable layer. At the PLS location in close proximity to the pumping station, the largest aggregates were most likely disaggregated by the increasing flow velocities once the second pump was activated. This explains why the largest particles disappeared from the particle size distribution of this location, but could persist at the lower flow velocities in the backfield ditch of SLT. According to Gailani et al. (1991), the volume of the easily resuspendable surface layer is small compared to other sediment sources, which could explain the absence of an increase in SM concentration in response to the mobilization of the resuspendable layer.

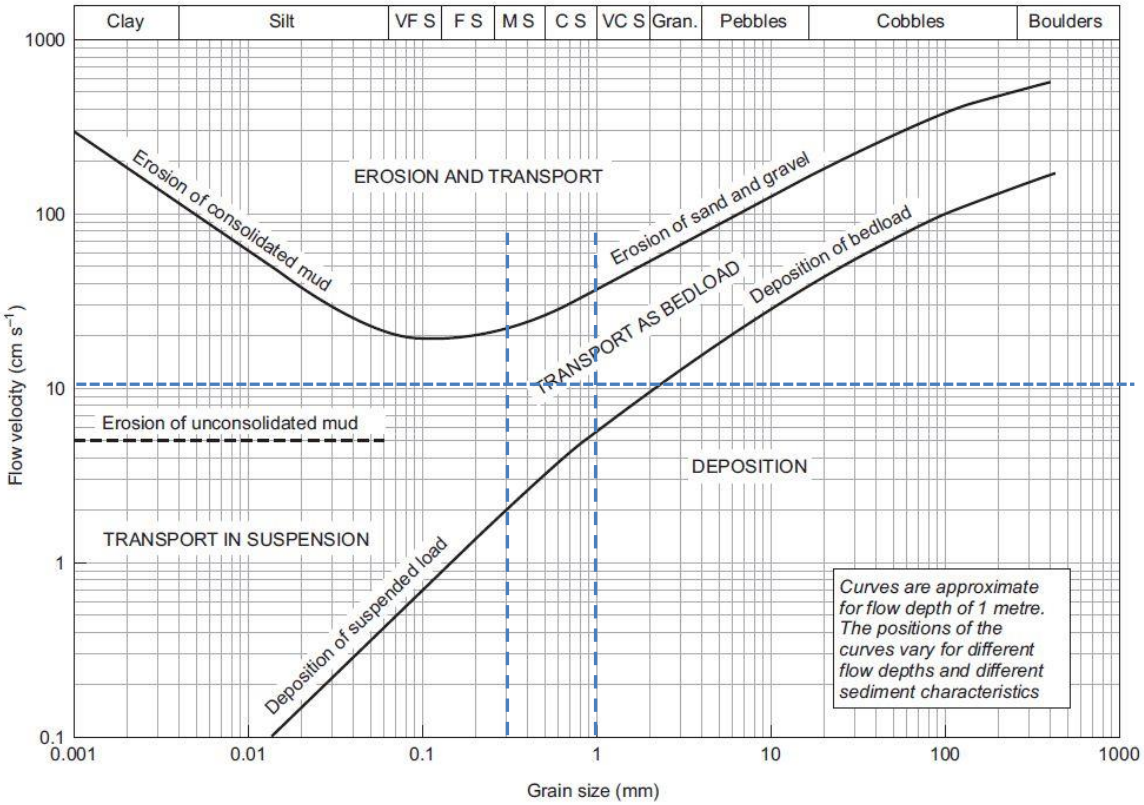

Figure 5.2 Hjülstrom diagram, taken from Press & Siever (1986). The original was modified with dashed lines, depicting the 0.2-1.0 mm size range of the observed peak at the locations PLS and SLT (dashed vertical lines) and the minimal flow velocity at the time that the peak in this size range was noted (horizontal line).The point of intersection indicates that transport (mainly as bedload) was an option.

5.2.3 Understanding P speciation

The variation in the relative contribution of P fractions is not expected to have played a significant role in determining the change in P concentration in the water column. Not only was the total

P/SM ratio of no significant influence, the relative contribution was also rather stable. The results indicate that Fe-P is by far the most significant P fraction for all locations and (flow) conditions in this case study, comprising 65-84% of the total PP. The second-largest fraction is at all times Orga-P, comprising 9-28% of the PP. The lower boundary of Fe-P and upper boundary of Orga-P are the results of outshoots in a single sample. The high importance of Fe-P in this study is confirmed by the scatter plot in Figure 5.3, which shows that the correlation pattern between the Fe-P content of SM and the total P/SM content is much stronger than the correlation between the Orga-P content of SM and the total P/SM content.

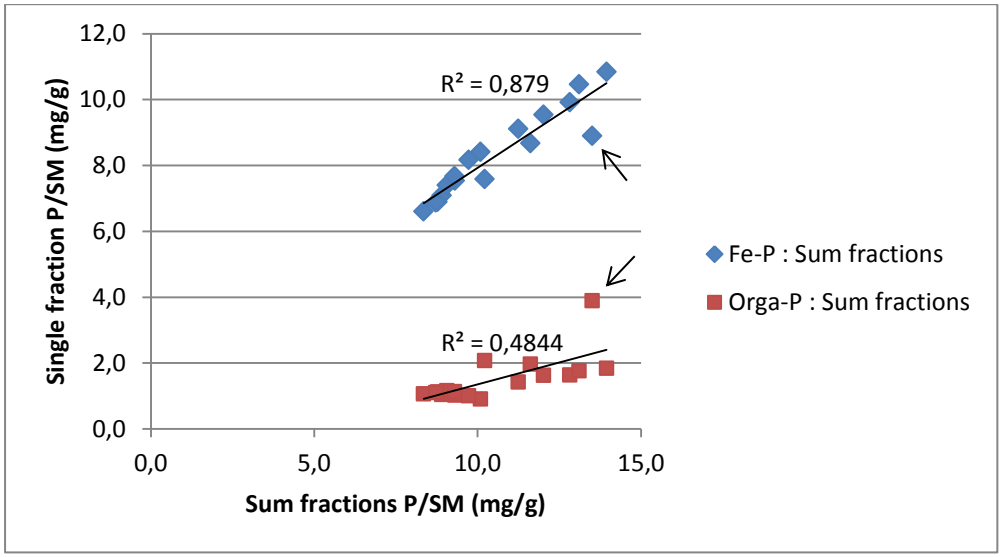

Figure 5.3 Scatter plot of separate fractions (Fe-P and Orga-P) against the sum of all P fractions for P/SM, using all filter-based SEDEX data of PLS, SLT and STW. The data points indicated by arrows belong to outshoot stw4.

Table 5.1 shows the results of previous P speciation studies for SM in free-flowing riverine systems. While not entirely comparable to the landscape of a polder and its constructed water infrastructure, the numbers do show that the average Fe-P contribution measured by this study is relatively much higher, while the Orga-P contribution is lower than that of other studies. Furthermore the Authi & Ca-P contribution found in the literature (3-25%) exceeds the maximum contribution found in this study (6%). Pacini & Gächter (1999) also showed that Exch-P can be a significant (12-25%) component of PP. Overall the observed Fe-P domination in this study is extreme compared to the results found in literature for studies in foreign areas. Compared to the unpublished PhD results of Bas van der Grift, who measured Fe-P contributions of 50-90% to the total SM bound P for two Dutch polders (pers. communication, B. van der Grift), the 79% average Fe-P contribution of this study is much less extreme. Soil type and geohydrological setting could therefore certainly be a factor in the Fe-P domination.

5.3 Temporal variability in phosphorus transport

The results show that large temporal variability in TP and SM concentrations can occur at small time scales. This is most evident in the concentrations in the channel near the pumping station (PLS), caused by different pumping rates of the Palenstein pumping station, and the concentrations in the stagnant water upstream of the closed weir (STW), caused by groundwater input and subsequent authigenic production. Gathering representable data by spot sampling while dealing with temporal variability poses a difficult task. This is illustrated by Figure 8.3 in appendix 8.4, which shows the TP concentration measurements performed by the water board at the same location as PLS. The 0.45-0.5 mg/L TP concentrations measured in this study are higher than any point that Figure 8.3 shows for the period 2012-2013.

The strong temporal variation is not only reserved to systems with a high PP:TP ratio and low DP. Claassen et al. (2012) investigated P concentrations shortly upstream of a pumping station in a Dutch polder where DP concentrations were relatively high, about 64% of the TP pool. Activating the pumping station caused almost a doubling of the TP concentration at this location.

Table 5.1 Results of previous P speciation studies for suspended matter in riverine systems. IP is defined as the sum of all mineral fractions.

Study	Temporal scale	Location	P/SM	OP	IP	Exch-P	Fe-P	Authi & Ca-P
			(mg/g)	(%PP)	(%PP)	(%PP)	(%PP)	(%PP)
Poulenard et al. 2008	Spot samples	Redon river, UK	n.a.	21 [a]	79 [a]	10 [a]	42 [a]	<15 [a]
	Spot samples	Mercube river, UK	n.a.	11 [a]	89 [a]	5 [a]	50 [a]	<25 [a]
Pacini & Gachter 1991	Storm event (<1 day)	Kleine Aa river, Switzerland	2.5-1.0	25-41	75-59	12-25	45-18	3-17
Ballantine et al. 2008	Storm event (5 hrs)	Hook stream, UK	n.a.	26-41 [a]	59-74	n.a.	n.a.	n.a.
	Storm event (3.5 hrs)	Devil's Brook, UK	n.a.	44-73	27-56	n.a.	n.a.	n.a.

[a] Calculated values, based on data provided in article

5.4 Practical implications

The mentioned outcomes of the present study, particularly the Fe-P dominance, peaks in P concentration at higher flow velocities and general vulnerability of P monitoring to temporal variation, have implications for risk assessment that warrant the attention of policy makers and managers of pumping stations. Biological availability and sedimentation behaviour of specific fractions are two factors which belong on this list as well, even if they were not included in the scope of this project.

Several studies investigated the biological availability of different P fractions. The consensus is that Fe-P is to be considered largely or entirely bio-available (Pacini & Gächter 1999; Golterman 2001). The biological availability of Fe-P is mostly related to release of P under anoxic conditions, meaning that the greatest risk of mass release is during summer periods, when anoxic conditions occur most frequently and biological life, including harmful algae, is most active.

Sedimentation behaviour is an important addition to the knowledge of resuspension behaviour and risk management, as it indicates how long the particles suspended by high flow events will remain mobile. For the PLS location, the percentage of SM/Particle concentration/obscuration measurements had already decreased to about 75% of peak value within 30 minutes of deactivating the pumps, with values for pre-event conditions at about 50%. This indicates that the system is able to restore relatively quickly to pre-pumping SM concentrations levels; the TP concentration follows more or less the same pattern, but is even closer to pre-pumping levels. Claassen et al. (2012) also observed a relatively quick decline of P concentration to baseflow after a drop of flow velocity. However, P speciation was not a part of that study. Additional experiments are needed to characterize the sedimentation behaviour of different PP fractions in the studied polder.

There are also P retention efforts to consider. TP concentrations near the station when using one pump amounted to about 0.25 mg/L. When using two pumps the TP concentration went up to about 45 mg/L. Given that the pumping station has to remove the same amount of excess water, no matter how fast, using two pumps effectively increases P loading to the system outside the polder by almost a factor two.

5.5 Recommendations for future research

For future research it is advised that the field experiment is to be repeated in summer, in order to assess the effect of increased biological activity and different weather, including precipitation patterns and possible anoxic state of the aquatic sediment. The rapid changes in P and SM concentrations around the shifts in pumping regime call for a greater emphasis on these particular moments. An experiment to determine if the mix of P transported at different times has a different sedimentation rate would also be a useful addition.

6 Conclusion

The transport of suspended matter and the speciation of the contained particulate phosphorus was analysed by means of a controlled flow event in the Dutch Noordplas polder, with the goal of allowing a more detailed characterization of phosphorus (P) mobility during high flow events. A pumping station and a weir were used to force a controlled high flow event without the interference of overland and sub-surface drain flow. Samples were collected from three different locations: 350 meters upstream from the Palenstein pumping station, in a ditch further upstream with an open flow connection to the pumping station and in a ditch separated from the pumping station, upstream of a weir. The polder is characterized by strong saline groundwater exfiltration, containing high concentrations of iron and phosphorus.

The results for the three different sampling locations show significant differences in the development and correlation of P concentration, suspended matter concentration and other water quality parameters. Suspended matter concentration did not consistently increase with flow velocity. The location near the pumping station was the only point where the trend of flow velocity was followed perfectly by the trend of the suspended matter concentration. In the backfield ditch and at the weir, maximum suspended matter concentrations did not coincide with maximum flow velocity, although partial correlation was indeed observed in segments of the time line. The most likely explanation for the lack of a uniform relationship is that critical shear stress thresholds determine if flow velocity leads to increased suspended matter concentrations, for the latter two locations the threshold is presumed to have been too high for the flow velocity to overcome. High suspended matter concentrations at the weir location were primarily related to trapping of suspended matter by the weir, the suspended matter was formed by authigenic and biological production in the week prior to the field experiment.

The overall development of total P concentrations in the water column varied greatly for all three locations, but was in all cases determined predominantly by the change in suspended matter concentrations. The P concentration in suspended matter, although also highly variable for the pumping station location and the weir location, had little influence on the total P concentrations in the water column. What exactly drove the change in the P in suspended matter remains uncertain, the particle size distribution analysis did not yield enough data to draw any conclusions on this matter. The relative contribution of the P fractions showed remarkable stability throughout all flow velocities and conditions; iron bound P (65-84% of the total) and to a lesser extent organic P (9-28% of the total) were at all times the most important fractions. The only factor that seemed to have any significant influence on the relative contribution was increased biological and authigenic suspended matter production due to large local groundwater influx at the weir location. This is presumed to have formed uncommonly large stocks of suspended matter and led to a minor shift in fractions when opening the weir replacing the stored water with fresh water from further upstream.

The size fractions of the transported sediment changed for all three locations during the experiment. As hypothesized, higher flow velocities were able to entrain larger particles. This was visible in the shifting d(0.9) values of the particle size distribution, but the d(0.1) and d(0.5) were also affected. Furthermore, peaks developed in the sand-size category of samples taken at the pumping station location and the backfield ditch. However, only for the samples taken during the highest flow velocity at the pumping station is it assumed that these peaks actually represent sandy particles. For all other samples, the sand-size peaks are assumed to be aggregates. Overall the results show that major changes in the particle size distribution are possible without a simultaneous noticeable change in suspended matter concentration (and vice versa). Further application of particle size specification proved difficult however.

This study has led to the insight that there are only two important findings that remain constant throughout the results of the entire field campaign. First, iron bound P is the dominant PP fraction under all conditions. Second, the only parameter that can be directly correlated to the TP

concentration in the water column is the suspended matter concentration. Other parameters explain only a minor part of the variations in TP concentration. The impact of flow velocity on suspended matter concentration, and by extension also on TP concentration, is dependent on overcoming critical shear stress thresholds and therefore not a constant factor throughout the experiment. In situations where erosion did occur, suspended matter and phosphorus concentrations went up greatly.

7 Bibliography

Baken, S. et al., 2013. Characterisation of hydrous ferric oxides derived from iron-rich groundwaters and their contribution to the suspended sediment of streams. *Applied Geochemistry*, 39, pp.59–68. Available at: dx.doi.org/10.1016/j.apgeochem.2013.09.013 [Accessed December 16, 2013].

Ballantine, D.J. et al., 2008. The phosphorus content of fluvial suspended sediment in three lowland groundwater-dominated catchments. *Journal of Hydrology*, 357(1-2), pp.140–151. Available at: http://linkinghub.elsevier.com/retrieve/pii/S0022169408002369 [Accessed December 16, 2013].

Borah, D.K., Bera, M. & Xia, R., 2004. Storm Event Flow and Sediment Simulations in Agricultural Watersheds using DWSM. , 47(2003), pp.1539–1560.

Correll, D.L., 1998. The Role of Phosphorus in the Eutrophication of Receiving Waters: A Review. *Journal of Environment Quality*, 27(2), p.261.

De Louw, P. et al. 2013. Het effect van waterbeheer op de chloride - en nutriëntenbelasting van het oppervlaktewater in Polder de Noordplas. Synthese rapport: definitieve water- en stoffenbalans en effecten van verschillende waterbeheerscenario's, Nederlands Instituut voor Toegepast Onderzoek (TNO).

Evans, D.J. & Johnes, P.J., 2004. Physico-chemical controls on phosphorus cycling in two lowland streams. Part 1--the water column. *The Science of the total environment*, 329(1-3), pp.145–163. Available at: http://www.ncbi.nlm.nih.gov/pubmed/15262164 [Accessed December 16, 2013].

Evans, D.J., Johnes, P.J. & Lawrence, D.S., 2004. Physico-chemical controls on phosphorus cycling in two lowland streams. Part 2--the sediment phase. *The Science of the total environment*, 329(1-3), pp.165–82. Available at: http://www.ncbi.nlm.nih.gov/pubmed/15262165 [Accessed August 3, 2014].

Gailani, J., Ziegler, C.K. & Lick, W., 1991. Transport of Suspended Solids in the Lower Fox River. *Journal of Great Lakes Research*, 17(4), pp.479–494. Available at: http://linkinghub.elsevier.com/retrieve/pii/S0380133091713841 [Accessed December 16, 2013].

Golterman, H.L., 2001. Fractionation and bioavailability of phosphates in lacustrine sediments: a review, 20(1), pp.15–29.

Gunnars, A. et al., 2002. Formation of Fe(III) oxyhydroxide colloids in freshwater and brackish seawater, with incorporation of phosphate and calcium. *Geochimica et Cosmochimica Acta*, 66(5), pp.745–758.

Hyacinthe, C. & Van Cappellen, P., 2004. An authigenic iron phosphate phase in estuarine sediments: composition, formation and chemical reactivity. *Marine Chemistry*, 91(1-4), pp.227–251. Available at: http://linkinghub.elsevier.com/retrieve/pii/S0304420304001884 [Accessed December 16, 2013].

Hoogheemraadschap Rijnland. 2014. Interactive water quality map: pumping station Palenstein-phosphate. Taken from http://rijnland.webgispublisher.nl

Konert, M. & Vandenberghe, J., 1997. Comparison of laser grain size analysis with pipette and sieve analysis : a solution for the underestimation of the clay fraction. , pp.523–535.

Malvern Instruments Ltd .2007. Mastersizer 2000 User Manual Issue 1.0

Ministerie van Verkeer en Waterstaat, 1990. Effectiviteitsonderzoeken doorstroomcentrifuges periode 1980-1990. *Werkdocument 90.156x*.

Pacini, N. & Gächter, R., 1999. Speciation of riverine particulate phosphorus during rain events. *Biogeochemistry*, 47(1), pp.87–109.

Poulenard, J., Dorioz, J.-M. & Elsass, F., 2008. Analytical Electron-Microscopy Fractionation of Fine and Colloidal Particulate-Phosphorus in Riverbed and Suspended Sediments. *Aquatic Geochemistry*, 14(3), pp.193–210. Available at: http://link.springer.com/10.1007/s10498-008-9032-5 [Accessed December 16, 2013].

Press, F. and Siever, R. 1986. Earth. (4th edition). Published by Freeman and Co, New York

Reddy, K.R. et al., 1999. Phosphorus Retention in Streams and Wetlands: A Review. *Critical Reviews in Environmental Science and Technology*, 29(1), pp.83–146. Available at: http://www.tandfonline.com/doi/abs/10.1080/10643389991259182 [Accessed December 11, 2013].

Ruttenberg, K.C., 1992. Ruttenberg, 1992.pdf. *Limnology and Oceanography*, 37(7), pp.1460–1482.

Van der Salm, C. et al., 2012. Water and Nutrient Transport on a Heavy Clay Soil in a Fluvial Plain in The Netherlands. *Journal of Environment Quality*, 41(1), p.229. Available at: http://www.ncbi.nlm.nih.gov/pubmed/22218191 [Accessed December 16, 2013].

Slomp, C.I. et al., 1996. A key role for iron-bound phosphorus in authigenic apatite formation in North Atlantic continental platform sediments. , 54(6), pp.1179–1205.

Vanlierde, E. et al., 2007. Estimating and modeling the annual contribution of authigenic sediment to the total suspended sediment load in the Kleine Nete Basin, Belgium. *Sedimentary Geology*, 202(1-2), pp.317–332. Available at: http://linkinghub.elsevier.com/retrieve/pii/S0037073807001558 [Accessed December 16, 2013].

Vidon, P. & Cuadra, P.E., 2011. Phosphorus dynamics in tile-drain flow during storms in the US Midwest. *Agricultural Water Management*, 98(4), pp.532–540. Available at: http://linkinghub.elsevier.com/retrieve/pii/S037837741000315X [Accessed December 16, 2013].

Wang, C. et al., 2013. Sequential extraction procedures for the determination of phosphorus forms in sediment. *Limnology*, 14(2), pp.147–157. Available at: http://link.springer.com/10.1007/s10201-012-0397-1.

8 Appendix

8.1 Appendix A – SEDEX procedure

8.1.1 Extraction procedure

Day 1- Extraction of Exchangeable P

- Add 10ml $MgCl_2$ to each sample tube
- Shake for 30 minutes, centrifuge to pellet sediment, weigh tubes, filter and store filtrate at 4°C (label as $MgCl_2$ 1)
- **$MgCl_2$ 1 is analysed to give the Exchangeable P fraction**

Day 2- Extraction of Fe-bound P

- Dissolve 12g Na dithionite in 480ml Na-citrate and 60ml Na-bicarbonate (pH ≈ 7.5) and add 9ml to each sample tube
- Shake for 8 hours, weigh tubes, centrifuge, filter and store filtrate at -20°C (label as **CDB**)
- Add 10ml $MgCl_2$ to each sample tube (label as $MgCl_2$ 2)
- Shake for 30 minutes, weigh tubes, centrifuge, filter and store filtrate at 4°C
- **CDB + $MgCl_2$ 2 results combined return the Fe-bound P fraction**

Day 3 and 4- Extraction of Authigenic Ca-P and Detrital P

- Add 10 ml acetate buffer (pH 4) to each sample tube
- Shake for 6 hours, weigh tubes, centrifuge, filter and store filtrate at 4°C (label as Acetate)
- Add 10ml $MgCl_2$ to each sample tube
- Shake for 30 minutes, weigh tubes, centrifuge, filter and store filtrate at 4°C (label as $MgCl_2$ 3)
- Add 10ml HCl to each sample tube
- Shake for 24 hours, weigh tubes, centrifuge, filter and store filtrate at 4°C (label as HCl 1)
- **Acetate and $MgCl_2$ 3 represents the Authigenic Ca-P fraction**
- **HCl 1 represents the Detrital P fraction**

Day 4 and 5- Ashing to extract Total Organic P

- Convey sediment from sample tubes to labelled ceramic crucibles by flushing sample tubes contents 2-3 times with UHQ; air dry the emptied sample tubes
- Dry sediment at 50°C for ≈24 hours (or 90°C for ≈12 hours, or 80°C for ≈16 hours)
- Ash samples for 2 hours at 550°C in a muffle oven (total oven time, including pre-heating is ≈3 hours)

- Convey ashed samples to the air-dried sample tubes (loosen the sediment using a spatula and grind them slightly in the crucible before transfer)
- Add 10 ml HCl to ashed samples
- Shake for 24 hours, weigh tubes, centrifuge, filter and store filtrate at 4°C (label as HCl 2)
- **HCl 2 represents the Organic P fraction**

8.1.2 Colorimetric analysis procedure

The colorimetric analysis was calibrated on a phosphorus concentration range of 0-30 µM, using extraction solvent (e.g. $MgCl_2$, HCl) from the same bottle that was also used in the extraction procedure as matrix solution. If the measured values exceeded calibrated concentration range, a new batch of further diluted samples was made and analysed. This procedure was repeated untill measurements fell within range of the calibration series. Calibration series were measured before and after the samples and checked for linearity. Calibrations were only accepted if the R^2 scores had a minimum value of 0.95.

The standard recipe for filling one measuring cuvette was 800 µL sample fluid, 800 µL mixing reagent (ammonium heptamolybdate and ascorbic acid) and 2400 µL UHQ. Volumes were pipetted into the cuvette using disposable tips to prevent sample pollution. The absorbance was measured at a wavelength of 880 nm, between 10-100 minutes after adding the ammonium heptamolybdate mixing reagent.

8.1.3 Samples selected for doubles

- pls1,2,4,5 (filter), representing moments of baseflow, one pomp active, two pomps active, inactivation of pumps, respectively.
- pls2,4 (centrifuge), representing moments with one pomp active and two pomps active, respectively.
- stw1,5,8 (filter), representing moments of baseflow (weir closed), initial flatting of flow velocity curve, stop flow, respectively.
- stw1,5,8 (centrifuge), representing moments of baseflow (weir closed), initial flatting of flow velocity curve, stop flow, respectively.
- pls4 (centrifuge), chosen because the available sample quantity is very high (750 mg). The double is used to validate if the 100 mg subsample is representable.
- stw1,6 (centrifuge), chosen because the available sample quantities are very high (550 mg and 460 mg, respectively). The double is used to validate if the 100 mg subsample is representable. stw1 and stw6 are also important moments in time (representing moments of baseflow and the initial flattening of the flow velocity curve, respectively).
- Blanks, chosen because no uncertainty can be allowed regarding any pollution of the extraction fluids.

8.1.4 Selection criteria within sets of samples

-If using only one sample per filter or centrifuge set; choose the sample with maximum weight (provided its SM concentration is not of extreme level).
-If using two samples per filter or centrifuge set; choose a secondary sample of average weight (i.e. not an extreme minimum), which also has a different SM concentration than the first filter and preferably not was not sampled directly pre/proceeding the first filter (increasing the chance of covering the whole spectrum of the water that was once in the Scott bottle).

8.2 Appendix B – Calculation of average flow velocity for stw2 centrifuge

The stw2 centrifuge samples cover the time period 00:25-00:53. This part of the graph can be divided up in three different sections. The ∆t values for A,B and C are respectively 18, 2 and 8 minutes. For sections A and B there are only begin -and end measurement points, the average flow velocity for these two sections can be calculated using the formula:

$$Average = \frac{Begin + End}{2} * \Delta t/\Delta t$$

For C there is one data point per five seconds available from the P-EMS, for which the average can simply be calculated within the respective Excel file. The total

$$Average\ flow\ velocity\ A = \frac{0.138 + 0.154}{2}$$

$$Average\ flow\ velocity\ B = \frac{0.154 + 0.1533}{2}$$

$$Average\ flow\ velocity\ C = [Excel] = 0.157$$

$$Average\ flow\ velocity\ stw2 = \frac{\frac{0.138 + 0.154}{2} * 18 + \frac{0.16 + 0.1533}{2} * 2 + 0.157 * 8}{28} = \mathbf{0.150\ m/s}$$

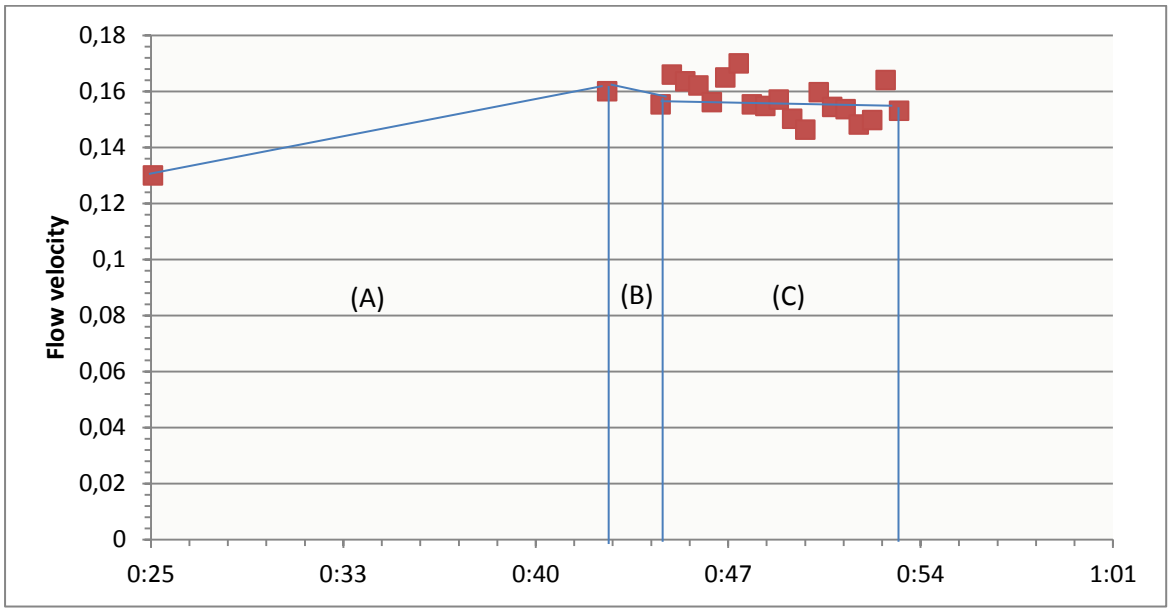

8.3 Appendix C – Figures and data tables

8.3.1 Water quality parameters

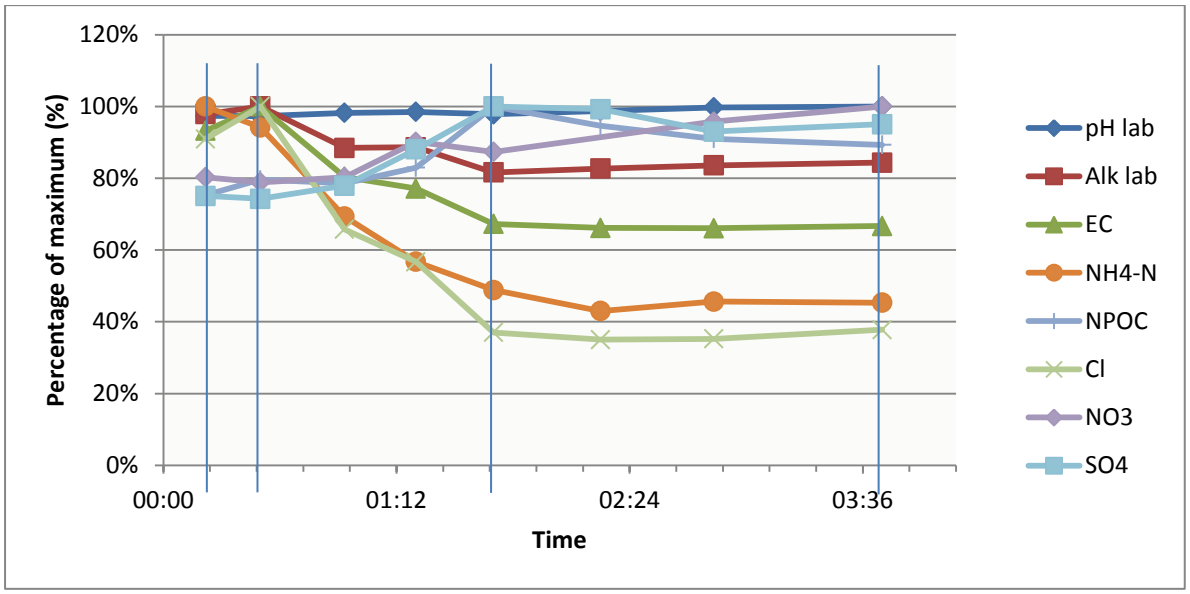

Figure 8.1 Development of water quality parameters (pH, alkalinity, EC, NH4, NPOC, Cl, NO3, SO4) at STW. The vertical lines indicate the boundaries of stable states

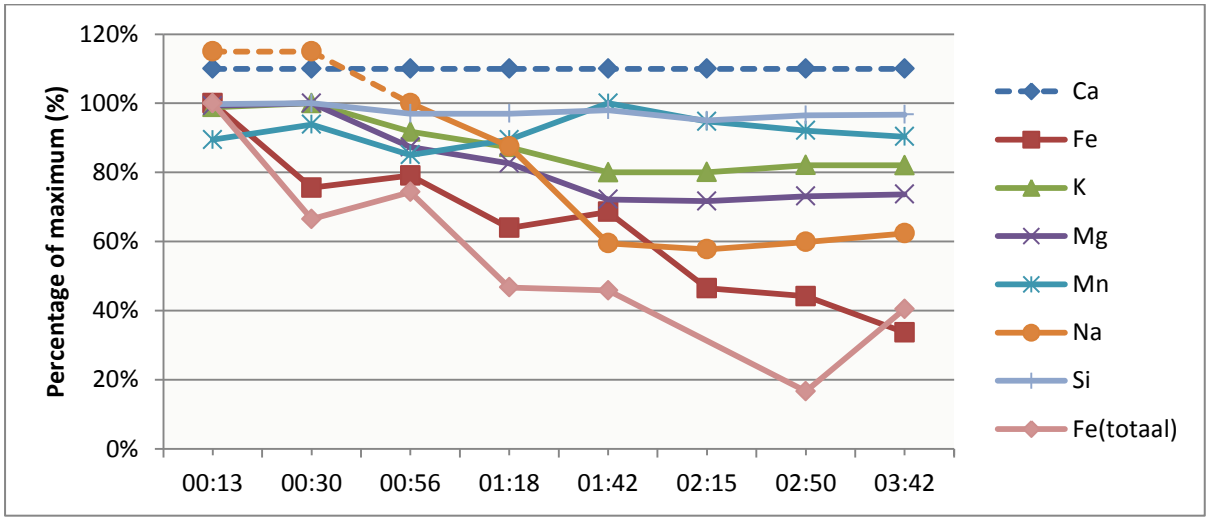

Figure 8.2 Development of cations (dissolved) and iron (extracted during SEDEX). Dashed lines indicate that the measurements fell outside the calibration range of the equipment and is thus marked as general continuation of the trend..

8.3.2 SEDEX data tables

Tables for the Palenstein location (PLS)

Table 8.1 Relative P contribution of the different fractions towards the total of the fractions (PLS), separated for filter and centrifuge (c.f.) samples.

	Time	Exch-P	Fe-P	Authi & Ca-P	Res-P	Orga-P
pls1 filter	00:08	2,8%	81,7%	2,4%	0,2%	12,9%
pls2 filter	00:58	2,1%	78,6%	6,2%	0,3%	12,8%
pls3 filter	01:28	2,6%	82,6%	2,2%	0,4%	12,2%
pls4 filter	01:53	1,8%	79,2%	6.0%	0,3%	12,8%
pls5 filter	02:18	2,4%	79.0%	5,9%	0,2%	12,6%
pls1 c.f.	00:00-00:20	1,4%	88,6%	0,4%	0,2%	9,4%
pls2 c.f.	00:48-01:09	2,3%	88,4%	0,4%	0,3%	8,6%
pls3 c.f.	01:17-01:42	0,7%	89,3%	0,4%	0,2%	9,4%
pls4 c.f.	01:47-02:10	3.0%	87,1%	0,5%	0,3%	9,1%

Table 8.2 P/SM ratio (mg/g) for the Palenstein location (PLS). Results depicted for filter and centrifuge (c.f.) samples.

	Time	Exch-P	Fe-P	Authi & Ca-P	Detri-P	Orga-P	Sum of fractions
	h:mm	mg/g	mg/g	mg/g	mg/g	mg/g	mg/g
pls1 filter	0:08	0,25	7,40	0,22	0,02	1,17	9,1
pls2 filter	0:58	0,18	6,90	0,55	0,03	1,12	8,8
pls3 filter	1:28	0,24	7,67	0,20	0,04	1,14	9,3
pls4 filter	1:53	0,15	6,61	0,50	0,03	1,07	8,4
pls5 filter	2:18	0,20	6,88	0,51	0,02	1,10	8,7
pls1 c.f.	00:00-00:20	0,12	7,37	0,03	0,02	0,78	8,3
pls2 c.f.	00:48-01:09	0,16	6,18	0,03	0,02	0,60	7,0
pls3 c.f.	01:17-01:42	0,06	7,01	0,03	0,02	0,73	7,9
pls4 c.f.	01:47-02:10	0,20	5,93	0,04	0,02	0,62	6,8

Table 8.3 $P_{waterSEDEX}$ (in mg/L) for PLS. Results depicted for filter and centrifuge (c.f.) samples.

	Time	Exch-P	Fe-P	Authi & Ca-P	Detri-P	Orga-P	Sum fractions
	h:mm	mg/L	mg/L	mg/L	mg/L	mg/L	mg/L
pls1 filter	0:08	0,01	0,22	0,01	0,00	0,03	0,26
pls2 filter	0:58	0,01	0,22	0,02	0,00	0,04	0,28
pls3 filter	1:28	0,01	0,27	0,01	0,00	0,04	0,33
pls4 filter	1:53	0,01	0,38	0,03	0,00	0,06	0,48
pls5 filter	2:18	0,01	0,28	0,02	0,00	0,05	0,36
pls1 c.f.	0:00-0:20	0,00	0,22	0,00	0,00	0,02	0,24
pls2 c.f.	0:48-1:09	0,01	0,20	0,00	0,00	0,02	0,23
pls3 c.f.	1:17-1:42	0,00	0,25	0,00	0,00	0,03	0,28
pls4 c.f.	1:47-2:10	0,01	0,34	0,00	0,00	0,04	0,39

Tables for the ditch location (SLT)

Table 8.4 Relative P contribution of the different fractions towards the total of the fractions (SLT).

	Time	Exch-P	Fe-P	Authi & Ca-P	Res-P	Orga-P
slt1 filter	0:05	3,7%	79,6%	5,1%	0,2%	11,8%
slt3 filter	0:40	3,2%	81.0%	4,4%	0,3%	11,1%
slt5 filter	2:09	4,1%	83,4%	3,2%	0,3%	9,0%
slt7 filter	2:57	3,8%	84,0%	1,6%	0,3%	10,3%
slt1 c.f.	0:00-0:25	1,0%	92,6%	0,4%	0,2%	5,8%
slt3 c.f.	0:30-1:10	1,0%	92,6%	0,4%	0,2%	5,7%
slt5 c.f.	1:57-2:22	1,8%	91,9%	0,6%	0,2%	5,5%
slt7 c.f.	2:53-3:20	2,1%	91,4%	0,4%	0,2%	5,9%

Table 8.5 P/SM ratio (in mg/g) for SLT. Results depicted for filter and centrifuge (c.f.) samples.

	Time	Exch-P	Fe-P	Authi & Ca-P	Res-P	Orga-P	Total fractions
	h:mm	mg/g	mg/g	mg/g	mg/g	mg/g	mg/g
slt1 filter	0:05	0,29	7,09	0,45	0,02	1,05	8,9
slt3 filter	0:40	0,30	7,54	0,41	0,03	1,03	9,3
slt5 filter	2:09	0,41	8,42	0,32	0,03	0,91	10,1
slt7 filter	2:57	0,37	8,17	0,15	0,03	1,01	9,7
slt1 c.f.	0:00-0:25	0,09	8,36	0,03	0,02	0,52	9,0
slt3 c.f.	0:30-1:10	0,09	8,13	0,04	0,02	0,50	8,8
slt5 c.f.	1:57-2:22	0,16	8,31	0,05	0,02	0,50	9,0
slt7 c.f.	2:53-3:20	0,18	8,06	0,03	0,02	0,52	8,8

Table 8.6 $P_{WATER.SEDEX}$ (in mg/L) for SLT. Results depicted for filter and centrifuge (c.f.) samples.

Label	Time	Exch-P	Fe-P	Authi & Ca-P	Detri-P	Orga-P	Total fractions
	h:mm	mg/L	mg/L	mg/L	mg/L	mg/L	mg/L
slt1 filter	0:05	0,01	0,35	0,02	0,00	0,05	0,44
slt3 filter	0:40	0,01	0,28	0,01	0,00	0,04	0,34
slt5 filter	2:09	0,01	0,24	0,01	0,00	0,03	0,29
slt7 filter	2:57	0,01	0,27	0,00	0,00	0,03	0,32
slt1 c.f.	0:00-0:25	0,00	0,41	0,00	0,00	0,03	0,44
slt3 c.f.	0:30-1:10	0,00	0,30	0,00	0,00	0,02	0,32
slt5 c.f.	1:57-2:22	0,00	0,24	0,00	0,00	0,01	0,26
slt7 c.f.	2:53-3:20	0,01	0,26	0,00	0,00	0,02	0,29

Tables for the weir location (STW)

Table 8.7 Relative contribution of P fraction towards the sum of all fractions for STW. Results depicted for filter and centrifuge (c.f.) samples.

	Time	Exch-P	Fe-P	Authi & Ca-P	Detri-P	Orga-P
stw1 filter	0:18	2,9%	81,0%	3,2%	0,2%	12,6%
stw2 filter	0:30	4,4%	74,6%	3,8%	0,2%	17,0%
stw3 filter	0:59	3,9%	74,3%	1,2%	0,2%	20,4%
stw4 filter	1:22	4,3%	65,9%	0,8%	0,2%	28,8%
stw5 filter	1:46	7,4%	79,4%	-0,6%	0,3%	13,6%
stw6 filter	2:18	9,7%	77,4%	-0,1%	0,3%	12,8%
stw7 filter	2:55	7,6%	79,8%	-1,1%	0,2%	13,5%
stw8 filter	3:43	8,7%	77,8%	0,0%	0,3%	13,2%
stw1 c.f.	0:00:0-20	1,9%	81,4%	0,1%	0,1%	16,6%
stw2 c.f.	0:25-0:53	1,8%	85,2%	0,1%	0,1%	12,9%
stw3 c.f.	0:54-1:12	1,7%	84,1%	0,1%	0,0%	14,1%
stw4 c.f.	1:13-1:35	1,5%	83,5%	0,5%	0,2%	14,4%
stw5 c.f.	1:36-2:03	0,7%	89,8%	0,1%	0,1%	9,3%
stw7 c.f.	2:29-3:00	3,1%	85,7%	0,2%	0,2%	10,9%
stw8 c.f.	3:28-3:43	1,6%	87,8%	0,1%	0,0%	10,5%

Table 8.8 P/SM ratio (in mg/g) for STW. Results depicted for filter and centrifuge (c.f.) samples.

Label	Time	Exch-P	Fe-P	Authi & Ca-P	Detri-P	Orga-P	Sum fractions
	h:mm	mg/g	mg/g	mg/g	mg/g	mg/g	mg/g
stw1 filter	0:18	0,33	9,11	0,36	0,02	1,42	11,3
stw2 filter	0:30	0,51	8,67	0,44	0,03	1,97	11,6
stw3 filter	0:59	0,40	7,59	0,13	0,02	2,08	10,2
stw4 filter	1:22	0,58	8,90	0,11	0,02	3,89	13,5
stw5 filter	1:46	0,88	9,54	-0,07	0,04	1,63	12,0
stw6 filter	2:18	1,24	9,92	-0,02	0,04	1,64	12,8
stw7 filter	2:55	0,99	10,46	-0,14	0,03	1,77	13,1
stw8 filter	3:43	1,22	10,85	0,00	0,04	1,84	14.0
stw1 c.f.	0:00:0-20	0,24	9,99	0,01	0,01	2,03	12,8
stw2 c.f.	0:25-0:53	0,19	9,08	0,01	0,01	1,37	10,7
stw3 c.f.	0:54-1:12	0,23	10,96	0,01	0,00	1,83	13,0
stw4 c.f.	1:13-1:35	0,17	9,08	0,05	0,02	1,56	10,9
stw5 c.f.	1:36-2:03	0,08	10,36	0,01	0,01	1,07	11,5
stw7 c.f.	2:29-3:00	0,19	5,25	0,02	0,01	0,67	6,1
stw8 c.f.	3:28-3:43	0,19	10,63	0,01	0,00	1,28	12,1

Table 8.9 $P_{WATER.SEDEX}$ (in mg/L) for the ditch location (STW). Results depicted for filter and centrifuge (c.f.) samples.

Label	Time	Exch-P	Fe-P	Authi & Ca-P	Detri-P	Orga-P	Sum fractions
	h:mm	mg/L	mg/L	mg/L	mg/L	mg/L	mg/L
stw1 filter	0:18	0,33	9,11	0,36	0,02	1,42	11,3
stw2 filter	0:30	0,51	8,67	0,44	0,03	1,97	11,6
stw3 filter	0:59	0,40	7,59	0,13	0,02	2,08	10,2
stw4 filter	1:22	0,58	8,90	0,11	0,02	3,89	13,5
stw5 filter	1:46	0,88	9,54	-0,07	0,04	1,63	12,0
stw6 filter	2:18	1,24	9,92	-0,02	0,04	1,64	12,8
stw7 filter	2:55	0,99	10,46	-0,14	0,03	1,77	13,1
stw8 filter	3:43	1,22	10,85	0,00	0,04	1,84	14.0
stw1 c.f.	0:00:0-20	0,24	9,99	0,01	0,01	2,03	12,8
stw2 c.f.	0:25-0:53	0,19	9,08	0,01	0,01	1,37	10,7
stw3 c.f.	0:54-1:12	0,23	10,96	0,01	0,00	1,83	13,0
stw4 c.f.	1:13-1:35	0,17	9,08	0,05	0,02	1,56	10,9
stw5 c.f.	1:36-2:03	0,08	10,36	0,01	0,01	1,07	11,5
stw7 c.f.	2:29-3:00	0,19	5,25	0,02	0,01	0,67	6,1
stw8 c.f.	3:28-3:43	0,19	10,63	0,01	0,00	1,28	12,1

8.3.3 Other tables and figures

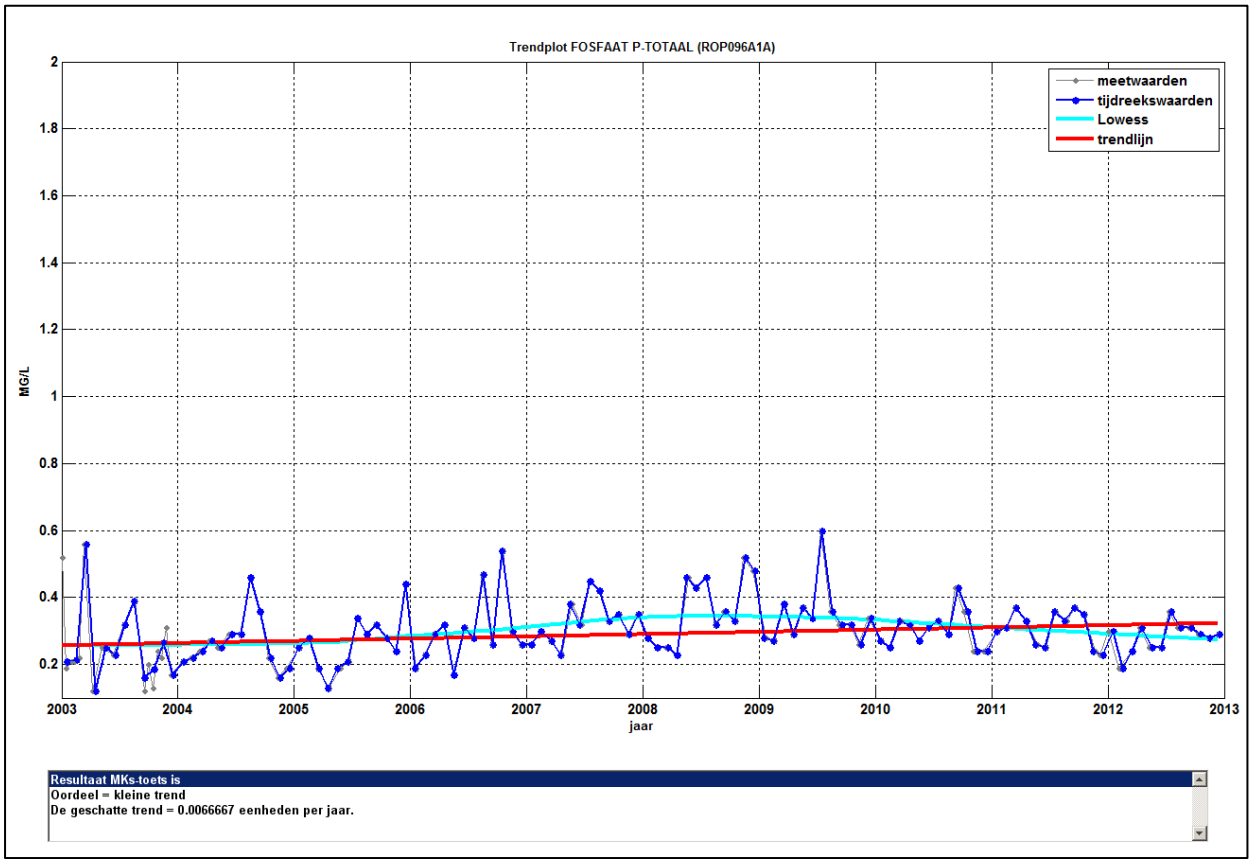

Figure 8.3 Overview of total P measurements performed by the water board at the same location as PLS. Graph taken from Hoogheemraadschap Rijnland (2014)